NUTRIENT POSTINGESTIVE SIGNALLING:

THE ASYMMETRY OF THE RESPONSE OF DOPAMINERGIC NEURONAL CIRCUITS

CAROLINA QUADRADO

A dissertation submitted in partial fulfilment of the requirements for the Degree of Master's in Biomedical Research (Specialisation Area: Neuroscience) at Faculdade de Ciências Médicas | NOVA Medical School of NOVA University Lisbon

November 2022

NUTRIENT POSTINGESTIVE SIGNALLING:

THE ASYMMETRY OF THE RESPONSE OF DOPAMINERGIC NEURONAL CIRCUITS

Carolina Quadrado

Supervisor: Ana B. Fernandes, Post-doctoral researcher at the Champalimaud Foundation Research Centre and Associate Professor at NOVA Medical School

A dissertation submitted in partial fulfilment of the requirements for the Degree of Master's in Biomedical Research (Specialisation Area: Neuroscience)

November 2022

All the work presented in this thesis was developed at the Neuropsychiatry unit at the Champalimaud Research Centre, Champalimaud Foundation.

Financial support

All the required financial support to perform this work was provided by the Portuguese entity Fundação para a Ciência e a Tecnologia under the projects "Viscerosensorial pathways in nutrient postingestive signalling" (PTDC/SAU-NUT/3507/2021) and "Reinforcement learning from postingestive rewards" (PTDC/MED-NEU/1552/2021).

Dedication

Before anything else I must thank one of the most important people to me, my father. You were my rock and my beacon, the one person I could always count on. I will forever miss our talks, your hugs, your advice, and wise words. All these moments have helped shape me as a person and, consequently, as a scientist.

This was the first career milestone I reached without having you by my side and I must confess there were moments I thought I was not going to reach it. However, the guidance you gave me throughout the years worked as lights leading me here. I can only hope to continue to make you proud by continuing to reach my goals and enjoy the good things life has to offer.

You gave true meaning to the word *saudade*.

Your daughter

''Aqueles que passam por nós não vão sós. Deixam um pouco de si, levam um pouco de nós.''

Antoine de Saint-Exupéry

Acknowledgments

In this long year full of challenges, it would not be possible for me to accomplish as much as I did without the people I had around me. They showed me new ways of thinking, new perspectives, and endless comprehension.

First and foremost, I must thank the person who gave me the incredible opportunity to work in the neuronal circuits field, Ana Fernandes. I deeply appreciated you letting me be part of this incredible and demanding project. You taught me new techniques, how to develop my critical thinking, improve my analysis skills and, altogether, how to become a better scientist. You guided me with patience, compassion, and rigorousness and for that I am truly grateful.

I would also like to thank Albino Oliveira-Maia for accepting me in the lab and giving me an incredible and indispensable number of opportunities and resources.

I want to thank all the Neuropsychiatry lab members from whom I had the privilege to learn from. Particularly, to Joaquim Alves da Silva for all the endless hours of code debugging and suggestions. To Tatiana and Margarida, for welcoming me with open arms. I am very grateful for all the patience, support, and advice.

A special thanks to the Champalimaud platforms, in particular to the Vivarium staff, for all the training provided. Of course, this work would not be possible without the mice for which I am incredible thankful for. Without our tiny helpers we would not be able to take such long strides forward in knowledge.

An enormous and warm thank you to my family, for every time you heard me talk about my thesis and my theories and for the support you showed in the toughest moments. This would not be a proper acknowledgement if I did not thank my sister, Madalena, I am forever grateful for your energy, your kindness, and your unconditional support.

A very special thank you to Mariana, we have been friends for years and you have always stood by me and helped me through the worst times and celebrated the best times with me. To *Tuch Tuch* you were all essential for my undergraduate studies and continued to show me your appreciation and full support throughout the Masters. Thanks to Mauro and Maria for all the *boleias*, coffee breaks, for being my lunch buddies and for looking out for me. A big thank you to all the friends I met at the NBR, for believing in me even when I did not. To Patrícia for showing me the ropes and for the daily support. To Dinis and Tiago for helping me blow off steam and always discussing science with me. Lastly, to Joana you are a kind, soft and overall incredible person. I must thank you *a lot a lot* for all the late-night calls, the never-ending pep talks and for always believing in me.

This work has a piece of all of you.

Abstract

Feeding behaviour encompasses any action an animal performs to obtain and consume food. This complex process is affected by pre and postingestive (PI) signals. The former occurs prior and during food consumption, while the latter are related to the mechanisms that occur once food is swallowed. Both these signals shape food-seeking behaviour and convey important information to the central nervous system (CNS).

Currently, it is known that both homeostatic and non-homeostatic circuits, within the CNS, respond to PI stimuli. Homeostatic circuits are controlled by several hypothalamic nuclei. Non-homeostatic circuits are mostly related to the rewarding properties of food and involve dopamine activation and consequent release in the striatum. In fact, several authors have shown that dopamine release in the nucleus accumbens (NAc), a nucleus from the ventral striatum, increases upon PI carbohydrate detection. Additionally, there is robust evidence that PI stimuli from carbohydrates increases neuronal dopaminergic activity in the ventral tegmental area (VTA). Recently, it was described that gut infusions of fat increased dopamine release in the dorsal striatum, However, much less is known about central nervous responses to PI stimuli from other nutrients, such as fat or proteins.

On the other hand, the usage of different nutrients to understand PI feedback in feeding behaviour has been extensively studied using classical associative learning. There is clear evidence that animals prefer flavours paired with calories, carbohydrates, fat or proteins, to flavours paired with non-nutritive solutions. This indicates that the reinforcing properties of PI stimuli could be associated, mostly, to the caloric content of food.

Therefore, the hypothesis for this work is that dopaminergic neurons increase their activity when caloric solutions are infused directly into the stomach. More specifically, it is postulated that ventral areas of dopaminergic neurons will increase their activity when carbohydrates are infused, while intragastric (IG) lipids infusion will activate a more dorsal area of dopaminergic neurons activating substantia nigra dopaminergic neurons and dopamine release in dorsal striatum.

To test this hypothesis, this work focused on how dopaminergic neurons respond to different IG nutrient infusions and how PI feedback affects dopamine response in ventral and dorsal striatal and dopaminergic regions. Thus, calcium imaging and fibre photometry experiments were carried out in dopaminergic regions - VTA and substantia nigra pars compacta (SNc) - and striatal regions - NAc and dorsal-lateral striatum (DLS) -, respectively, while isocaloric solutions of fat and sucrose were infused directly into the stomach. Additionally, how PI stimuli impacts a reinforcement learning (RL) probabilistic behavioural task was also studied. For this, a novel two-action probabilistic instrumental task was developed to better asses how PI feedback modulates learning based on IG infusions of sucrose (caloric carbohydrate) or sucralose (non-caloric artificial sweetener) and how different reward probabilities can affect this type of behaviour.

Calcium imaging recordings revealed that the VTA responds specifically to sucrose, when compared to corn oil or a non-caloric artificial sweetener - sucralose. SNc responses were not nutrient-specific, since dopaminergic activity in this nucleus showed similar patterns of response for all the reinforcers tested. Evaluation of dopamine release in ventral and the dorsal striatum, simultaneously and in the same animal, corroborated previous evidence that dopamine release in the NAc increases when sucrose is infused. In opposition, DLS did not respond to any of the reinforcers administered. Additionally, preliminary data showed that dopaminergic SNc responses did not depend on the lipid administered since response to isocaloric SMOF lipid solution, composed of several types of fatty acids, was similar to corn oil response. Interestingly, NAc response to SMOF lipid was similar to sucrose response, which could mean that ventral response depends on lipid constitution.

The development of the instrumental two-action probabilistic task showed that, when given the choice, between a lever associated to IG infusion of a caloric solution and a lever associated to IG infusion of a non-caloric solution, mice develop a clear preference for the lever associated with caloric content. This preference was independent of the probability of delivering the reward associated with each lever.

Altogether, results from this work shed light on the postulated asymmetry of dopaminergic responses between mesolimbic (VTA to ventral striatum) and nigrostriatal (SNc to dorsal striatum) neuronal pathways, according to the type of postingestive stimuli. Results from the development of the two-action task inferred important parameters in decision making and RL based on PI stimuli.

Resumo

O comportamento alimentar engloba qualquer ação que um animal realiza para obter e consumir comida. Este processo complexo é afetado por sinais pré e pós-ingestivos. Os primeiros ocorrem antes e durante o consumo de comida enquanto os segundos estão relacionados com todos os mecanismos que ocorrem após o consumo da comida. Ambos influenciam o comportamento alimentar e transmitem informações relevantes ao sistema nervoso central (SNC).

Atualmente, sabe-se que existem, no SNC, circuitos homeostáticos e não homeostáticos que respondem a estímulos pós-ingestivos. Os circuitos homeostáticos são maioritariamente controlados por núcleos do hipotálamo. Os circuitos não homeostáticos estão maioritariamente relacionados com as propriedades recompensadoras da comida e envolvem ativação e consequente libertação de dopamina no estriado. De facto, vários autores mostraram que a concentração de dopamina no núcleo *accumbens* (NAc), um núcleo do estriado ventral, aumenta em resposta à deteção pós-ingestiva de carbohidratos. Também há evidência de que estímulos pós-ingestivos derivados da deteção de carbohidratos levam a um aumento de atividade dopaminérgica neuronal na área ventral tegmental (AVT). Recentemente, foi ainda descrito que infusões de lípidos no intestino levaram ao aumento de dopamina no estriado dorsal. Contudo, a resposta dopaminérgica a estímulos pós-ingestivos com o mesmo conteúdo calórico, mas de proveniência nutricional diferente continua por explorar.

Por outro lado, mecanismos pós-ingestivos com diferentes tipos de nutrientes foi extensivamente explorado através de paradigmas clássicos de aprendizagem de associação. Há várias evidências de que animais preferem sabores associados a infusão de substâncias calorias quando comparado com sabores associados a soluções não-nutritivas, o que parece indicar que estímulos pós-ingestivos dependentes do conteúdo calórico parecem ativar regiões neuronais de recompensa que explicam as preferências comportamentais.

Assim a hipótese para o trabalho descrito é de que neurónios dopaminérgicos aumentam a sua atividade quando soluções calóricas são administradas diretamente no estômago. Mais especificamente, foi postulado que neurónios dopaminérgicos de áreas centrais ventrais aumentam a sua atividade quando carbohidratos são administrados, enquanto lípidos devem ativar neurónios dopaminérgicos de áreas mais dorsais, levando a ativação da *substância negra pars compacta* e estriado dorsal.

Tendo em conta o descrito, este trabalho focou-se em perceber como neurónios dopaminérgicos respondem a infusões gástricas de diferentes nutrientes e como os estímulos pós-ingestivos afetam a resposta nas regiões dopaminérgicas ventral e dorsal, e das suas projeções axonais no estriado. Deste modo, experiências de microscopia de cálcio de e fotometria de fibra ótica foram executadas em regiões dopaminérgicas – AVT e porção compacta da substância negra (SNc) – e regiões do estriado – NAc e estriado dorsal-lateral (EDL) -, respetivamente, enquanto soluções isocalóricas de gordura e sucrose eram infundidas diretamente no estômago. Adicionalmente, procurou-se ainda perceber a forma como estímulos pós-ingestivos afetavam a aprendizagem de reforço no contexto de uma tarefa instrumental. Para isso, uma tarefa probabilística instrumental de duas ações foi desenvolvida de modo a avaliar como estímulos pós-ingestivos modulavam a aprendizagem com base em diferentes probabilidades de obtenção de recompensa que poderiam resultar na administração de soluções de sacarose (calórica) e sucralose (adoçante artificial sem conteúdo calórico) diretamente no estômago e simultaneamente uma recompensa oral sem conteúdo calórico.

Experiências de microscopia de cálcio revelaram que a AVT tem uma resposta mais aumentada para injeções intragástricas de sacarose, quando comparadas com injeções intragástrica de óleo de milho ou

sucralose. A resposta da SNc não depende do nutriente infundido uma vez que todos os estímulos utilizados resultaram em perfis de atividade dopaminérgica similares. Medição de níveis de dopamina no estriado ventral e dorsal, simultaneamente no mesmo animal, vão de encontro aos resultados previamente reportados que confirmam maior libertação de dopamina no NAc com a administração intragástrica de sacarose. Em oposição, e em conformidade com os resultados obtidos na SNc, o EDL não respondeu a nenhum dos estímulos administrados. Dados preliminares também revelaram que a resposta de neurónios dopaminérgicos da SNc não depende da constituição lipídica da solução administrada, visto que a resposta intragástrica de óleo de milho é semelhante à resposta intragástrica isocalórica de uma solução calórica - SMOF, composto por vários tipos de ácidos gordos. Interessantemente, a resposta do NAc a esta solução lipídica parece mais similar à resposta observada quando da administração intragástrica de sacarose, o que pode significar que a constituição lipídica da solução administrada pode influenciar vias ventrais dopaminérgicas.

O desenvolvimento da tarefa probabilística instrumental de duas ações mostrou que os animais, quando dada a opção de escolha, desenvolvem uma preferência clara para a alavanca associada a infusões gástricas de sacarose quando comparada a alavanca associada com infusões gástricas de sucralose. Curiosamente, esta preferência é independente da probabilidade que cada alavanca tem de entregar recompensa.

Os resultados deste trabalho permitiram clarificar a hipótese de que a resposta dopaminérgica entre a via mesolímbica (VTA e estriado ventral) e a via nigroestriatal (SNc e estriado dorsal) em resposta a diferentes tipos de estímulos pós-ingestivos é assimétrica. Os resultados do desenvolvimento da tarefa probabilística instrumental de duas ações permitiram inferir parâmetros importantes no contexto de aprendizagem de reforço e decisão baseada em estímulos pós-ingestivos.

Table of contents

List of figures

List of tables

Abbreviations

AAV	Adeno associated virus
AP	Anterior-posterior
CAG	Chicken beta-actin
CNS	Central Nervous System
CRF	Continuous reinforcement
DAT-IRES: Cre	Dopamine Transporter-Internal Ribosome Entry Site-linked Cre recombinase
DLS	Dorsal-lateral striatum
DV	Dorsal-ventral
GRIN	Gradient refractive index
IG	Intragastric
ML	Medial-lateral
NAc	Nucleus Accumbens
ns	non-significant
PI	Postingestive
PP	Postingestive probabilistic
R	Reversal
RL	Reinforcement learning
RR	Random reinforcement
SEM	Standard error of the mean
SNc	Substantia Nigra pars compacta
VTA	Ventral Tegmental Area
WT	Wild-type

1. Introduction

1.1. Feeding behaviour

Feeding behaviour encompasses any action that an animal performs to obtain and consume food. The study of feeding behaviour began in the 19th century with Claude Bernard. The physiologist associated homeostatic regulation with the regulation of the internal environment [1]. In the beginning of the 20th century, Curt Richter first used the term ''behavioural regulation of internal states'', which indicated how feeding behaviour functioned to maintain physiological homeostasis [2]. Since then, the field has evolved, and much progress has been made, in the past several decades, to identify the neural and biological pathways that control feeding behaviour.

Currently, it is known that regulation of feeding behaviour is a complex multifactorial mechanism that is regulated by homeostatic and non-homeostatic mechanisms [3]. The former regulates food intake in order to appease hunger and fulfil nutritional requirements. The latter includes hedonic pathways are mostly driven by sensory of food. Non-homeostatic circuits have been related to eating disorders associated with excessive food intake, such as obesity, as cognitive and hedonic factors are thought to override the inhibitory mechanism regulating caloric intake and energy homeostasis [4].

During food intake animals integrate the explicit orosensory properties of food such as taste, smell, texture and others. At the same time, and after food consumption, signals from interoceptive pathways, such as satiety, energy, nutritional balance and other metabolic states, are also integrated. [5] These signals constitute, in a simplistic model, the pre and postingestive (PI) signals, respectively, and will be explored throughout this thesis.

1.1.1. Preingestive signals and food preference

Orosensory cues are external and explicit signals that are an essential component of feeding behaviour and that include signals as taste, smell, temperature, texture, and others. From all of this, taste has been described as the major intervenient in feeding behaviour and it has been well studied in modulating feeding decisions [6].

Five major tastants have been described and immediately signal CNS the modality of taste that is being consumed: sweet, bitter, umami, salty or acid [7]. For the purpose of this work, sweet taste will be explored. Several species, including humans, show an innate positive response to sweet taste that is shaped throughout their lifetime [8]. Several sweet taste receptors have been identified the tongue of mice and have been shown to be essential to experience sweetness [9, 10]. Furthermore, studies have showed that improving the palatability of food by using artificial sweeteners - sweet non-caloric solutions - leads to an increase in food intake and weight gain [11]. In a two - bottle preference test, between water and artificial sweetener, mice consume a bigger volume of the latter indicating that animals prefer the sweet non-caloric solution [12, 13]. Preference for these non-caloric sweet tastant is usually dose-dependent, which means that an increase in the sweetness is accompanied by an increase in preference [14, 15].

In human adults, assessment of hedonic characteristics of sweet solutions is often done through self-report questionaries [16]. Several lines of evidence clearly show that sweet orosensorial characteristics are pleasant and increase with the sweetness intensity associated with the solution. Interestingly, sweetness preference increases with age and fasting, when compared to satiated counterparts, but tends to decrease for individuals that are more active, when compared to less active counterparts. [17] Moreover, it has been reported that sweet intensity appraisal and hedonic hunger scores, which reflect the rewarding properties

of highly palatable foods, are predictors of weight loss. A recent study also showed that hedonic hunger levels, rewarding properties of highly palatable foods in the environment, are positively associated with obesity status [18]. This mean that the higher the hedonic hunger, the most likely it was for the person to have a higher body mass index (BMI) score [19]. These results show orosensory processing and assessment are related with body weight in a matter that suggest that the more sensitive you are to sweet taste, the less likely you are to gain weight.

Moreover, animals exposed to a two - bottle preference test prefer sucrose – caloric carbohydrate - over sucralose – artificial sweetener-, which indicates that the caloric content of food is also important in defining feeding behaviour. Importantly, preference for carbohydrates over non-nutritive solutions was corroborated in a context of sham feeding, which is a procedure that allows animals to experience the tastant (orosensory cues) but not consume the solution (PI signals) [20-24]. In fact, sweet-blind mice, genetically modified animals that do not express a taste-specific receptor essential to experience sweet taste [25, 26], develop a clear short and long-term preference for the flavour associated with sucrose – caloric solution – but not sucralose – artificial sweetener based only on PI stimuli [27, 28]. Lastly, mice trained in an instrumental two-lever task press a lever to obtain an oral reward of sucrose significantly more than a lever associated with an equally sweet solution of sucralose [29]. These results indicate that feeding behaviour can be modulated by other factors rather than orosensorial sweet perception.

1.1.2. The impact of postingestive feedback on food seeking behaviour

The importance of PI signals in feeding behaviour was well demonstrated in classical flavour-nutrient conditioning (FNC) experiments. During several decades, studies, mostly published by Anthony Sclafani and co-workers, have consistently reported that animals develop a learned preference for flavours associated to calories over flavours associated to non-caloric solutions [30, 31].

Figure 1.1 represents the three phases of FNC assay. Briefly, in the pre-conditioning phase animals are exposed to two arbitrary novel flavours and flavour preference is measured based on the intake of each of the flavours consumed, in a two-bottle preference test. Afterwards, a conditioning phase starts with one of the flavours, is associated with a nutritive source - reinforcer. The other flavour is associated with a non-nutritive source, such as water or a non-caloric solution. To ensure that the solutions associated are not differentiated through their orosensory properties, the conditioning occurs by injection of the substances, through an intragastric (IG) catheter, whenever the animal licks for the flavour. After several consecutive conditioning sessions, preference between each flavour is measured using the same preconditioning two-bottle test. [30] During the pre and post conditioning tests flavours are presented without any administration of the IG solution associated during the conditioning phase. The duration of the test after conditioning is brief to ensure that the results are not affected by extinction.

Results obtained from this type of conditioning have robustly shown that animals prefer the flavour associated with IG delivery of calories to the flavour associated with IG water or non-caloric solutions [30]. This type of flavour-nutrient association has been consistently established using several carbohydrate sources, such as glucose, sucrose, and polycose, fat sources such as corn oil, intralipid and soybean oil [22, 27, 31], and protein sources such as glutamate [32]. However, even though that FNC association with fat and proteins sources also occurs, the absolute intake of the flavour associated with IG corn lipids or protein [33] is lower when compared to the absolute intake in protocols with carbohydrate conditioning [34]. Moreover, when performing a FNC assay with one flavour associated with IG lipid and another flavour associated with IG

carbohydrate, animals prefer the latter, indicating that, for the same caloric content, carbohydrates are preferred over lipids solutions [30].

When looking at the response of animals to other types of nutrients, the pattern of response is similar to the one observed for sugar. If given the choice between water and a carbohydrate solution, such as glucose, polycose or sucrose, animals prefer the caloric sweet solution [15]. Preference for carbohydrates is dose-dependent, which means that an increase in concentration is accompanied by an increase in preference [14, 15]. Moreover, lipidic solutions –, such as corn oil or intralipid, are also preferred to water [22].

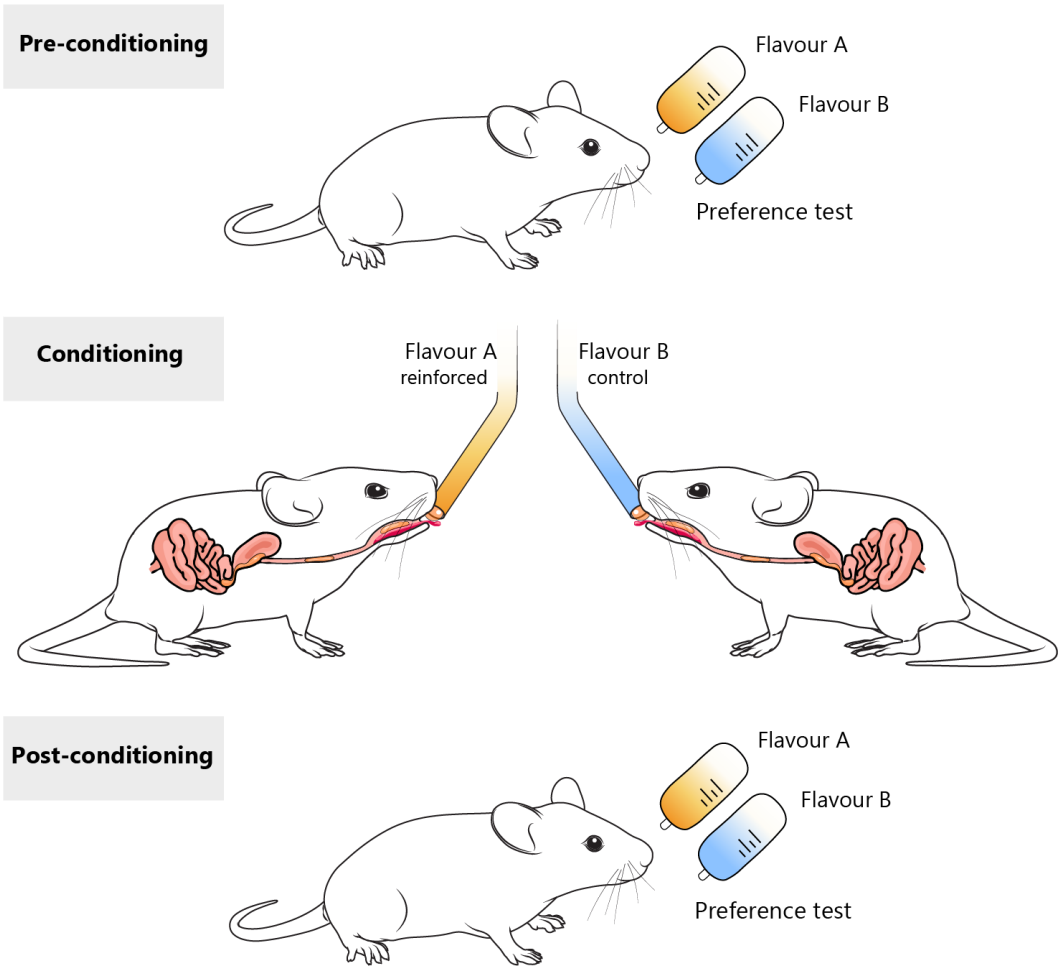

Figure 1.1 Schematic representation of the flavour-nutrient conditioning (FNC) behavioural assay.
In the pre-conditioning stage, animals are exposed to two arbitrary novel flavours – flavour A (orange) and B (blue). Preference for each flavour is assessed in the pre- and post-conditioning phases using a two-bottle preference test. In the conditioning stage, one flavour is reinforced with a caloric solution (flavour A), while the other is associated with a non-nutritive source (flavour B), for several consecutive sessions. The flavour association with the IG reinforcer during the conditioning phase is performed by exposing only one of the flavours at a time.

FNC assays have become the standard behavioural test for studying the impact of PI sensing and, therefore, the rationale has also been applied in humans [16]. For example, using the FNC paradigm in adults revealed that associating a non-palatable caloric solution – maltodextrin – to a flavour lead to an increase in consumption when compared to a flavour paired with lower calories. Importantly, both flavours were equally sweet since they had the same amount of sucralose (Unpublished work by Gabriela Ribeiro, Ana

Fernandes, and Oliveira-Maia). Proving, once again, that PI caloric stimuli shapes feeding behaviour and that this phenomenon is conserved in humans.

In mice, evidence that PI stimuli modulates feeding decisions has been extensively studied by Sclafani and co-workers. Corroborating these findings, de Araujo *et al.,* 2008 performed experiments with sweet-blind mice and showed that these animals prefer sucrose to a non-nutritive solution [27]. Additionally, Oliveira-Maia *et al.*, 2011 showed that most of the PI stimuli could occur after absorption of carbohydrates. In this study, the authors performed a side nutrient conditioning test, which is similar to FNC, but the association is performed on the position of the solution (left or right), rather the flavour. Animals developed a clear side preference for the side that was conditioned with jugular and hepatic-portal vein administrations of glucose. Results from this work revealed that conditioning using the jugular route occurred for higher concentrations of glucose, when compared to conditioning using the hepatic-portal vein route [35]. Thus, giving insight on the possibility that conditioning could depend on administration route or even where these nutrients are being detected after absorption in the gut.

More recently, Fernandes *et al.,* 2020 reported that mice sustain and increase lever pressing behaviour for a lever associated with IG infusion of sucrose. When the same protocol is applied to a group of animals pressing for IG infusions of sucralose, there is a progressive decrease in lever pressing behaviour. These results further corroborate the importance of PI stimuli in feeding behaviour. Additionally, in this work a two-lever instrumental task was designed with the intent to dissect the preference for IG sucrose over IG sucralose. In the same session, mice had two possible levers, one lead to an IG infusion of sucrose while the other lead to an IG infusion of sucralose. Results showed that mice significantly press more the lever associated with the caloric reinforcer (sucrose) when compared to the lever associated the non-caloric reinforcer (sucralose), [29] proving that PI delivery of sucrose can sustain operant food seeking behaviour.

Altogether, the findings described clearly demonstrate that PI signals modulate feeding behaviour, in associative Pavlovian learning, such as FNC experiments, and operant reinforcement learning tasks. However, how these signals are transmitted to the central nervous system (CNS) or how they are modulated within the reward related areas remains largely unknown.

1.2. Central nervous system and postingestive sensing

1.2.1. Peripheral-brain communication

Peripheral-brain communication has been extensively studied since the 18th century and has given rise to major discoveries regarding anatomical and physiological characteristics of gut-brain signalling [36]. Food sensing is one the most well-known system where neuronal, humoral, and hormonal peripheral signals converge information to CNS [37]. Abdominal peripheral sensory systems, from stomach, gut, and liver, convey information to the CNS regarding PI information. All these gastrointestinal organs are highly enervated by the peripheral nervous system and are directly or indirectly modulated by hormonal and humoral factors [37]. Thus, they are important organs in the communication between periphery and CNS.

The vagus nerve densely innervates the gastrointestinal tract and transmits sensory information to the brain. Vagal sensory neurons are robustly activated by both mechanical and chemical signals associated with food consumption. Mechanosensitive vagal afferents innervate the stomach and intestines, to directly detect distension. In contrast, chemosensitive vagal afferents innervate the intestine and liver and have been mostly described to monitor nutrients. Importantly, it has been reported that vagal afferents stimulation can modulate food intake [38-40].

Vagal afferents from intestine or liver have their cell bodies localized in the nodose ganglion and axons that terminate in the brainstem. Anatomical studies demonstrate that vagal fibres that innervate the duodenum and liver converge information to the left nodose ganglion (LNG). On the other hand, fibres that innervate the jejunum and ileum convey signals to the CNS through the right nodose ganglion (RNG) (**Figure 1.2**) [41, 42].

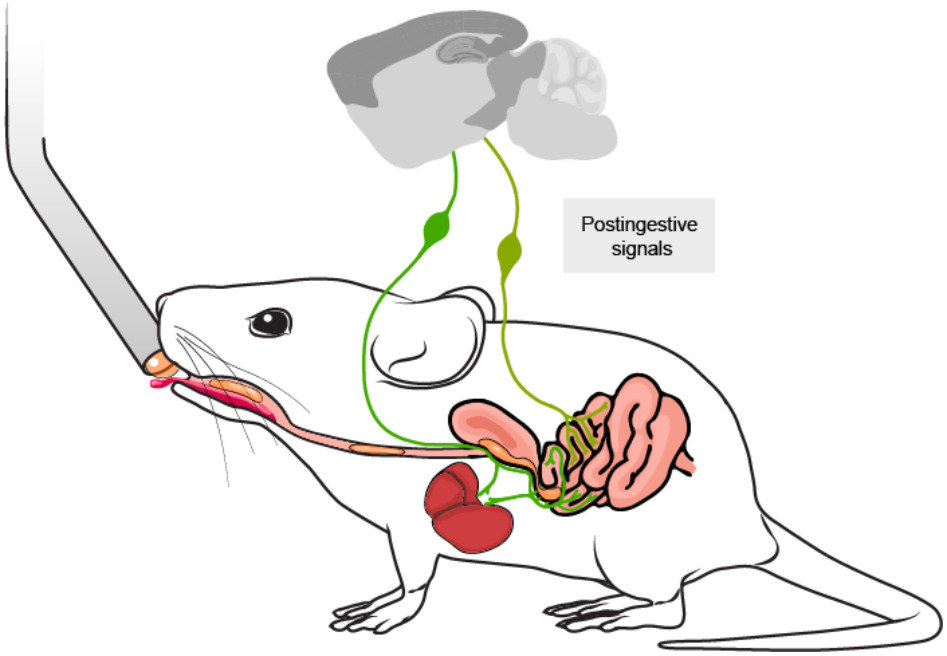

Figure 1.2 Schematic representation of vagal sensory afferent fibres in the context of gut-brain communication context.
Vagal fibres that innervate the duodenum and liver (dark green) and convey signals to central regions through to the left nodose ganglion (LNG). Vagal afferent fibres that innervate the jejunum and ileum (light green) and convey signals to central regions through to the right nodose ganglion (RNG).

The asymmetry observed for gastrointestinal vagal innervation has been postulated to differently transmit information regarding nutrients, such as carbohydrates and lipids, to central nervous circuits. In fact, there is evidence that sugar and fat are detected by different gastrointestinal vagal afferent fibres [3, 43, 44]. Consequently, information regarding nutrient detection could be transmitted to the CNS through different vagal signalling pathways.

Carbohydrates are firstly detected by intestinal vagal nerves [45] and then by the hepato-portal system, more specifically by hepatic vagal afferent fibres. This is supported by the fact that specific vagus nerve lesions disrupt flavour-nutrient conditioning [46, 47] and decrease, but do not abolish, instrumental operant responses to IG infusions of sugar, specifically sucrose [29].

Recent evidence has demonstrated that a population of nodose ganglion (NG) neurons are activated upon delivery of glucose in the intestine. Notably, these neurons were not stimulated upon delivery of a non-caloric artificial sweetener [44]. Furthermore, retrograde and anterograde tracing studies showed that the hepatic branch of the vagus nerves was connected to NG neurons, more specifically LNG [40]. Similarly, intestinal vagal afferent neurons respond to intestinal delivery of fat and that bilateral lesions to the vagus nerve are sufficient to abolish fat preference [43]. Han *et al.*, 2018 demonstrated that intestinal anterograde labelling activate vagal RNG neurons leads to infection of dopaminergic neurons. Moreover, results also

showed that labelling vagal upper intestine neurons that are connected to the RNG is sufficient to induce labelling in central dopaminergic regions [48], establishing a connection between the peripheral nervous system and central dopaminergic regions.

It is also important to refer that food consumption triggers the release of several hormones throughout the gastrointestinal tract. These hormones are released in response to specific nutrients and other stimuli and can have paracrine and endocrine effects.

In addition to the vagus nerve and the endocrine action of hormones, information from the gut is also transmitted to the brain by spinal nerves. [37, 42] However, the gastrointestinal signals that are encoded by spinal afferents, and how those signals might influence feeding behaviour, has not been well characterized.

1.2.2. Neuronal circuits involved in feeding behaviour

Currently, it is well established that PI mechanisms are able to drive food seeking behaviour. The physiological requirements are complex and involve both homeostatic and non-homeostatic mechanisms. Homeostatic circuits regulate homeostasis through energy and metabolic requirements and involves mostly the hypothalamus [49, 50]. On the other hand, certain type of food elicit clear rewarding responses within the central nervous system that can behaviourally override hypothalamic satiation mechanisms and ultimately lead to unhealthy feeding patterns [4].

From an evolutionary standpoint, our brain is optimized to ensure survival in an environment with scarce food availability and long fasting periods. Therefore, nutritive food, such as sugar, is encoded as highly rewarding and guides several decisions regarding what and when to eat. Even though the sweetness from sugars and artificial sweetener is detected by sweet taste receptor in the tongue, and immediately sensed in the CNS, there is a considerable part of sugar consumption response that derives from the gut detection and absorption. In fact, studies where measurements of dopamine concentration were performed, using microdialysis and cyclic voltammetry, have shown that PI signals per se consistently evoke dopamine release in the striatum [51].

Dopamine is a catecholamine neurotransmitter that has been associated with food seeking behaviour, motivation, and reinforcement value [51, 52]. Several studies have shown that disrupting dopamine production or signalling, through pharmacological and genetic techniques, resulted in deep aphagia that was reverted once animals had accesses to another source of dopamine [53, 54]. Dopamine is synthetized by neurons in the ventral tegmental area (VTA) and substantia nigra pars compacta (SNc), which, in turn, project to other central regions, such as the striatum (**Figure 1.3**) [55].

The striatum is composed by medium spiny neurons that receive projections from dopaminergic neurons, namely VTA and SNc neurons among others. VTA dopaminergic neurons project to the ventral striatum - mesolimbic pathway. This pathway is mostly related to reward-related functions [56], such as incentive salience, pleasure response and positive reinforcement. Evidence emerged showing that ventral areas of the striatum were the ones implicated in food stimuli, specifically from PI peripheral signals. On the other hand, SNc dopaminergic projections constitute the nigrostriatal pathway, and release dopamine mostly in the dorsal part of striatum [56]. Dysfunction of this pathway is mostly related to motor dysfunction and learning deficits.

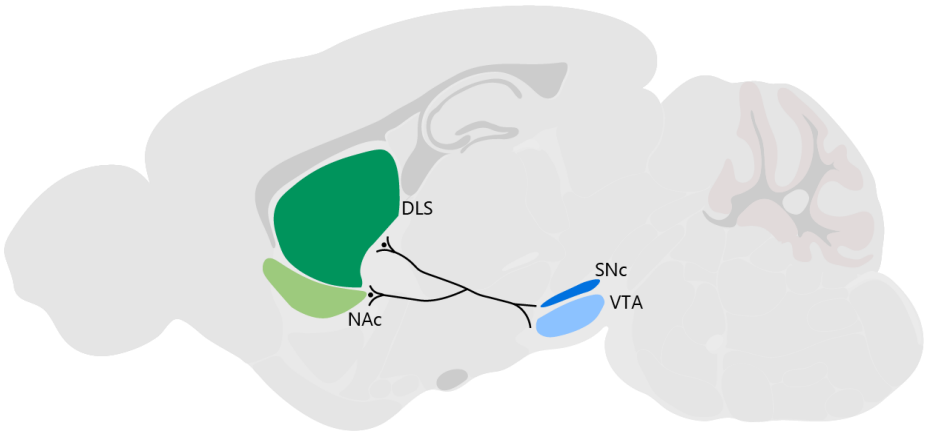

Figure 1.3 Dopaminergic central regions and their striatal projections.
Representation of the striatum (green) and regions where dopaminergic cell bodies are found (blue). Ventral tegmental area (VTA, light blue) and substantia nigra pars compacta (SNc, dark blue) communicate with the nucleus accumbens (NAc, light green) and the dorsal-lateral striatum (DLS, dark green), respectively. Black traces represent dopaminergic neurons (axons) stemming from VTA and SNc that project to the dorsal and ventral striatum. Sagittal slice was obtained from the Allen Brain References Mouse Atlas using the Application Programming Interface (API).

It is also important to note that striatal medium spine neurons are one of the main components of the basal ganglia nuclei, which have been heavily implicated in movement initiation [57]. Robust evidence has shown that the dorsal-lateral striatum (DLS) receives important inputs involved in movement control [58] and the loss of dopaminergic neurons in the SNc has been heavily implicated with issues in movement initiation, i.e., development of Parkinson's disease [59].

The nucleus accumbens (NAc) of the ventral striatum has been largely implicated in food reinforcement since NAc dopamine levels increases in response to orosensory food cues[14, 60]. Dopamine dynamics in this region are also affected by the PI properties of food, namely carbohydrates. Dopamine release in the ventral striatum on sweet blind mice, measured by microdialysis, revealed that extracellular dopamine levels increased after sucrose but not sucralose consumption [27]. Additionally, infusions of sucrose directly into the stomach showed a clear increase in dopamine levels in the same striatal region. Furthermore, portal vein infusions of glucose led to an increase of dopamine transient frequency, measured by cyclic voltammetry, in the NAc [35]. Using a high temporal and spatial resolution technique – calcium imaging – that allows to directly measure dopaminergic neuronal activity in mice, it was shown that VTA dopaminergic activity increased upon IG delivery of sucrose, when compared with IG sucralose [29]. Altogether, this data indicates that there is a robust increase in dopaminergic neuronal activity in VTA and, consequently, an increase in dopamine levels in ventral striatum as a response to PI stimuli from carbohydrates.

Although there is evidence that intragastric infusion of sugars causes an increase in dopamine in ventral striatum, there is also evidence that dopamine release in dorsal striatum is involved in gastrointestinal nutrient responses. Han *et al.,* 2018 performed experiments where the dopamine dynamics of the dorsal striatum were monitored while the SNc was stimulated. Additionally, infusions of fat directly into the gut led to increments in dopamine release in dorsal striatum indicating that central dorsal dopaminergic structures could be involved in PI feedback related to lipids.

Accordingly, experiments performed in humans using functional magnetic resonance imaging (fMRI) and a dopamine sensitive positron emission tomography (PET) showed that consumption of sweet caloric food led to the immediate and delayed release of dopamine in ventral and dorsal striatal areas [61]. Imaging

showed an immediate response is thought to be related with preingestive signals, and a second delayed response that was most likely related with PI stimuli from the consumed food. This evidence further corroborates dopamine dynamic patterns observed in the striatum of mice after food consumption.

Considering everything described above, the proposed model and the hypothesis tested was that dopamine could differently activate VTA or SNC dopaminergic neurons based on nutrient infusion, with carbohydrates activating ventral rewarding areas, while fat sources once sensed activate more dorsal areas of dopaminergic neurons namely SNc and dorsal striatum.

The study of feeding behaviour and its neurological underpinnings revealed important features of food stimuli and sensing, however, their impact on unhealthy feeding patterns, related with excessive eating, remains unknown. Evidence gather thus far, shows clear layers of feedback signals, which begins from the moment that food enters in our mouth or even prior. The nature of these signals is remarkably diverse and complex, they are integrated in several areas of the brain, and ultimately define food-seeking behaviour. Although clear evidence has shown key neurological circuits in the control of eating, the neurological underpinning controlling nutrient sensing, peripheral signals and their integration within the CNS needs further clarification.

1.2.3. Measuring neuronal activity in response to gut signalling

The understanding of gut signalling effects on neuronal activity has been studied in both humans and animal models. In humans, this effect has been explored through the use of fMRI [61, 62]. In animals, the study of *in vivo* neural dynamics in the context of feeding behaviour became possible with recent advances in transgenic models, neurotransmitter sensing, and development imaging techniques with high temporal and spatial resolution [63].

Currently, it is possible to monitor *in vivo* neurotransmitter dynamics and neuronal activity responses. The neurotransmitter that has been studied the most in the context of feeding behaviour is dopamine. Several works have reported the use of microdialysis [27] and cyclic voltammetry [35] to measure dopamine release while animals were exposed to caloric and non-caloric solutions. By measuring neurotransmitter dynamics these techniques are an indirect measure of neuronal activity. Microdialysis is performed in awake freely behaving animals and it is based on sampling of molecules from interstitial space that allows quantification of neurotransmitters, such as dopamine [63, 64]. Nevertheless, it has slow temporal dynamics [63]. On the other hand, cyclic voltammetry can be performed on anesthetized or awake animals and consists of measuring the current response of a redox solution with a linearly cycled potential sweep. Therefore, it involves applying voltage to induce oxidation and reduction of a chemical that, in this context, is a neurotransmitter [63, 65]. It has the advantage of having a higher temporal resolution, when compared to microdialysis but since it is an electrochemical technique, it is unspecific [65]. One disadvantage that these techniques presented was the inability to monitor and measure long-term changes which is crucial to understand how neurotransmitters can modulate feeding behaviour over time [63].

More recently, fibre photometry using dopamine sensors have been used. The development of dopamine sensors with high spatial and temporal resolution permitted the usage of this technique for measurements of dopamine dynamics in the striatum (**Figure 1.4**). This approach involves the implant of, at least, one small optical fibre that allows to monitor population-level dynamics. For most cases, fibre photometry relays on calcium indicators to measure overall calcium dynamic in neuronal population [66]. Additionally, this technique can also be used along with dopamine indicators in order to exclusively monitor and record dopamine dynamics. A recently developed dopamine indicator is DLight, which allows for high resolution dopamine

dynamics in awake freely behaving mice [67]. This indicator is sensitive to dopamine concentration changes because its conformation changes upon dopamine binding. Also, it was engineered to be couples to a green fluorescent protein (GFP) and, thus, when dopamine binds to this indicator it induces changes in fluorescence so the more dopamine binds, the more intense the fluorescence [67].

Calcium imaging, contrary to all the techniques mentioned above, allow to directly monitor and quantify neuronal activity of individual neurons (**Figure 1.4**). It relays on calcium indicators to measure activity, but the spatial resolution provided allows to monitor fluorescence changes of individual neurons and, consequently, identify neuronal subpopulations. Calcium indicators are proteins that change conformation upon calcium binding and, subsequently, emit fluorescence. These are a good proxy for neuronal activity since calcium floods neurons when action potentials are generated and, if the cell expresses a calcium indicator, fluorescence increases in this scenario. [66] Currently, the most common calcium indicator is green calmodulin protein – GCaMP. Fibre photometry is relatively non-invasive and has the advantage of allowing to measure neuronal dynamic in freely behaving animals [63].

Additionally, this approach also allows to image calcium dynamics of two cell populations by using calcium indicators that emit different colours. Calcium imaging involves the implant of a gradient index refractive (*GRIN*) lens and the use of a small head mounted microscope (miniscope) [68]. It is less invasive than, for example, 2-photon microscopy and allows to easily monitor neuronal activity in awake freely behaving animals [63].

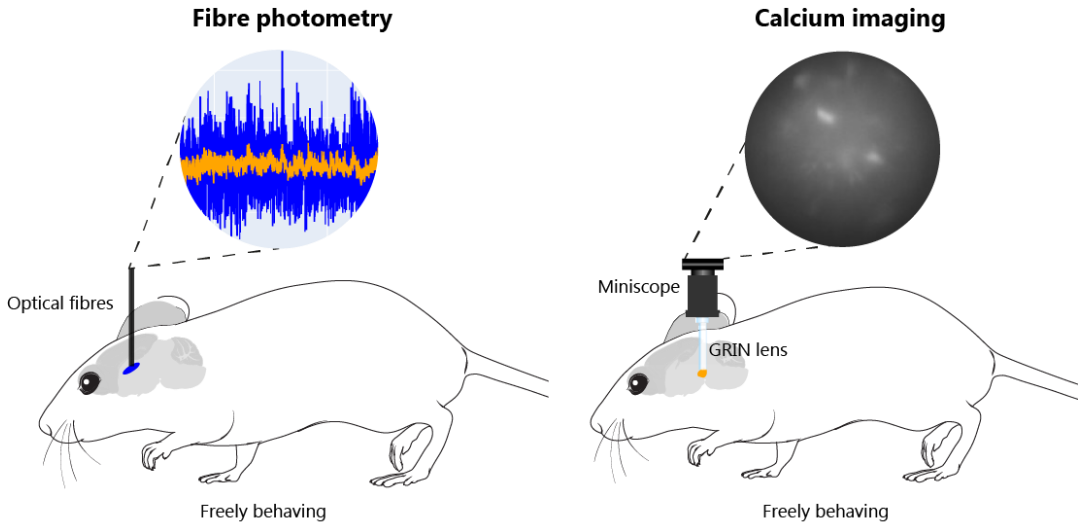

Figure 1.4 Optical imaging techniques for awake freely behaving animals.
Schematic representation of fibre photometry (left) and calcium imaging (right) experiments. In fibre photometry experiments mice undergo surgeries that allow to observe calcium dynamics with the help of optical fibres. For calcium imaging experiments, a *GRIN* lens and a miniscope is used to monitor neuronal activity. Fibre photometry is a has less temporal resolution and does not enable identification of subpopulation of neurons, therefore the spatial resolution is limited when compared to calcium imaging.

Most of the techniques described above take advantage of transgenic animal models in order to monitor activity of a specific neuronal population. These models allow to express calcium indicators in a specific cell type, for example, dopaminergic neurons by using the Cre-*loxP* system [69]. The Cre recombinase recognizes two consecutive *loxP* sites and enable the expression of the calcium indicator in cells that express the enzyme

Cre recombinase [69, 70]. Therefore, Cre transgenic mice are genetically modified animals that express Cre recombinase under a cell specific transporter.

These techniques along with nutrient infusions, FNC assays, and sham-feeding experiments have allowed to better understand how gut signalling influences neuronal activity. The constant development and optimization of brain imaging techniques has granted the possibility to image deep brain regions which was not possible until very recently [68]. At the same time, neuronal imaging has provided the opportunity to ask new questions and better understand the neuronal underpinnings behind food-seeking behaviour.

1.3. Bibliography

1. Gross CG. Claude Bernard and the Constancy of the Internal Environment. *The Neuroscientist*. 1998;4(5):380-385. doi:10.1177/107385849800400520

2. Richter C. Total self-regulatory functions in animals and human beings. *Harvey Lecture Series*. 1943;38:63-103.

3. de Araujo IE, Schatzker M, Small DM. Rethinking Food Reward. *Annu Rev Psychol*. 2020;71:139-64. doi:10.1146/annurev-psych-122216-011643

4. Rossi MA, Stuber GD. Overlapping Brain Circuits for Homeostatic and Hedonic Feeding. *Cell Metab*. Jan 9 2018;27(1):42-56. doi:10.1016/j.cmet.2017.09.021

5. Sclafani A. Oral and postoral determinants of food reward. *Physiology & Behavior*. 2004;81(5):773-79. doi:10.1016/j.physbeh.2004.04.031

6. Peng Y, Gillis-Smith S, Jin H, Tränkner D, Ryba NJ, Zuker CS. Sweet and bitter taste in the brain of awake behaving animals. *Nature*. 2015;527(7579):512-15. doi:10.1038/nature15763

7. Yarmolinsky DA, Zuker CS, Ryba NJ. Common sense about taste: from mammals to insects. *Cell*. Oct 16 2009;139(2):234-44. doi:10.1016/j.cell.2009.10.001

8. Venditti C, Musa-Veloso K, Lee HY, et al. Determinants of Sweetness Preference: A Scoping Review of Human Studies. *Nutrients*. 2020;12(3)doi:10.3390/nu12030718

9. Adler E, Hoon MA, Mueller KL, Chandrashekar J, Ryba NJ, Zuker CS. A novel family of mammalian taste receptors. *Cell*. 2000;100(6):693-702. doi:10.1016/s0092-8674(00)80705-9

10. Nelson G, Hoon MA, Chandrashekar J, Zhang Y, Ryba NJ, Zuker CS. Mammalian sweet taste receptors. *Cell*. 2001;106(3):381-90. doi:10.1016/s0092-8674(01)00451-2

11. Ramirez I. Stimulation of energy intake and growth by saccharin in rats. *J Nutr*. Jan 1990;120(1):123-33. doi:10.1093/jn/120.1.123

12. Strouthes A. Long-range two-choice saccharin and water consumption in rats. *J Comp Physiol Psychol*. Oct 1970;73(1):123-34. doi:10.1037/h0030019

13. Dess NK, Chapman CD, Monroe D. Consumption of SC45647 and sucralose by rats selectively bred for high and low saccharin intake. *Chem Senses*. 2009;34(3):211-20. doi:10.1093/chemse/bjn078

14. Hajnal A, Smith GP, Norgren R. Oral sucrose stimulation increases accumbens dopamine in the rat. *Am J Physiol Regul Integr Comp Physiol*. Jan 2004;286(1):31-37. doi:10.1152/ajpregu.00282.2003

15. Cagan RH, Maller O. Taste of sugars: brief exposure single-stimulus behavioral method. *J Comp Physiol Psychol*. 1974;87(1):47-55. doi:10.1037/h0036585

16. Yeomans MR, Leitch M, Gould NJ, Mobini S. Differential hedonic, sensory and behavioral changes associated with flavor-nutrient and flavor-flavor learning. *Physiol Behav*. 2008;93:798-806. doi:10.1016/j.physbeh.2007.11.041

17. Drewnowski A, Mennella JA, Johnson SL, Bellisle F. Sweetness and food preference. *J Nutr*. 2012;142(6):1142-48. doi:10.3945/jn.111.149575

18. Ribeiro G, Camacho M, Fernandes AB, Cotovio G, Torres S, Oliveira-Maia AJ. Reward-related gustatory and psychometric predictors of weight loss following bariatric surgery: a multicenter cohort study. *Am J Clin Nutr*. 2021;113(3):751-61. doi:10.1093/ajcn/nqaa349

19. Ribeiro G, Camacho M, Santos O, Pontes C, Torres S, Oliveira-Maia AJ. Association between hedonic hunger and body-mass index versus obesity status. *Sci Rep*. 2018;8(1)doi:10.1038/s41598-018-23988-x

20. Nissenbaum JW, Sclafani A. Sham-feeding response of rats to Polycose and sucrose. *Neurosci Biobehav Rev*. Summer 1987;11(2):215-22. doi:10.1016/s0149-7634(87)80029-5

21. Weingarten HP, Watson SD. Sham feeding as a procedure for assessing the influence of diet palatability on food intake. *Physiol Behav*. 1982;28(3):401-07. doi:10.1016/0031-9384(82)90131-7

22. Sclafani A. Fat and sugar flavor preference and acceptance in C57BL/6J and 129 mice: experience attenuates strain differences. *Physiol Behav*. 2007;90(4):602-11. doi:10.1016/j.physbeh.2006.11.012

23. Smith GP, Greenberg D. Orosensory stimulation of feeding by oils in preweanling and adult rats. *Brain Res Bull*. 1991;27(3-4):379-82. doi:10.1016/0361-9230(91)90128-7

24. Bachmanov AA, Tordoff MG, Beauchamp GK. Sweetener preference of C57BL/6ByJ and 129P3/J mice. *Chem Senses*. Sep 2001;26(7):905-13. doi:10.1093/chemse/26.7.905

25. Zhang Y, Hoon MA, Chandrashekar J, et al. Coding of sweet, bitter, and umami tastes: different receptor cells sharing similar signaling pathways. *Cell*. 2003;112(3):293-301. doi:10.1016/s0092-8674(03)00071-0

26. Pérez CA, Huang L, Rong M, et al. A transient receptor potential channel expressed in taste receptor cells. *Nat Neurosci*. 2002;5(11):1169-76. doi:10.1038/nn952

27. de Araujo IE, Oliveira-Maia AJ, Sotnikova TD, et al. Food reward in the absence of taste receptor signaling. *Neuron*. Mar 27 2008;57(6):930-41. doi:10.1016/j.neuron.2008.01.032

28. Glendinning JI, Beltran F, Benton L, et al. Taste does not determine daily intake of dilute sugar solutions in mice. *Am J Physiol Regul Integr Comp Physiol*. 2010;299(5):1333-41. doi:10.1152/ajpregu.00331.2010

29. Fernandes AB, Alves da Silva J, Almeida J, et al. Postingestive Modulation of Food Seeking Depends on Vagus-Mediated Dopamine Neuron Activity. *Neuron*. Jun 3 2020;106(5):778-88. doi:10.1016/j.neuron.2020.03.009

30. Sclafani A. Conditioned food preferences. *Bulletin of the Psychonomic Society*. 1991/02/01 1991;29(2):256-260. doi:10.3758/BF03335250

31. Sclafani A, Ackroff K. Flavor preferences conditioned by intragastric glucose but not fructose or galactose in C57BL/6J mice. *Physiol Behav*. Jun 25 2012;106(4):457-61. doi:10.1016/j.physbeh.2012.03.008

32. Ackroff K, Sclafani A. Flavor preferences conditioned by oral monosodium glutamate in mice. *Chem Senses*. 2013;38(9):745-58. doi:10.1093/chemse/bjt049

33. Sclafani A, Ackroff K. Role of gut nutrient sensing in stimulating appetite and conditioning food preferences. *Am J Physiol Regul Integr Comp Physiol*. 2012;302(10):1119-33. doi:10.1152/ajpregu.00038.2012

34. Lucas F, Sclafani A. Differential reinforcing and satiating effects of intragastric fat and carbohydrate infusions in rats. *Physiol Behav*. May 1999;66(3):381-88. doi:10.1016/s0031-9384(98)00275-3

35. Oliveira-Maia AJ, Roberts CD, Walker QD, et al. Intravascular food reward. *PLoS One*. 2011;6(9)doi:10.1371/journal.pone.0024992

36. Miller I. The gut-brain axis: historical reflections. *Microb Ecol Health Dis*. 2018;29(1)doi:10.1080/16512235.2018.1542921

37. Cummings DE, Overduin J. Gastrointestinal regulation of food intake. *J Clin Invest*. 2007;117(1):13-23. doi:10.1172/jci30227

38. Travagli RA, Anselmi L. Vagal neurocircuitry and its influence on gastric motility. *Nature Reviews Gastroenterology & Hepatology*. 2016/07/01 2016;13(7):389-401. doi:10.1038/nrgastro.2016.76

39. Bai L, Mesgarzadeh S, Ramesh KS, et al. Genetic Identification of Vagal Sensory Neurons That Control Feeding. *Cell*. 2019;179(5):1129-43. doi:10.1016/j.cell.2019.10.031

40. Berthoud HR. Anatomy and function of sensory hepatic nerves. *Anat Rec A Discov Mol Cell Evol Biol*. Sep 2004;280(1):827-35. doi:10.1002/ar.a.20088

41. Berthoud HR, Blackshaw LA, Brookes SJ, Grundy D. Neuroanatomy of extrinsic afferents supplying the gastrointestinal tract. *Neurogastroenterol Motil*. Apr 2004;16 Suppl 1:28-33. doi:10.1111/j.1743-3150.2004.00471.x

42. Berthoud H-R, Neuhuber WL. Functional and chemical anatomy of the afferent vagal system. *Autonomic Neuroscience*. 2000/12/20 2000;85(1):1-17. doi:10.1016/S1566-0702(00)00215-0

43. Li M, Tan H-E, Lu Z, Tsang KS, Chung AJ, Zuker CS. Gut–brain circuits for fat preference. *Nature*. 2022/09/07 2022;doi:10.1038/s41586-022-05266-z

44. Tan HE, Sisti AC, Jin H, et al. The gut-brain axis mediates sugar preference. *Nature*. Apr 2020;580(7804):511-16. doi:10.1038/s41586-020-2199-7

45. Buchanan KL, Rupprecht LE, Kaelberer MM, et al. The preference for sugar over sweetener depends on a gut sensor cell. *Nat Neurosci*. Feb 2022;25(2):191-200. doi:10.1038/s41593-021-00982-7

46. Sclafani A, Lucas F. Abdominal vagotomy does not block carbohydrate-conditioned flavor preferences in rats. *Physiol Behav*. Aug 1996;60(2):447-53. doi:10.1016/s0031-9384(96)80018-7

47. Zafra MA, Molina F, Puerto A. Learned flavor preferences induced by intragastric administration of rewarding nutrients: role of capsaicin-sensitive vagal afferent fibers. *Am J Physiol Regul Integr Comp Physiol*. Aug 2007;293(2):635-41. doi:10.1152/ajpregu.00136.2007

48. Han W, Tellez LA, Perkins MH, et al. A Neural Circuit for Gut-Induced Reward. *Cell*. 2018;175(3):665-78. doi:10.1016/j.cell.2018.08.049

49. Ahima RS, Antwi DA. Brain regulation of appetite and satiety. *Endocrinol Metab Clin North Am*. 2008;37(4):811-23. doi:10.1016/j.ecl.2008.08.005

50. Chambers AP, Sandoval DA, Seeley RJ. Integration of satiety signals by the central nervous system. *Curr Biol*. 2013;23(9):379-88. doi:10.1016/j.cub.2013.03.020

51. McCutcheon JE. The role of dopamine in the pursuit of nutritional value. *Physiol Behav*. 2015;152:408-15. doi:10.1016/j.physbeh.2015.05.003

52. Schultz W. Behavioral dopamine signals. *Trends Neurosci*. 2007;30(5):203-10. doi:10.1016/j.tins.2007.03.007

53. Szczypka MS, Kwok K, Brot MD, et al. Dopamine production in the caudate putamen restores feeding in dopamine-deficient mice. *Neuron*. Jun 2001;30(3):819-28. doi:10.1016/s0896-6273(01)00319-1

54. Sotak BN, Hnasko TS, Robinson S, Kremer EJ, Palmiter RD. Dysregulation of dopamine signaling in the dorsal striatum inhibits feeding. *Brain Res*. Nov 9 2005;1061(2):88-96. doi:10.1016/j.brainres.2005.08.053

55. Baik JH. Dopamine signaling in reward-related behaviors. *Front Neural Circuits*. 2013;7doi:10.3389/fncir.2013.00152

56. McKinley MPOL, Valerie Dean. *Human Anatomy*. 2 ed. McGraw-Hill Higher Education; 2008:913.

57. Da Silva JA, Tecuapetla F, Paixão V, Costa RM. Dopamine neuron activity before action initiation gates and invigorates future movements. *Nature*. 2018;554(7691):244-48. doi:10.1038/nature25457

58. Voorn P, Vanderschuren LJMJ, Groenewegen HJ, Robbins TW, Pennartz CMA. Putting a spin on the dorsal–ventral divide of the striatum. *Trends in Neurosciences*. 2004/08/01 2004;27(8):468-74. doi:doi.org/10.1016/j.tins.2004.06.006

59. Damier P, Hirsch EC, Agid Y, Graybiel AM. The substantia nigra of the human brain. II. Patterns of loss of dopamine-containing neurons in Parkinson's disease. *Brain*. 1999;122 1437-48. doi:10.1093/brain/122.8.1437

60. Hernandez L, Hoebel BG. Food reward and cocaine increase extracellular dopamine in the nucleus accumbens as measured by microdialysis. *Life Sci*. 1988;42(18):1705-12. doi:10.1016/0024-3205(88)90036-7

61. Thanarajah SE, Backes H, DiFeliceantonio AG, et al. Food Intake Recruits Orosensory and Post-ingestive Dopaminergic Circuits to Affect Eating Desire in Humans. *Cell Metab*. 2019;29(3):695-706. doi:10.1016/j.cmet.2018.12.006

62. Dalenberg JR, Patel BP, Denis R, et al. Short-Term Consumption of Sucralose with, but Not without, Carbohydrate Impairs Neural and Metabolic Sensitivity to Sugar in Humans. *Cell Metab*. 2020;31(3):493-502. doi:10.1016/j.cmet.2020.01.014

63. Alhadeff AL. Monitoring In Vivo Neural Activity to Understand Gut-Brain Signaling. *Endocrinology*. 2021;162(5)doi:10.1210/endocr/bqab029

64. Chefer VI, Thompson AC, Zapata A, Shippenberg TS. Overview of brain microdialysis. *Curr Protoc Neurosci*. 2009;Chapter 7doi:10.1002/0471142301.ns0701s47

65. Fortin SM, Cone JJ, Ng-Evans S, McCutcheon JE, Roitman MF. Sampling phasic dopamine signaling with fast-scan cyclic voltammetry in awake, behaving rats. *Curr Protoc Neurosci*. 2015;70doi:10.1002/0471142301.ns0725s70

66. Chen TW, Wardill TJ, Sun Y, et al. Ultrasensitive fluorescent proteins for imaging neuronal activity. *Nature*. Jul 18 2013;499(7458):295-300. doi:10.1038/nature12354

67. Patriarchi T, Cho JR, Merten K, et al. Ultrafast neuronal imaging of dopamine dynamics with designed genetically encoded sensors. *Science*. 2018;360(6396)doi:10.1126/science.aat4422

68. Resendez SL, Jennings JH, Ung RL, et al. Visualization of cortical, subcortical and deep brain neural circuit dynamics during naturalistic mammalian behavior with head-mounted microscopes and chronically implanted lenses. *Nature Protocols*. 2016;11(3):566-97. doi:10.1038/nprot.2016.021

69. Kim H, Kim M, Im S-K, Fang S. Mouse Cre-LoxP system: general principles to determine tissue-specific roles of target genes. *Laboratory Animal Research*. 12 2018;34(4):147-59. doi:10.5625/lar.2018.34.4.147

70. Sauer B, Henderson N. Site-specific DNA recombination in mammalian cells by the Cre recombinase of bacteriophage P1. *Proc Natl Acad Sci U S A*. Jul 1988;85(14):5166-70. doi:10.1073/pnas.85.14.5166

2. Objectives

Food-seeking behaviour is shaped by pre and postingestive (PI) signals. Preingestive stimuli encompass information about orosensory properties of food, while PI feedback is related to the pathways that are activated after food consumption. PI signals transmit important information about food features, such as nutrient type and the caloric content of food to the central nervous system (CNS) through neuronal, hormonal, and humoral pathways. After food consumption, PI stimuli immediately convey information regarding satiety to the CNS homeostatic circuits, namely several nuclei within the hypothalamus. On the other hand, the PI stimuli also activate non-homeostatic circuits mostly related to the rewarding properties of food involving, therefore, dopaminergic neurons.

PI feedback has emerged as an important feature of feeding behaviour. It is consensual that a flavour associated to caloric PI stimuli is preferred to a flavour associated to non-caloric solutions. Moreover, PI conditioning can occur even in the absence of any explicit preingestive feedback, as observed in genetically modified sweet-blind mice. However, given the purely Pavlovian structure of the task they provide limited insight regarding food seeking behaviours. Experiments where the differential impact of pre-and PI factors on action values are assessed remains to be described.

Currently, it is also known that dopamine transients in the nucleus accumbens (NAc) increase in response to PI delivery of sucrose. Additionally, studies have shown that PI feedback from carbohydrates is sufficient to induce an increased in activity of ventral tegmental area (VTA) dopaminergic neurons, however, the nature of this response is totally unknown.

Therefore, the present work was divided into two main objectives. The first objective is to understand the nature of the dopaminergic signals, specifically in an attempt to further clarify whether neuronal dopaminergic activity is nutrient-specific. The second aim will focus on how sucrose PI feedback impacts operant food seeking behaviour by developing a novel two-action probabilistic instrumental task that can assess PI feedback on action value and reinforcement learning (RL).

To accomplish the first objective, mice will perform two assays. First, calcium imaging will be used to record neuronal dopaminergic activity, in the VTA and SNc, in sessions with IG delivery of different reinforcers. The reinforcers will be isocaloric solutions of sucrose and corn oil and a non-caloric artificial sweetener, sucralose, as a control. In a second group of animals, fibre photometry will be employed to monitor, simultaneously and in the same animals, dopamine dynamics in the NAc and DLS in sessions with IG delivery of the same reinforcers described. The hypothesis for this part of the work is that ventral regions - VTA and NAc - respond specifically to PI delivery of carbohydrates, whereas dorsal regions - SNc and DLS - respond to lipids, which was tested through infusion of sucrose and corn oil, respectively.

To accomplish the second objective, deprived mice will learn and perform a task where there is choice between two actions that, with a given probability, will lead to an oral and an intragastric (IG) reward. The oral reward will always be an artificial non-caloric sweetener – sucralose. However, while one action will lead to the IG infusion of sucrose, the other action will lead to an IG infusion of sucralose. The expected outcome is that mice will press more to obtain IG delivery of sucrose regardless of probability.

This project will allow to shed light on the postulated asymmetry of dopaminergic responses between the ventral and dorsal central regions according to the type of PI stimuli. Additionally, the development of the two-action task may infer important parameters in decision making and reinforcement learning based on PI stimuli.

3. Methodology

3.1. Experimental model

All animal procedures, including housing and breeding, were performed at the Champalimaud Research Centre. The institution is licensed for animal experimentation by the Portuguese Directorate-General for Animal Welfare (Direção Geral de Alimentação e Veterinária - DGAV). It also complies with the European guidelines (Directive 2010/63/UE), Federation of European Laboratory Animal Science Associations (FELASA) recommendations, and national laws (Decree-Law 113/2013) regarding scientific use, animal welfare and proper personnel training. All experimental procedures were conducted in accordance with DGAV approval, the rodent facility at Champalimaud Research Centre, and the Ethical Committee at NOVA Medical School (Lisbon, Portugal).

Mice were housed in ventilated racks at 19-22 °C with 30-70 % relative humidity in a light cycle of 12 h light/ 12 h dark Animals were individually housed, and their cages changed biweekly. All experimental procedures were performed during the light cycle. Mice had *ad libitum* access to food and water.

Experiments were conducted with DAT-IRES: Cre (dopamine transporter-internal ribosome entry site-linked Cre recombinase gene, B6.SJL-Slc6a3$^{tm1.1(Cre)Bkmn}$/J) and wild-type (WT) B6 (C57BL6/J) mice, both inbred at Champalimaud Research Centre.

3.2. Surgical procedures

All surgical procedures were performed under anaesthesia using a mix of 1.5-2 % oxygen and 4-5 % isoflurane for induction, followed by 1.5-2 % oxygen and 1-2 % isoflurane mix during surgery. The animals were placed on a thermostatically controlled heating pad (World Precision Instruments, #ATC1000) kept at 37 °C to maintain body temperature for the duration of the surgeries, and their eyes were covered with an ophthalmic gel to prevent drying.

After each surgery, the animals were placed in a clean home cage on a heating pad until they recovered fully. Postoperative analgesia was administered as needed - subcutaneous injection of buprenorphine 0.05 – 0.1 mg/Kg.

3.2.1. Gastric catheter implantation

The implantation of a gastric catheter was performed in order to later administer solutions directly into the stomach.

First, hair on the mid abdomen and dorsal neck was shaved, the animal was placed on a surgical table, a vertical midline incision was made on the abdomen, and a small incision was performed on the should blades. Next, a polyethene tube (Instech Solomon) was tunnelled subcutaneously from the abdomen to the dorsum of the animal and exteriorised through the shoulder blades. Afterwards, the stomach was exteriorised, and a purse string suture using non-absorbable sutures (Silkam, B. Braun) was made in the proximal part of the stomach, a small cut was performed in the stomach, into which the tube was inserted. The purse string was tightened around the catheter to keep it in place. To the externalised extremity of the catheter was connected to a vascular button (Instech Solomon), Finally, incisions were sutured using absorbable sutures (Novosyn, B. Braun) and disinfected.[1] Animals recovered for about a week or until their weight was similar to the value registered before surgery.

3.2.2. Viral injection, gradient refractive index *(GRIN)* lens implantation, and baseplate fixation

Stereotaxic central nervous system (CNS) surgeries were done on DAT-IRES: Cre mice to perform calcium imaging studies in dopaminergic regions. This strain enabled the use of the Cre – *loxP* system. The Cre-*loxP* system is a widely used powerful technology for gene editing. Cre recombinase is able to recognize two consecutive *loxP* sites and, consequently, enable the expression of a protein [2, 3]. Therefore, the Cre-*loxP* system is used to study the role of specific peptides and proteins in a given population of cells. In this study, DAT-IRES: Cre mice, a genetically modified strain that expresses Cre recombinase under the dopamine transporter (DAT), were used [4]. This strain enables the targeting of exclusively dopaminergic neuronal population when paired with neuronal infection. To selectively target dopaminergic neurons in DAT-IRES Cre mice, a recombinant adeno-associated virus (AAV) whose transgene expression is activated by Cre was injected enabling the expression of an encoded protein. In this case, the protein expressed a genetically encoded fluorescent calcium sensor – green calmodulin protein (GCaMP).

To express a fluorescent calcium sensor – GCaMP - and record calcium transients, CSN surgeries were performed. Surgeries included two steps, a viral injection and a gradient refractive index (*GRIN*) lens implantation [5] in two different regions of interest: the ventral tegmental area (VTA) and the substantia nigra pars compacta (SNc).

Male and female DAT-IRES: Cre mice were placed on the stereotaxic apparatus (KOPF Instruments, #962LS), the head was shaved, and a vertical skin incision was performed to expose the skull; connective and muscle tissues were precisely removed. Next, the exposed area was cleaned, allowing for visual identification of bregma and lambda. These reference points indicate where the sagittal and coronal converge – bregma - and where the sagittal and lambdoid sutures converge – lambda (**Figure 3.1**). The skull surfaced was then levelled at less than a 0.05 mm difference by comparing the dorsal-ventral (DV) and medial-lateral (ML) values of bregma and lambda.

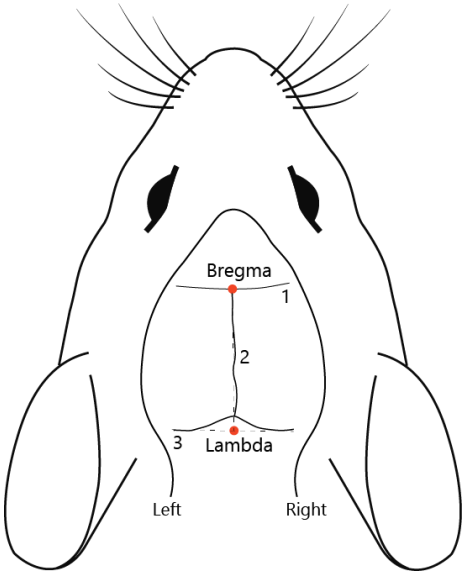

Figure 3.1 Representation of reference points used for skull alignment
Bregma indicates the point where the (1) coronal and (2) sagittal sutures converge. Lambda indicates the point where the (2) sagittal and (3) lambdoidal sutures converge. Mouse drawing obtained from Scidraw.io.

For mice to express a calcium sensor in dopaminergic neurons, a unilateral viral injection was performed using a glass pipette (inner diameter 0.53 mm ± 25 µm and outer diameter 1.14 mm, fire polished glass; World Precision Instruments, #504950). To target the VTA, 1 µL of the AAV GCaMP6f (AAV5-CAG-Flex-GCaMP6f-WPRE-SV40, UPENN)[6] was injected with nanojet II (Drummond Scientific) at anterior-posterior (AP): -2.80 mm, ML: ±0.40 mm from bregma, and DV: -4.50 from brain surface (**Figure 3.2 A**) at the rate of 4.6 nL/ 5 seconds (s). The injection lasted for approximately 18 min, and the glass pipette was retracted 20 min after the injection was completed.

To target the SNc 1 µL of the AAV GCaMP7f (pGP-AAV1-syn-FLEX-jGCaMP7f-WPRE, Addgene)[7] was injected at AP: -3.16 mm and ML: ±1.40 mm from bregma, and DV: -4.30 mm from brain surface [8] (**Figure 3.2 B**). The rate of injection was similar to the VTA injections. The coordinates of the of both regions were optimized.

The virus chosen to target both areas of interest was a recombinant AAV since it is non-pathogenic and elicits a moderate immune system response. These characteristics allowed for an efficient viral expression [9]. However, the virus used to target the VTA and SNc were slightly different (AAV5-CAG-Flex-GCaMP6f-WPRE-SV40 vs pGP-AAV1-syn-FLEX-jGCaMP7f-WPRE). Two minor differences are the types of AAV used, AAV serotype 5 and AAV serotype 1, and a slight variation in the calcium sensor, GCaMP6f and GCaMP7f. The latter has been developed more recently allowing a better pattern of expression under serotype 1 [6, 10]. The most significant difference is the type of promoter that drives protein expression, chicken beta-actin (CAG) vs synapsin (syn) promoter. The CAG promoter is a robust synthetic promoter that can drive adequate protein expression in the VTA but leads to very high protein expression levels in the SNc, that could impair fluorescence detection based on the levels of expression and high expression levels and is also associated with neuronal death. Therefore for the SNc experiments, the syn promoter was used since it enables optimal levels of expression, when compared to the CAG in this region [11].

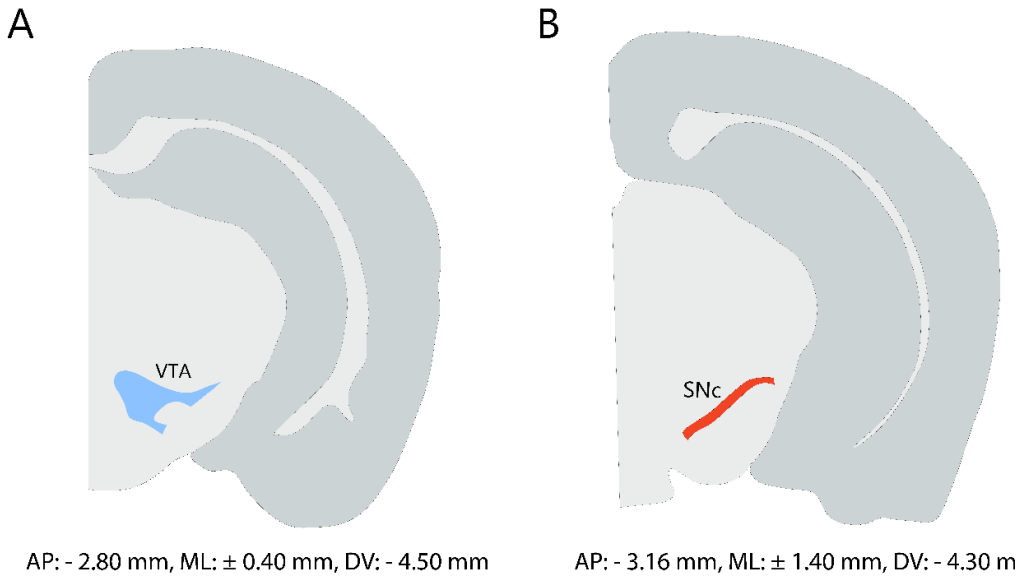

Figure 3.2 Representation of Ventral Tegmental Area (VTA) and Substantia Nigra pars compacta (SNc) structures in the mouse brain atlas.
Anatomical structures and their representations were obtained from the Allen Brain Reference Mouse Atlas using the Application Programming Interface (API). **A** Representation of the VTA structure (blue) for the virus injection and lens placement coordinates. The coordinates used were anterior-posterior (AP): -2.80 mm, medial-lateral (ML): ±0.40 mm from

bregma, and dorsal-ventral (DV): -4.50 from brain surface. **B** Representation of the SNc structure (red) for the final virus injection and lens placemen coordinates. The coordinates used were AP: -3.16 mm and ML: ±1.40 mm from bregma, and DV: -4.30 mm from brain surface.

Afterwards, a 30 G blunted needle (Thermo Scientific) was slowly lowered to 0.2 mm above the indicated DV coordinate and slowly upraised. This procedure was important to prepare for lens implantation, minimise tissue damage, and alleviate cranial pressure. A gradient refractive index (*GRIN*) lens (diameter: 0.5 mm, length: 8.4 mm, Inscopix) was lowered at increments of 0.1 mm every 5 s until it reached the indicated DV coordinate (VTA: -4.5 mm and SNc: -4.3 mm from brain surface). The *GRIN* lens was fixed with Super-Bond C&B (CTBA), a biocompatible superglue, and the head cap was built with black dental cement (Lang Dental), anchored to two screws (Antrin miniature Specialties, #00-90x) in the skull surface. Lastly, a layer of paper and adhesive tape was applied to the top of the head cap to prevent lens damage. **Supplementary Figure 7.1** and **Supplementary Figure 7.2** show representative images of brain slices of the *GRIN* lens track in the VTA and SNc, respectively.

Three to four weeks after *GRIN* lens implantation, mice were placed on the stereotaxic apparatus under anaesthesia to fixate the baseplate to the head cap. First, the lens was exposed, and a baseplate (Inscopix), previously attached to the miniature microscope (nVistaHD, Inscopix), was positioned above the lens [12]. The focal plane was adjusted for each mouse to observe neuronal structures, mainly cell bodies, and black dental cement was used to secure the baseplate to the head cap permanently. Lastly, the miniscope was detached, and a baseplate cover (Inscopix) was attached to the baseplate to protect the lens. [5] After baseplate fixation, the intragastric (IG) catheter was implanted (3.2.1) [13].

3.2.3. Viral injection and fibre implantation

Stereotaxic CNS surgeries were performed on male and female C57Bl6/J to perform fibre photometry studies of dopamine dynamics in the striatum. For this purpose, a genetically encoded fluorescent-based dopamine indicator – dLight1.2 - was injected. This highly sensitive dopamine indicator works by coupling the conformational changes that occur on dopamine receptor upon dopamine binding to changes in fluorescence intensity of a green fluorescent protein (GFP). As a result, when dopamine binds to a dLight1.2 receptor, fluorescence increases. Importantly, this dopamine indicator was engineered so that dopamine binding could occur regardless of type of dopamine receptor [14].

Considering that all experiments were performed *in vivo*, the dopamine sensor was delivered through an AAV that was injected into the central regions of interest [15]. The areas of interest were the nucleus accumbens (NAc) and dorsal-lateral striatum (DLS).

CNS surgeries included two steps, a viral injection and a dual optical fibre implantation [14]. These steps allowed for the recording of dopamine release on the NAc and DLS.

Mice were placed on the stereotaxic apparatus, the head was shaved, and a vertical skin incision was performed to expose the skull. Connective and muscle tissue were precisely removed, and the exposed area was clean, allowing for visual identification of bregma and lambda (**Figure 3.1**). The skull surfaced was levelled at less than 0.05 mm difference by comparing the DV and ML values of the reference points.

For mice to express dLight1.2, a bilateral viral infection in the NAc and DLS was performed using a glass pipette. To target the NAc, 500 nL of the AAV dLight1.2 (AAV5-hSyn-dLight1.2, Addgene)[14] was injected using nanojet II at AP: +1.30 mm and ML: ±1.25 mm from bregma, and DV: -3.93 from the brain surface. To

target the DLS, the same volume of the dLight1.2 virus was injected at AP: +0.50 mm and ML: ±2.60 mm from bregma and DV: -2.40 from the brain surface (**Figure 3.3**).[8] Each injection was performed at the rate of 4.6 nL/ 5 s (0.40 Hz). The injection lasted for approximately 9 min and the glass pipette was retracted 10 min after the injection was completed. Importantly, the number of animals injected and implanted on NAc left and DLS right was similar to the number of animals injected and implanted on NAc right and DLS left.

Afterwards, two optical fibres (diameter: 200 µm, length: 10 mm, Neurophotometrics Ltd.) were slowly lowered until they were 0.20 mm above each indicated DV coordinate for viral injections. [14, 16] The optical fibre was fixed with Super-Bond, and the head cap was built with black dental cement, anchored to one screw that was previously implanted in the skull surface. **Supplementary Figure 7.3** shows a representative images of brain slice with dLight1.2 expression in the NAc and DLS and optical fibre track in the DLS.

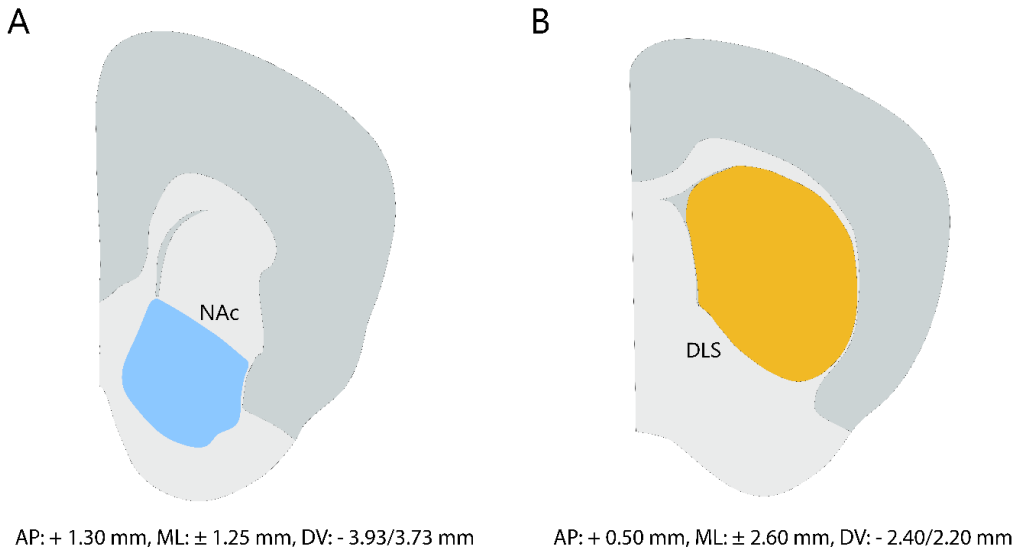

Figure 3.3 Representation of Nucleus Accumbens (NAc) and Dorsal-lateral Striatum (DLS) structures in the mouse brain atlas.
Anatomical structures and their representations were obtained from the Allen Brain Reference Mouse Atlas using the API. **A** Representation of the NAc structure (blue) for the virus injection and optical fibre coordinates. The coordinates were AP: +1.30 mm, ML: ±1.25 mm from bregma, and DV: -3.93/3.73 mm from brain surface. **B** Representation of the NAc structure (orange) for the virus injection and optical fibre coordinates. The coordinates were AP: +0.50 mm, ML: ±2.60 mm from bregma, and DV: -2.40/2.20 mm from brain surface.

Mice were allowed to recover for about three to four weeks before an IG catheter was implanted (3.2.1).

3.3. Calcium imaging assay

DAT-IRES: Cre mice were infected with a virus to express a calcium indicator, GCaMP, implanted with a *GRIN* lens in the VTA or SNc, and implanted with an IG catheter, as previously described above. Both surgeries allowed for the monitorisation and recording of calcium dynamics of dopaminergic neurons during IG infusions of different reinforcers.[5]

Mice had *ad libitum* access to food and water in their home cage.

Animals were infused with 2 isocaloric solutions, sucrose 20 % (w/v, 0.6 M) (Sigma Aldrich, #57-50-1), corn oil 9 % (w/v) (Sigma Aldrich, #8001-30-07), and a control non-caloric solution of sucralose 0.02 % (1,6 – dichloro - 1,6 – dideoxy – b – D - fructofuranosyl – 4 – chloro – 4 – deoxy – a - D-galactopyranoside; Sigma

Aldrich, #56038-13-2) (w/v, 0.5 mM).[17] In animals injected and implanted in the SNc, SMOF lipid 10 % (w/v) (Fresenius Kabi, 63323-820-00) was also administered. All the solutions were diluted in water. Corn oil 9% solution was prepared in two steps: (1) adding an emulsifier – Emplex® 0.2 % (Corbion, #124692) - to water and stirring the solution for a couple of hours and (2) adding the oil to the previously made solution and stirring it overnight.

Before each calcium imaging session, mice were anaesthetised with a mix of 1.5-2 % oxygen and 1-2 % isoflurane. The miniature microscope was connected to the baseplate and the button was connected to a pump (PHM-100A-EURO, Med-Associates Inc). A 20 min acclimatisation period occurred to fully recover from anaesthesia. At this point animals were placed in. sound-attenuating operant chambers (length: 21.6 cm, width: 17.8 cm, height 12.7 cm, Med-Associates Inc) equipped with a camera to track animal movement throughout the session.

Fluorescence images were acquired using nVistaHD acquisition software (Inscopix) at 10 Hz, with light-emitting diode (LED) power set at 30 % - 50 %, and gain level 4. Acquisition features, including the focus plane, were initially adjusted for each mouse and constant across sessions. Animals were allowed to freely move in the MedPC box throughout the session. Each session began with the illumination of the house light followed by a 5 min baseline period. After this period, one of the four possible reinforcers was infused directly into the stomach (Terumo syringe without needle 10 mL, Thermo Scientific), with a pump, at a rate of approximately 20 µL/ 3 s for 90 s, making up a total volume of 600 µL. The pump was coupled to a polyethene tube that passed through a metallic swivel (Instech Solomon) which connected to the vascular button in the mouse - an interface between the exterior and the IG. The time and rate of injection was programmed using the Med-PC IV software (Med-Associates Inc). The session ended 20 min after the start of the injection – total 25 min session. Calcium recordings, pump and session starting timestamps were recorded and synchronised using Bonsai, a modular open-source software[18].

Behaviour was recorded across the entire session using a top-mounted camera (Navitar, NMV-6WA 6 mm F/1.4, at a rate of 15 frames per second using the FlyCapture2, 2.12.3.31 software) for posterior movement analysis.

Once the imaging session was completed, mice were anaesthetised with isofluorane, the microscope and the exteriorized catheter was detached, and baseplate and catheter covers were placed.

The experimental procedure was repeated for several consecutive workdays with reinforcers delivered 4 times in a randomised order. Protocol lasted for twelve days.[13] Between sessions the box was cleaned and prepared for the next animal.

3.3.1. Calcium imaging data processing and analysis

Calcium imaging data acquired for both dopaminergic neuronal regions, VTA and SNc, was processed similarly. First, imaging data was processed in a custom-made MATLAB software (MATLAB R2021a) to detect and replace frames incorrectly captured during acquisition – corrupt frames. The code was based on frame-to-frame correlation, and it allowed to maintain the temporal integrity of the video by replacing corrupt frames with the previous correctly acquired frame. Afterwards, the video was pre-processed to remove artifacts and reduce size.

The Inscopix Data Processing software (Inscopix) was used to bin the video in the spatial domain and cropped it to remove margin values. Since animals were freely behaving, it was important to correct for movement artifacts. For that, a motion correction algorithm (Inscopix Data Processing, Inscopix) was

employed. The motion correction algorithm estimates a translation that allows to minimize the difference between the current frame and the reference frame [19]. In this case, motion correction was used to remove frame-to-frame motion in each video by using the first frame as the reference frame.

To extract calcium fluorescence responses associated with individual neurons, a constrained non-negative matrix factorisation (CNMF) was used [20, 21]. CNMF has been proposed as a framework that allows simultaneously denoise, deconvolve, and demix calcium imaging data. The framework also identifies neuronal cell locations and manages spatial overlap between the identified neurons.[22] CNMF-e is one of the extensions available for this framework specific for processing microendoscopic data. The CNMF-e algorithm automatically identifies the spatial location of the cells present in each video (regions of interest, ROIs) and allows for the association between cell and activity via fluorescence changes. This extension was used to process the calcium imaging data acquired. The analysis through this framework entails four steps: (1) initialise spatial and temporal components of the detected single neurons; (2) estimate the background based on the previously estimated neuronal spatiotemporal activity; (3) update the spatiotemporal components of the identified neuron while resolving the background fluctuation; (4) iteratively repeat steps (2) and (3) (MATLAB R2018a) [21, 23].

To track animal movement during each session DeepLabCut, a software used for posing estimation based on transfer learning with neural networks [24, 25], was used. The software allowed for an unbiased and efficient labelling of the previously acquired behaviour recordings for the body part of interest, which in this case was the catheter button and tail base. Labelling and subsequent network training was done for 80 frames extracted from different reinforcers session videos. Frame selection was randomized for animal and time point in the video, while ensuring the same number of frames was used for each reinforcer session. Afterwards, a custom-made Python code based on frame-by-frame pixel change was used. Briefly, frame-by-frame pixel change was used to calculate a metric of movement by using previously labelled reference point. The obtained signals were smoothed using a moving average filter. Finally, smooth signals were binned and aligned to the beginning of the session and start of IG reinforcer infusion.

3.3.1.1. Receiver operating characteristics (ROC) analysis

A receiver operating characteristics (ROC) analysis was applied to characterise dopaminergic neuronal responses in both areas of interest. This analysis was similar to one described previously [26] For each dopaminergic neuron identified, the ROC for each 10 s bin before and after baseline was produced. Importantly, as previously mentioned, the baseline was defined as the 5 min (300 s) before reinforcer delivery of each calcium imaging session. The ROC for baseline was calculated by comparing the histogram of the calcium fluorescence traces of each 10 s bin to the histogram during baseline, before and after IG injection. The area under the curve ROC (auROC) for each bin was calculated using trapezoidal numerical integration [26].

3.3.1.2. Dopaminergic neuron classification

Dopaminergic neurons were classified as positively or negatively modulated by reinforcer administrations.[27] Briefly, the mean activity of the 5 min (300 s) of baseline was chosen as a threshold and mean fluorescence changes, based on the GCaMP traces, were calculated for 10 s bins within the first 300 s after reinforcer delivery. Neurons with at least three consecutive bins (30 s) that were 2.56 standard deviations above the mean baseline activity threshold - 99% confidence interval - were classified as positively modulated by the reinforcer.

3.3.1.3.Cell pairing between different reinforcer sessions

Analysis of same ROIs between different sessions was performed based on nearest neighbour cell maps (MATLAB R2018a) [28]. Cell pairing between sessions was analysed for the last recording sessions, comparing the last session of a given reinforcer and the previous or following session of a second distinct reinforcer. Cell maps from the sessions to be matched were registered to the spatial map of the respective reference image, with registered coordinates calculated by applying the transformation to the original coordinates. Reference images were the first frame of each session to be matched and were extracted using Fiji (open-source software)[29]. To calculate nearest-neighbour distances between imaging sessions of the same animal, distances were measured in one of the sessions to the most proximate cell acquired from the session to match. Based on these metrics, pairs of neurons between 2 sessions with a distance greater than 15 pixels were considered distinct neurons.

3.4. Fibre photometry assay

Fibre photometry experiments consisted of using a dual optical fibre approach in combination with the expression of a dopamine indicator – dLight1.2 - that measures dopamine release.

Mice had *ad libitum* access to food and water in their home cage.

C57Bl6/J mice were infected with a virus to express dLight1.2 and implanted with two optical fibres in the ventral and dorsal striatum, NAc and DLS, respectively. Animals were also implanted with an IG catheter, which allowed for reinforcer infusion directly into the stomach. Mice were infused with 3 different isocaloric reinforcers and a control solution. Reinforcing solution included isocaloric solutions of sucrose 20 % (w/v), corn oil 9 % (w/v), and SMOF lipid 10 % (w/v), and a control non-caloric solution of sucralose 0.04 % (w/v).[17]

Dopamine dynamics were acquired using the FP3002 acquisition hardware (Neurophotometrics, CA) and Bonsai software (open-source). As previously stated, each animal was implanted with two optical fibres. For each fibre, two channels, 415 and 470 nm were simultaneously recorded at a frame rate of 50 Hz. The 415 nm or isosbestic channel was used to later correct for movement artifacts since animals were freely behaving. The 470 nm excitation channel was used since dLight1.2 couples conformational changes, upon dopamine binding, to a green fluorescent protein (GFP), which has peak excitation around 470 nm.

Before dopamine dynamics acquisition, the ROIs were defined for each channel. Additionally, the LED power for each channel was calibrated by modulating the amount of amperage supplied. The total LED power provided adjusted to ensure 50 mA at the tip of the fibre measured using a multimeter. The total LED power was adjusted to 8.33 and 6.16 %, to the 415 and 470 nm channels, respectively [14, 16]. Settings were maintained for all mice throughout all reinforcer sessions.

Each session began with the illumination of the house light within each box (Med Pc sound attenuating external box Med-Associates Inc and hardware platform HARP, Champalimaud Foundation) where mice were placed. After a 5 minute baseline recording, one of the four possible reinforcers was infused directly into the stomach (10 mL Terumo syringe without needle, Thermo Scientific), with a pump (HARP, Champalimaud Foundation), at a rate of approximately 20 µL/ 3 s for 90 s, making up a total volume of 600 µL. The pump was coupled to a polyethene tube that passed through a metallic swivel (Instech Solomon) connected to the catheter button. The metallic swivel rotated and, therefore, prevented tube twingle while the animal freely behaves. The session ended 20 min after the start of the IG injection – total of 25 min session [13].

Fibre photometry recordings and pump timestamps were recorded and synchronised using a clock synchronizer (Bonsai, open-source) with a sub-millisecond resolution.

Behaviour was recorded across the entire session using a top-mounted camera (Navitar, NMV-6WA 6 mm F/1.4, at a rate of 15 frames/ s using the FlyCapture2, 2.12.3.31 software).

The experimental procedure was repeated for several consecutive workdays, with reinforcers delivered in a randomised order. Protocol lasted for twelve days.[13]

3.4.1. Fibre photometry data processing analysis

Fibre photometry data acquired for the DLS and NAc was processed similarly. Data processing analysis was based on a standard strategy [30] and optimized for the current data set. Signals for both channels, 415 and 470 nm, were smoothed using a low pass filter fitted to a polynomial of 3 degrees. Next, signals were corrected for photobleaching. For this, smooth signals were fitted to a polynomial of 9 degrees function, and the resulting signals were subtracted from the raw signals - corrected signals (**Figure 3.4**).

Afterwards, it was necessary to correct for movement artifacts since animals were freely behaving during acquisition. This was accomplished by applying a linear regression to the isosbestic signal and normalizing it to the corrected 415 nm signal (**Figure 3.4**).

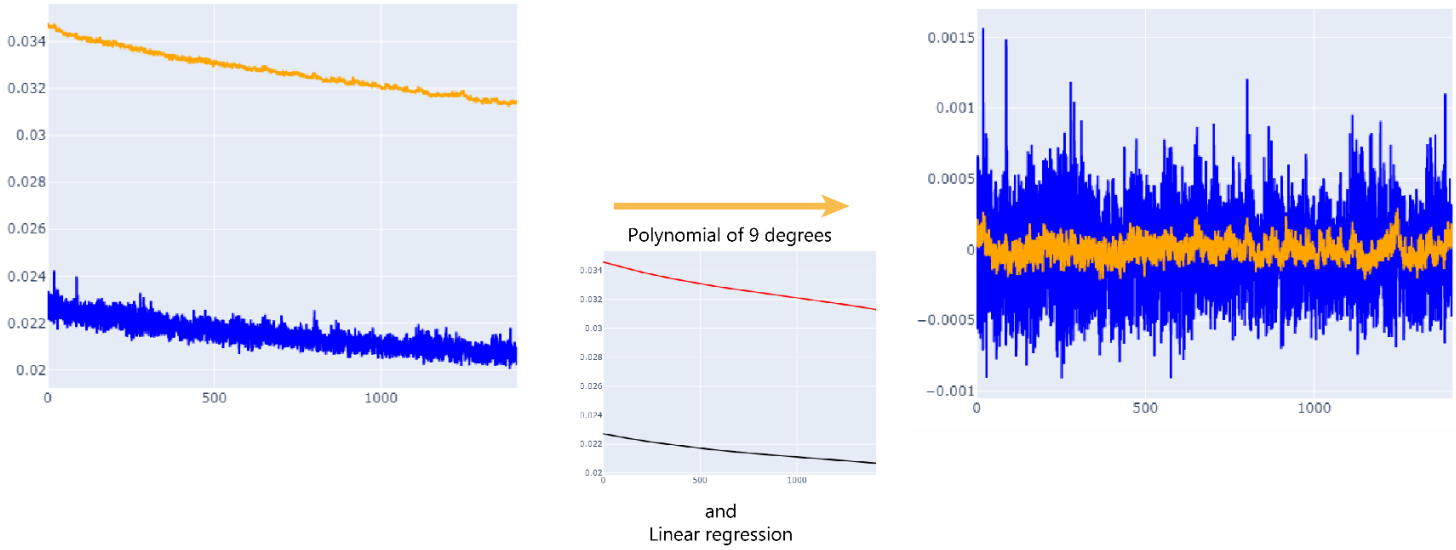

Figure 3.4 Schematic representation of the fibre photometry data processing pipeline.
Left panel represents the smooth signals for the 415 and 470 nm channels, represented in orange and blue, respectively. Smoothing was achieved by using a low pass filter and a polynomial of 3 degrees. Afterwards, smooth signals were fitted to a polynomial of 9 degrees and a linear regression was applied (middle panel), which was designated by corrected signals (right panel).

Afterwards, Δ470 nm (**Figure 3.5**) was calculated using the following equation:

$$\Delta 470 = \text{corrected } 470 - \text{corrected } 415 \,/\text{normalized } 415.$$

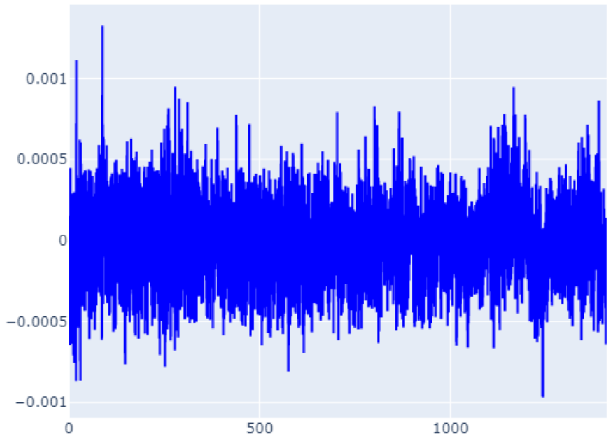

Figure 3.5 Example of Δ470 signal for the dorsal striatum.
Representative image of the Δ470 for the DLS signal in a mouse.

The Δ470 nm signal obtained was then z-scored, assuming a normal distribution: z-score = x-mean / standard deviation , in which x is any value within Δ470 nm. Lastly, z-scored signal was binned and aligned with the beginning the baseline period and beginning of injection.

To track animal movement during each session DeepLabCut, a software used for posing estimation based on transfer learning with neural networks [24, 25], was used as previously described.

3.5. Two levers probabilistic instrumental task

A novel probabilistic two-action task was developed with deprived C57Bl6/J mice that underwent surgery to implant a gastric catheter.

The only two reinforcers used in the instrumental task were sucrose 20 % (w/v, 0.6 M) and a control non-caloric solution of sucralose 0.04 % (w/v, 1 mM).[17]

For this assay, mice were under a water and food deprivation protocol that started two days before behavioural training. The deprivation protocol was used to initiate and maintain motivational states during behavioural training [13, 31]. Importantly, mice had a minimum daily water consumption [32, 33]. These parameters were adjusted to ensure hydration levels. For the food deprivation protocol, 1.8-2.5 g of standard food pellets were given daily. Notably, the weight of the pellet was adjusted daily and depended on the weight of the animal to ensure that mice maintained at 80 - 85 % of their initial body weight. Animals were weighted daily after finishing the behavioural task. Water and food provision was given at least 2 hours after finishing the behavioural task to ensure no association between the task and the food/water given.

Behaviour training occurred in sound attenuating operant boxes (Med-Associates Inc), allowing for exterior light and sound isolation. In addition, each behaviour box was equipped with a house light, a food magazine, and two retractable levers placed on each side of the magazine.

During each session Med-PC IV software (Med-Associates Inc) was used to record timestamps of lever presses, reinforcer delivery, licks, and head entries with 10 ms resolution. Head entries were recorded and measured via infrared detection. Licks were recorded and measured via a contact lickometer controller (Med-PC IV, Med-Associates Inc) that connects the magazine and the grid floor. Lever pressing was measured

based on 45 degrees change in the angle of the lever. Additionally, the number of lever presses, rewards and blocks were counted throughout each session.

Each session began with the illumination of the house light and the insertion of one or both levers. Sucralose 0.04 % solution was delivered in a metal cup for oral consumption in the food magazine using a syringe (10 mL Terumo syringe without needle, Thermo Scientific) connected to a pump (PHM-100A-EURO, Med-Associates Inc). Simultaneously, sucralose 0.04 % or sucrose 20 % solutions were delivered directly into the stomach through the IG catheters using a syringe connected to a pump. The pump was coupled to a polyethene tube that passed through a metallic swivel (Instech Solomon) attached to the catheter button. The volume of IG reward was always 10 µL, however, volume of oral reward changed depending on the training phase, starting with 40 during learning and decreased to 20 µL after lever pressing behaviour. Each session ended with the retraction of both levers and the offset of the house light[13, 34].

3.5.1. Training schedule

Mice were trained in a single daily session on consecutive days. Training started with a 30 min magazine training session, in which the oral reward – non-caloric sucralose 0.04 % – had a 50 % probability of being delivered every 60 s. Magazine training is essential since it led mice to understand that there is a place within the box where oral reinforcer was delivered to consume. To ensure lever pressing behaviour, mice were exposed to one lever at a time, with the starting side always randomised (**Figure 3.6**). At this stage, food and water deprived mice were on a continuous reinforcement (CRF) schedule in which animals obtained a reinforcer after each lever press (**Figure 3.6 A**). Training sessions ended after 60 min or when mice completed the number of presses necessary to reach the criteria. The CRF criteria – the number of lever presses per session - was gradually increased and contingent on completing previously set criteria. These criteria included:

(1) CRF5: press each lever 5 times, enabling a total of 10 oral rewards. Each lever press led to a 40 µL of oral sucralose 0.04 % reward delivered at the magazine.
(2) CRF10: press each lever 10 times, enabling a total of 20 oral rewards. Each lever press led to a 40 µL of oral sucralose 0.04 % reward delivered at the magazine.
(3) CRF25: press each lever 25 times, enabling a total of 50 oral rewards. Each lever press led to a 20 µL of oral sucralose 0.04 % reward delivered at the magazine. The volume was adjusted to ensure similar volumes within session.
(4) CRF25 cached and retractable: press each lever 25 times, enabling a total of 50 oral rewards. Each press was followed by lever retraction (0.1 s after lever press) and delivery of a 20 µL of oral sucralose 0.04 % at the magazine. Lever insertion occurred 1 s after a head entry into the magazine.

After mice had successfully reached the last criteria and acquired lever-pressing behaviour, water deprivation was slowly tapered. From this point on, both levers were simultaneously inserted at the beginning of the session, and animals were free to choose whichever to press. Additionally, each press was followed by lever retraction and lever insertion contingent on a head entry into the magazine.

At this stage, lever pressing led to an oral reward paired with an IG reward infused directly into the stomach. One lever had an 80 % probability of delivering reward - high probability lever -, while the other lever had a 20 % probability of delivering reward - low probability lever (**Figure 3.6 B**). After the animal had, on average, 25 rewards, the reward probability of each lever shifted, the high probability lever became a low probability lever and vice-versa. The switch of probability associated with each lever was designated as a transition. The attainment of, on average, 25 rewards and the consequent probability switch was designated

as a block. At first, and with the intent that mice would be able to track the change in probability, IG rewards were always sucralose 0.04 % independently of which lever was pressed. After approximately 7 sessions, one lever was associated with an IG reward of a non-caloric solution - sucralose 0.02 % - while the other was associated with a caloric carbohydrate solution - sucrose 20 % (**Figure 3.6 B**). The association between the lever side and IG reinforcer was counterbalanced between left and right lever but remained constant for each animal throughout training. Sessions ended after 60 min.

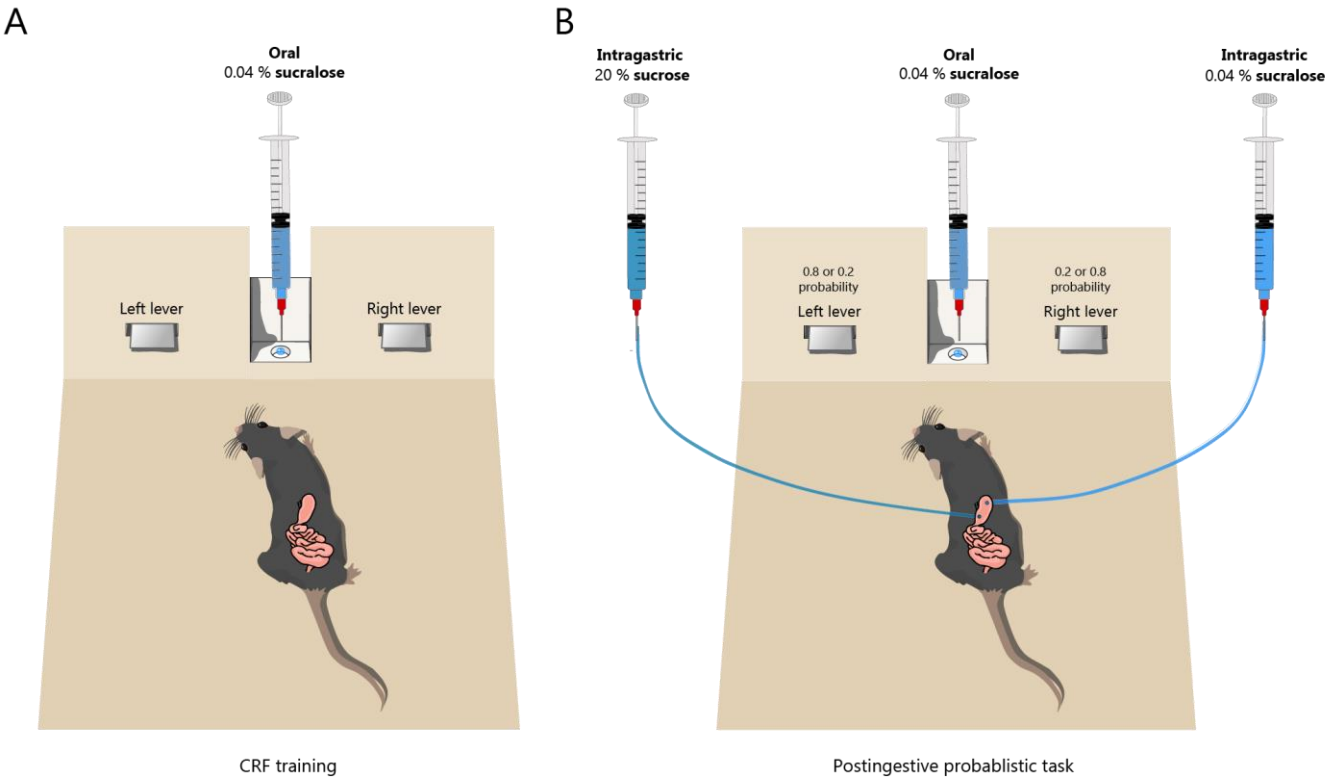

Figure 3.6 Two levers probabilistic instrumental task set-up schematics.
A Instrumental task set-up during the continuous reinforcement (CRF) schedule. In the CRF training phase, WT mice were trained to press a lever and obtain an oral reward, 0.04 % sucralose. **B** Instrumental task set-up during the postingestive probabilistic (PP) training schedule. For this portion of the two-action instrumental task, mice trained to press both levers could obtain an oral reward, sucralose 0.04 %, paired with an intragastric (IG) reward of 20 % sucrose or 0.02 % sucralose. The delivery of the reward was contingent on the lever that mice pressed, and the probability associated with that lever upon pressing. Mouse drawing was obtained from Scidraw.io.

3.5.2. Two levers probabilistic instrumental task data processing and analysis

Timestamps of lever presses, reinforcer delivery, licks and head entries were recorded during each session. The number of lever presses, rewards and blocks were counted throughout each session. This information allowed a detailed analysis of the behaviour for each animal across all sessions by using a custom-made Python program. Behaviour analysis included calculating the total number of lever presses, preference for each lever, and mean preference for each lever when the probability of obtaining a reward was high (80 %) or low (20 %). Values were analysed according to the IG reinforcer associated with each lever. The total number of levers represents the mean number of lever presses per mouse for a given session. Total lever preference was calculated by dividing the number of lever presses for a lever by the total number of lever presses for a given session. These values were calculated independently of the probability associated with each lever.

Next, the preference for each lever during a transition was determined by using a moving window of 5 lever presses, which was denominated as a trial. Mean preference was calculated using the preference for the last 5 trials when the lever had a high probability (80 %) and the last 5 trials had a low probability (20 %).

3.6. Histology and immunohistochemistry

Histological procedures were executed for mice injected with fluorescent sensors: GCaMP and dLight1.2 and implanted with a *GRIN* lens or optical fibres, respectively, to observe viral expression and lens/ fibre placement.

3.6.1. Mouse perfusion and brain slice preparation

After experiments were completed, animals were anesthetised with isoflurane followed by intraperitoneal injection (U-100 0.5 mL syringe with 29 G needle, Thermo Scientific) of ketamine-xylazine (mix of 100 mg/kg ketamine and 5 mg/kg xylazine). Once entirely insensitive to a toe pinch, mice were perfused with 1 X phosphate-buffered saline (PBS) and 4 % paraformaldehyde (PFA).

Briefly, an incision on the skin was made to expose the diaphragm, and a cut was made to expose the heart completely. A small calibre needle (26 G, Thermo Scientific), connected to a pumping system (Ismatec, Masterflex), was inserted in the left ventricle and the right atrium was cut. These steps allowed to pass both 1 X PBS and 4 % PFA through the systemic circulation at a flux of 10 mL/min. Afterwards, the brains were carefully dissected, placed in 4 % PFA overnight, and then transferred to 1 X PBS at 4 °C for further histological processing.

For histological analysis brains were placed in agarose 2.4 % (Thermo Scientific, #17852) and sectioned in coronal 50 µm slices using a vibratome (Leica VT1000 S, Leica Germany) at a speed of 0.225 mm/s and frequency of 45 Hz. Slices were collected into 24-well plates (Nunclon, Thermo Scientific) previously filled with PBS, stored at 4 °C and covered with aluminium foil until further use.

Brain slices from samples of all groups of animals were stained. Briefly, slices were washed 3 times with PBS for 5 min, then incubated at room temperature (RT) with a 1:1000 anti-GFP Polyclonal Alexa Fluor™ 488 antibody (Thermo Scientific, #A-21311) in 1:10 1 X PBS with Triton (PBST) 40 % in PBS overnight. Lastly, slices are washed 3 times in PBS for 5 min.

For imaging purposes, previously cut and stained brain slices were mounted on slides (Superfrost Plus, Thermo Scientific) with a mowiol mounting medium (refractive index 1.41 – 1.49). Glass coverslips (24 x 50 mm, Thermo Scientific) were then mounted onto the slides and sealed with clear nail polish and stored in an opaque box at 4 °C.

3.6.2. Microscopy image acquisition

Images of the mounted slices were acquired using the AxioScan.Z1 (Zeiss) microscope with the Plan - Apochromat 10 X/0.45 M27 (Zeiss). A green wavelength laser (channel Alexa Fluor (AF) 488, excitation filter 555 nm) was used with exposure time of 30 ms and a LED power of 20 %. Finally, the output images were transformed into 2D maximum intensity images using the ZEN 2.6 blue edition (Zeiss) software.

3.7. Statistical analysis

Statistical analysis was conducted using GraphPad Prism 8.0.1 (GraphPad Software Inc., CA). Data is presented as mean ± standard error of the mean (SEM) unless stated otherwise. Statistical significance was considered for $p < 0.05$. Normal distribution of the sample was assumed. One-way and two-way ANOVAs were used to investigate the main effects, post-hoc comparisons (Tukey test) were performed when appropriate. Mixed model was applied whenever there was corresponding missing data. Paired t-tests were used for planned comparisons. Statistical tests used for each panel are explained in detail in the corresponding figure legend. **Table 7.1** shows detailed description of the statistical analysis for all relevant figures.

3.8. Bibliography

1. Ueno A, Lazaro R, Wang P-Y, Higashiyama R, Machida K, Tsukamoto H. Mouse intragastric infusion (iG) model. *Nature Protocols*. 2012;7(4):771-81. doi:10.1038/nprot.2012.014

2. Kim H, Kim M, Im S-K, Fang S. Mouse Cre-LoxP system: general principles to determine tissue-specific roles of target genes. *Laboratory Animal Research*. 12 2018;34(4):147-59. doi:10.5625/lar.2018.34.4.147

3. Sauer B, Henderson N. Site-specific DNA recombination in mammalian cells by the Cre recombinase of bacteriophage P1. *Proc Natl Acad Sci U S A*. Jul 1988;85(14):5166-70. doi:10.1073/pnas.85.14.5166

4. Bäckman CM, Malik N, Zhang Y, et al. Characterization of a mouse strain expressing Cre recombinase from the 3' untranslated region of the dopamine transporter locus. *Genesis*. 2006;44(8):383-90. doi:10.1002/dvg.20228

5. Resendez SL, Jennings JH, Ung RL, et al. Visualization of cortical, subcortical and deep brain neural circuit dynamics during naturalistic mammalian behavior with head-mounted microscopes and chronically implanted lenses. *Nature Protocols*. 2016;11(3):566-97. doi:10.1038/nprot.2016.021

6. Chen TW, Wardill TJ, Sun Y, et al. Ultrasensitive fluorescent proteins for imaging neuronal activity. *Nature*. Jul 18 2013;499(7458):295-300. doi:10.1038/nature12354

7. Dana H, Sun Y, Mohar B, et al. High-performance calcium sensors for imaging activity in neuronal populations and microcompartments. *Nature Methods*. 2019/07/01 2019;16(7):649-657. doi:10.1038/s41592-019-0435-6

8. Paxinos GF, K. *Paxinos and Franklin's the Mouse Brain in Stereotaxic Coordinates*. 5th ed. 2019.

9. Sen D, Balakrishnan B, Gabriel N, et al. Improved adeno-associated virus (AAV) serotype 1 and 5 vectors for gene therapy. *Scientific Reports*. 2013/05/13 2013;3(1)doi:10.1038/srep01832

10. Dana H, Sun Y, Mohar B, et al. High-performance calcium sensors for imaging activity in neuronal populations and microcompartments. *Nat Methods*. Jul 2019;16(7):649-57. doi:10.1038/s41592-019-0435-6

11. Jackson KL, Dayton RD, Deverman BE, Klein RL. Better Targeting, Better Efficiency for Wide-Scale Neuronal Transduction with the Synapsin Promoter and AAV-PHP.B. *Front Mol Neurosci*. 2016;9doi:10.3389/fnmol.2016.00116

12. Ziv Y, Ghosh KK. Miniature microscopes for large-scale imaging of neuronal activity in freely behaving rodents. *Current Opinion in Neurobiology*. 2015/06/01 2015;32:141-47. doi:10.1016/j.conb.2015.04.001

13. Fernandes AB, Alves da Silva J, Almeida J, et al. Postingestive Modulation of Food Seeking Depends on Vagus-Mediated Dopamine Neuron Activity. *Neuron*. Jun 3 2020;106(5):778-88. doi:10.1016/j.neuron.2020.03.009

14. Patriarchi T, Cho JR, Merten K, et al. Ultrafast neuronal imaging of dopamine dynamics with designed genetically encoded sensors. *Science*. 2018;360(6396)doi:10.1126/science.aat4422

15. Bartel MA, Weinstein JR, Schaffer DV. Directed evolution of novel adeno-associated viruses for therapeutic gene delivery. *Gene Therapy*. 2012/06/01 2012;19(6):694-700. doi:10.1038/gt.2012.20

16. Martianova E, Aronson S, Proulx CD. Multi-Fiber Photometry to Record Neural Activity in Freely-Moving Animals. *JoVE*. 2019/10/20 2019;(152)doi:10.3791/60278

17. Beeler JA, McCutcheon JE, Cao ZFH, et al. Taste uncoupled from nutrition fails to sustain the reinforcing properties of food. *European Journal of Neuroscience*. 2012;36(4):2533-46. doi:10.1111/j.1460-9568.2012.08167.x

18. Lopes G, Bonacchi N, Frazão J, et al. Bonsai: an event-based framework for processing and controlling data streams. Technology Report. *Frontiers in Neuroinformatics*. 2015-April-08 2015;9doi:10.3389/fninf.2015.00007

19. Thévenaz P, Ruttimann UE, Unser M. A pyramid approach to subpixel registration based on intensity. *IEEE Trans Image Process*. 1998;7(1):27-41. doi:10.1109/83.650848

20. Maruyama R, Maeda K, Moroda H, et al. Detecting cells using non-negative matrix factorization on calcium imaging data. *Neural Networks*. 2014/07/01 2014;55:11-19. doi:10.1016/j.neunet.2014.03.007

21. Zhou P, Resendez SL, Rodriguez-Romaguera J, et al. Efficient and accurate extraction of in vivo calcium signals from microendoscopic video data. *eLife*. 2018;7doi:10.7554/elife.28728

22. Pnevmatikakis EA, Soudry D, Gao Y, et al. Simultaneous Denoising, Deconvolution, and Demixing of Calcium Imaging Data. *Neuron*. 2016;89(2):285-99. doi:10.1016/j.neuron.2015.11.037

23. Klaus A, Martins GJ, Paixao VB, Zhou P, Paninski L, Costa RM. The Spatiotemporal Organization of the Striatum Encodes Action Space. *Neuron*. 2017/08/30/ 2017;95(5):1171-80. doi:10.1016/j.neuron.2017.08.015

24. Mathis A, Mamidanna P, Cury KM, et al. DeepLabCut: markerless pose estimation of user-defined body parts with deep learning. *Nat Neurosci*. 2018;21(9):1281-89. doi:10.1038/s41593-018-0209-y

25. Mathis A, Schneider S, Lauer J, Mathis MW. A Primer on Motion Capture with Deep Learning: Principles, Pitfalls, and Perspectives. *Neuron*. 2020;108(1):44-65. doi:10.1016/j.neuron.2020.09.017

26. Cohen JY, Haesler S, Vong L, Lowell BB, Uchida N. Neuron-type-specific signals for reward and punishment in the ventral tegmental area. *Nature*. 2012;482(7383):85-88. doi:10.1038/nature10754

27. Da Silva JA, Tecuapetla F, Paixão V, Costa RM. Dopamine neuron activity before action initiation gates and invigorates future movements. *Nature*. 2018;554(7691):244-48. doi:10.1038/nature25457

28. Jennings JH, Ung RL, Resendez SL, et al. Visualizing Hypothalamic Network Dynamics for Appetitive and Consummatory Behaviors. *Cell*. 2015/01/29/ 2015;160(3):516-27. doi:10.1016/j.cell.2014.12.026

29. Schindelin J, Arganda-Carreras I, Frise E, et al. Fiji: an open-source platform for biological-image analysis. *Nature Methods*. 2012/07/01 2012;9(7):676-82. doi:10.1038/nmeth.2019

30. *FP3002 Manual*. 2021.

31. Tabbara RI, Maddux JM, Beharry PF, Iannuzzi J, Chaudhri N. Effects of sucrose concentration and water deprivation on Pavlovian conditioning and responding for conditioned reinforcement. *Behav Neurosci*. Apr 2016;130(2):231-42. doi:10.1037/bne0000138

32. Toth LA, Gardiner TW. Food and water restriction protocols: physiological and behavioral considerations. *Contemp Top Lab Anim Sci*. Nov 2000;39(6):9-17.

33. Tucci V, Hardy A, Nolan PM. A comparison of physiological and behavioural parameters in C57BL/6J mice undergoing food or water restriction regimes. *Behav Brain Res*. Oct 2 2006;173(1):22-29. doi:10.1016/j.bbr.2006.05.031

34. Dias-Ferreira E, Sousa JC, Melo I, et al. Chronic Stress Causes Frontostriatal Reorganization and Affects Decision-Making. *Science*. 2009;325(5940):621-25. doi:10.1126/science.1171203

4. Results

4.1. Monitoring neuronal activity during intragastric infusions of different nutrients

Previous work demonstrated that postingestive (PI) carbohydrate sensing, more specifically glucose injected into stomach, upper part of the duodenum or the hepatic portal vein, significantly increased dopamine levels in the ventral striatum, more specifically in the nucleus accumbens (NAc) [1, 2]. Moreover, recent findings showed that ventral tegmental area (VTA) dopaminergic neurons respond significantly more to intragastric (IG) infusions of a caloric carbohydrate solution, sucrose, when compared to IG infusions of a non-caloric solution, sucralose [3]. Moreover, stimulation of gut afferent neurons activates substantia nigra pas compacta (SNc) and dopamine release in the dorsal striatum, an observation also seen with intralipid infusions in the gut [4].

Thus, the working hypothesis for this work was based on a possible asymmetry of responses based on nutrient detection [3-6]. It was hypothesized that the VTA dopaminergic neurons would respond to IG infusions of carbohydrates (sucrose) and convey this information to NAc. In contrast, SNc neurons would respond to IG infusions of lipids (corn oil) and communicate with the dorsal-lateral striatum (DLS).

To test the hypothesis, two types of assays were performed. First, VTA and SNc neuronal dopaminergic activity were recorded during IG infusions of isocaloric different macronutrients – carbohydrate, lipid, and a control. In the second assay, dopamine dynamics in the NAc and DLS, within the same animal, were recorded during IG infusions of the same macronutrients.

4.1.1. Dopaminergic neurons of the VTA respond differently to different macronutrients

As previously described, DAT-IRES mice were injected with a Cre-dependent fluorescent calcium sensor and implanted with a *GRIN* lens in the VTA. Afterwards, a gastric catheter was implanted. The surgeries allowed for the monitorisation and recording of dopaminergic neuronal activity in the VTA during IG infusion of different reinforcers.

The reinforcers chosen - sucrose 20 % and corn oil 9 % - were isocaloric solutions of different macronutrients that were able to sustain lever pressing behaviour when given orally (**Supplementary Figure 7.4**). Additionally, a sweet non-caloric solution – sucralose 0.02 % - was chosen as a control. It is also important to note that the lipidic solution (corn oil) was dissolved in water with an emulsifier. In control experiments the activity of VTA dopaminergic neurons in response to sucrose and sucralose was tested with and without the emulsifier (**Figure 4.9**).

Figure 4.1 A summarizes the deep-brain calcium imaging study. Calcium recordings were acquired in 15 DAT-IRES: Cre mice for 25 min sessions using a miniature microscope (miniscope, Inscopix). During the session animals were freely behaving. For each session, one of 3 reinforcers was delivered directly into the stomach through a previously implanted IG catheter. Reinforcer delivery occurred after a 5 min baseline period at a rate of 20 µL/ 3 s. The 3 reinforcers administered were a carbohydrate - sucrose 20 %-, a lipid - corn oil 9% -, and a non-caloric artificial sweetener - sucralose 0.02 %.

Figure 4.1 B exemplifies VTA dopaminergic neurons calcium transients during a session where sucrose 20 % was administered (left top panel) directly into the stomach. The corresponding areas of interest for each neuron detected (10 neurons) and a time course (10 min) of the calcium fluorescence traces of the 4 highlighted neurons (yellow, green, light blue and dark blue) are represented in the left bottom panel and

right panel, respectively (**Figure 4.1 B**). Importantly, in this and the following figures, the light orange bar represents IG reinforcer delivery (90 s).

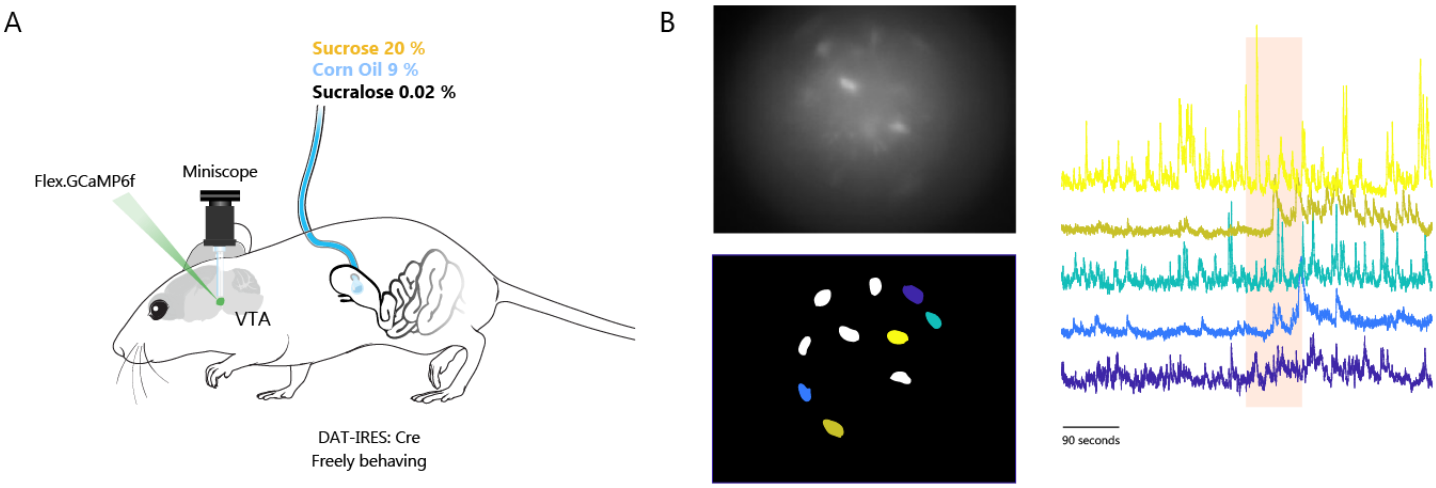

Figure 4.1 Monitoring ventral tegmental area (VTA) dopaminergic neuronal activity during intragastric (IG) delivery of reinforcers in freely behaving mice.
A A group of 15 freely behaving DAT-IRES: Cre mice were injected with a calcium sensor, AAV.CAG.Flex.GCaMp6f, and implanted with a gradient refractive index (*GRIN)* lens in the VTA for deep-brain calcium imaging. Calcium recordings were acquired using a miniature microscope (miniscope) during IG delivery of 3 different reinforcers directly into the stomach, through a previously implanted IG catheter. The 3 reinforcers were 2 isocaloric solutions of a carbohydrate - sucrose 20 %-, and a lipid - corn oil 9% -, as well as a non-caloric sweetener solution - sucralose 0.02 %. Only one reinforcer was delivered per session. Mouse drawing was obtained from Scidraw.io. **B** Example of VTA dopaminergic neurons during a session where sucrose 20 % was administered (top left panel) and the corresponding areas of interest (bottom left panel). A time course (10 min) of the calcium fluorescence traces of the highlighted neurons, according to colour (dark blue, blue, green, mustard yellow, and yellow), are shown in the right panel. For this and following figures, the light orange bar represents reinforcer delivery (90 s).

The activity of, on average, 9 (± 1) neurons per animal was recorded (**Figure 4.2 A**). No significant difference was found in the number of neurons recorded per animal between different reinforcer sessions (**Figure 4.2 B**, one-way repeated measures ANOVA ns $p = 0.5$).

Figure 4.3 shows the mean activity, in area under the receiver operating characteristics (auROC), for all the VTA dopaminergic neurons detected per reinforcer during 15 min. The first 5 min (- 300 to 0 s) represent the baseline – period before reinforcer delivery - and the highlighted orange bar (0 to 90 s) represents reinforcer delivery. Results were calculated using a ROC analysis for each VTA dopaminergic neuron identified and then averaged per mouse. Values higher or lower than 0.5 indicated that activity is higher or lower when compared to 5 min baseline activity, respectively.

The total number of neurons detected for the 15 animals with all sessions was 214 neurons for sucrose 20 % sessions, 240 neurons for corn oil 9 % sessions, and 261 neurons for sucralose 0.02 % sessions.

Mean VTA dopaminergic neuronal traces, are significantly different between different reinforcer sessions (**Figure 4.3**, two-way repeated measures ANOVA main effect for reinforcer $^{*}p = 0.01$). Post-hoc analysis indicate that mean activity for neurons in a sucrose session (**Figure 4.3** in yellow) is significantly higher when compared with both corn oil (**Figure 4.3** in blue, Tukey test IG sucrose vs IG corn oil $^{\#\#\#\#}p < 0.0001$) and sucralose (**Figure 4.3** in black, Tukey test IG sucralose vs IG sucrose $^{\#\#\#\#}p < 0.0001$) sessions.

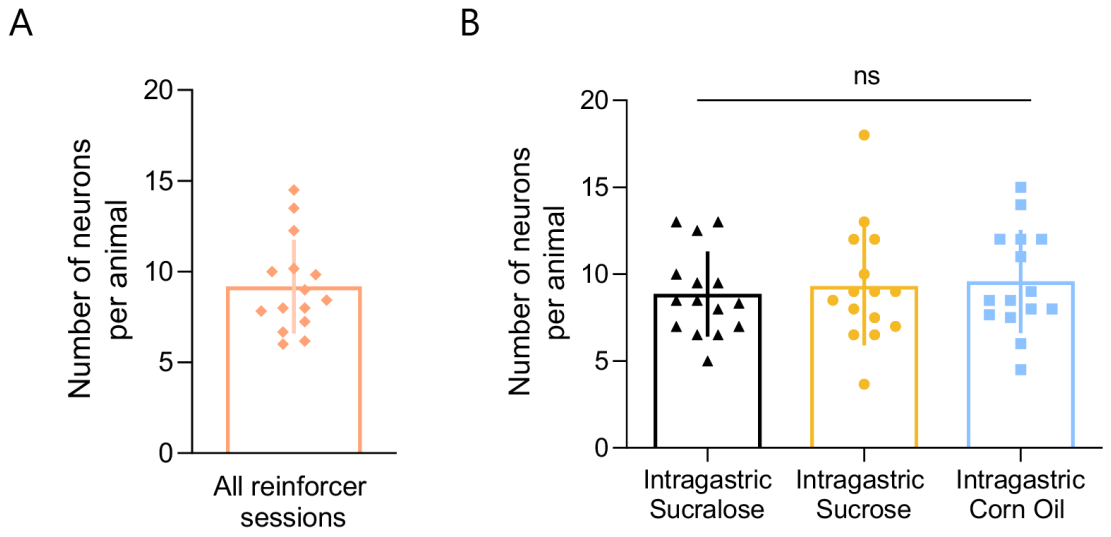

Figure 4.2 Number of neurons recorded in the VTA was constant between different reinforcer sessions.
A Number of neurons recorded per animal in the VTA for all sessions. **B** Number of neurons recorded per animal in the VTA in different reinforcer sessions. The black bar (black filled triangles) represents sessions where intragastric (IG) sucralose 0.02 % was delivered, the yellow bar (yellow filled circles) represents sessions where IG sucrose 20 % was administered, and the blue bar (blue filled squares) represents sessions where IG corn oil 9 % was administered. One-way repeated measures ANOVA $F_{14,28}$= 6.9, ns p = 0.5. Data is represented as mean ± standard error of the mean (SEM).

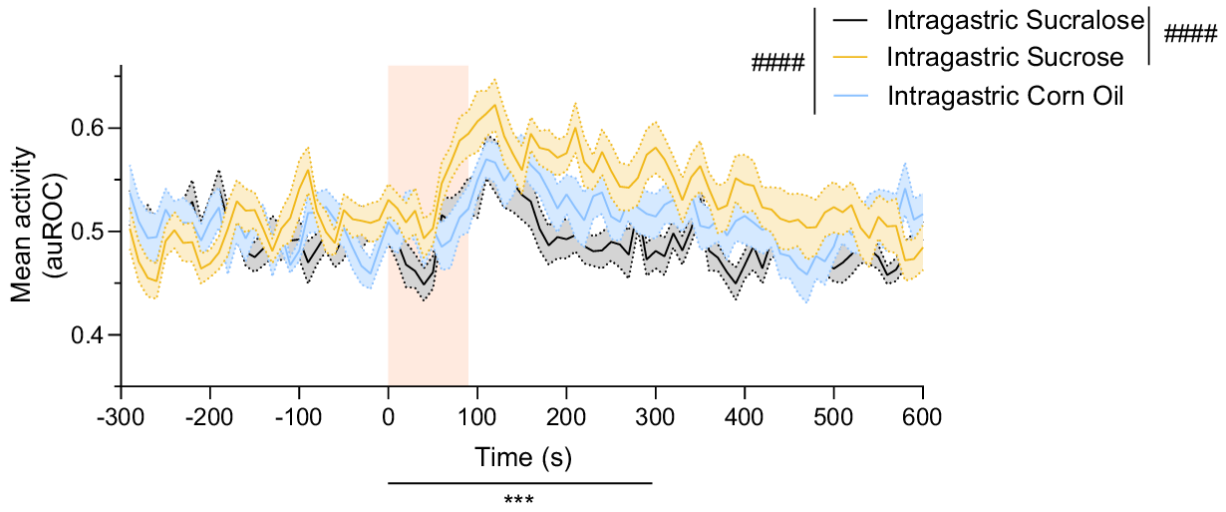

Figure 4.3 Mean area under the curve receiver operating (auROC) VTA dopaminergic neuronal traces are distinct between different reinforcer sessions.
Mean activity, in auROC, of all the neuronal activity recorded for all the VTA dopaminergic neurons detected per reinforcer session per animal. IG sucralose 0.04 % sessions are presented in black (261 neurons), IG sucrose 20 % sessions are represented in yellow (214 neurons), and IG corn oil 9 % sessions are represented in blue (240 neurons). Two-way repeated measures ANOVA main effect for time $F_{8,117}$= 4.3. ***p = 0.0001; main effect for reinforcer $F_{2,27}$= 5.0, *p = 0.01. Post-hoc (Tukey test) analysis IG sucrose vs IG corn oil $^{\#\#\#\#}$p < 0.0001; IG sucralose vs IG sucrose $^{\#\#\#\#}$p < 0.0001; IG sucralose vs IG corn oil $^{\#\#\#\#}$p < 0.0001, blue line). Data is presented as mean ± SEM. Shading indicates SEM.

To further explore the difference observed in the mean activity of VTA dopaminergic neurons between different reinforcer sessions, the percentage of positively modulated neurons per reinforcer session was calculated. Neurons were classified as positively modulated if their activity was 2.56 standard deviations (SD)

above the mean baseline activity threshold (99 % confidence interval) for at least 30 s. The classification was made concerning the first 300 s after reinforcer delivery and compared to the 5 min baseline period.

Figure 4.4 A represents the percentage of positively modulated VTA dopaminergic neurons, per reinforcer session. The results show that the percentage of positively modulated neurons is significantly higher in sucrose (yellow bar) sessions when compared with sucralose (black bar) and corn oil (blue bar) sessions (**Figure 4.4 A**, mixed-effects analysis ** p = 0.002; Tukey test IG sucrose vs IG sucralose $^{\#\#}$p= 0.006 and IG sucrose vs IG corn oil $^{\#}$p = 0.03). Interestingly, the percentage of VTA neurons positively modulated by sucralose and corn oil is similar (**Figure 4.4 A** Tukey test IG sucralose vs IG corn oil ns p = 0.6).

Additionally, the curves that represent the mean activity of the positively modulated VTA neurons (total of 155 neurons) per reinforcer are also significantly different (**Figure 4.4 B**, mixed-effects main effect for reinforcer * p = 0.04). Interestingly, although the percentage of positively modulated neurons for IG sucrose is significantly higher when compared to IG corn oil sessions, their activity pattern is similar and superimposable (**Figure 4.4 B** yellow and blue traces, respectively). Additionally, IG sucrose and corn oil traces are significantly higher and more sustained in time than sucralose neuronal traces (**Figure 4.4 B** black traces).

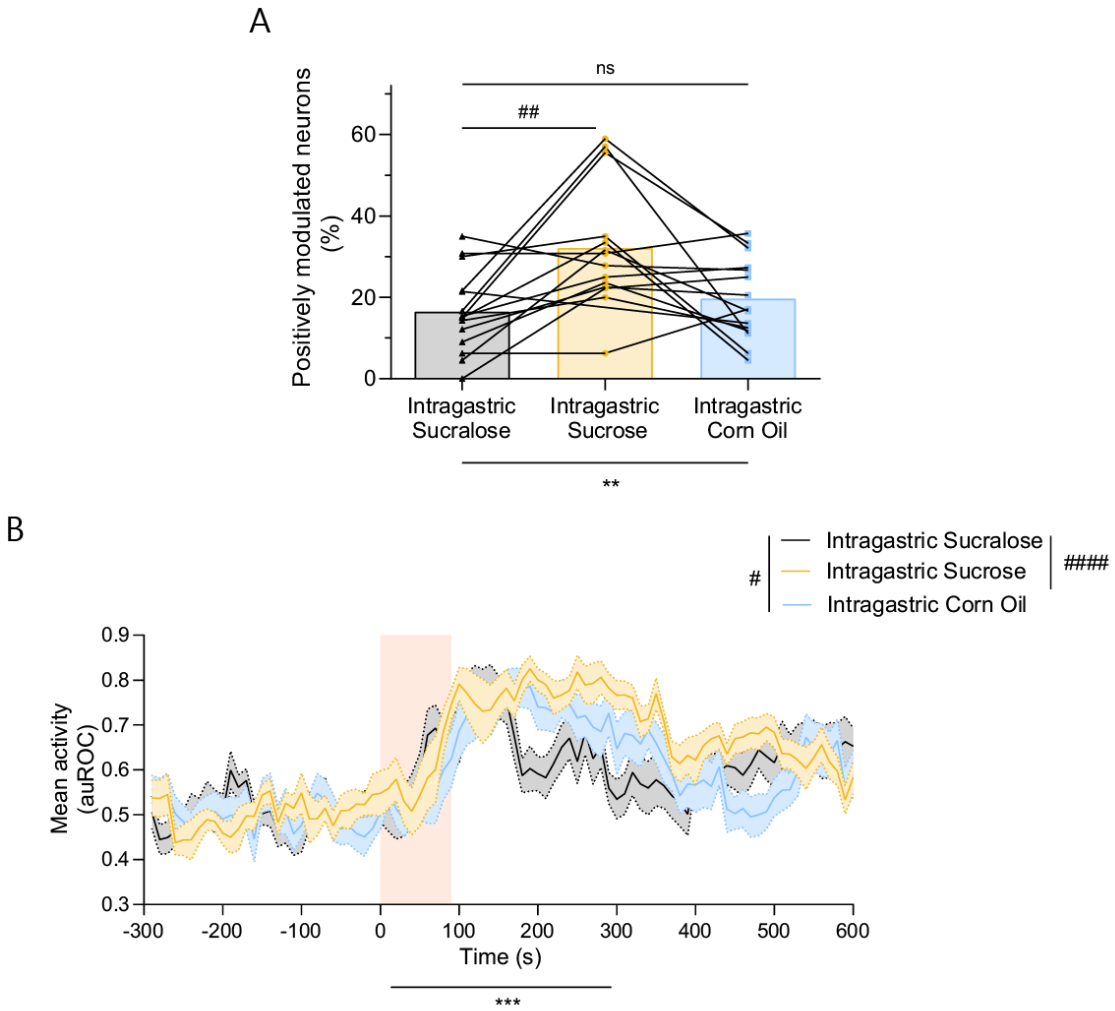

Figure 4.4 Percentage of positively modulated VTA dopaminergic neurons is significantly higher for intragastric sucrose when compared with an isocaloric lipid, corn oil, and a non-caloric control, sucralose.

A Positively modulated VTA neurons, in percentage, per mouse for the first 300 s after infusion of the IG reinforcers. The black bar (black filled triangles) represents the sessions where IG sucralose 0.02 % was delivered, the yellow bar (yellow filled circles)

represents the sessions where IG sucrose 20 % was administered, and the blue bar (blue filled squares) represents where IG corn oil 9 % was administered (n = 15). Mixed-effects analysis $F_{2,25}$= 8.8, ** p = 0.002. Post-hoc (Tukey test) IG sucrose vs IG corn oil $^{\#}$p = 0.03, IG sucralose vs IG sucrose $^{\#\#}$p= 0.006, and IG sucralose vs IG corn oil ns p = 0.6. Data is represented as mean. **B** Mean activity, in auROC, of the VTA neurons that were positively modulated by the different reinforcers. The number of positively modulated neurons was calculated for the for the first 300 s after IG infusion of each reinforcer. IG sucralose sessions are presented in black (53 neurons), IG sucrose sessions are represented in yellow (55 neurons), and IG corn oil sessions are represented in blue (47 neurons). The light orange bar represents reinforcer delivery (90 s). Mixed-effects, main effect for time $F_{7,98}$=11.4, **** p < 0.0001; main effect for reinforcer $F_{2,26}$= 4.1, * p = 0.04. Post-hoc (Tukey test) analysis IG sucrose vs IG corn oil $^{\#\#\#}$p = 0.004; IG sucralose vs IG corn oil $^{\#}$p= 0.01; IG sucralose vs IG sucrose $^{\#\#\#\#}$p < 0.0001. Data is presented as mean ± SEM. Shading indicates SEM.

Values for positively modulated VTA dopaminergic neurons were also calculated for the first 600 s after injection (**Figure 4.5**). As observed, the percentage of positively modulated neurons is very similar to the one obtained when the analysis was performed based on the first 300 s (**Figure 4.5 A**). Furthermore, profile for VTA positively modulated neuronal traces analysis for the first 600 and 300 s after injection are superimposable. These results indicate that the period of time for the analysis of positively modulated neurons does not interfere with the results output.

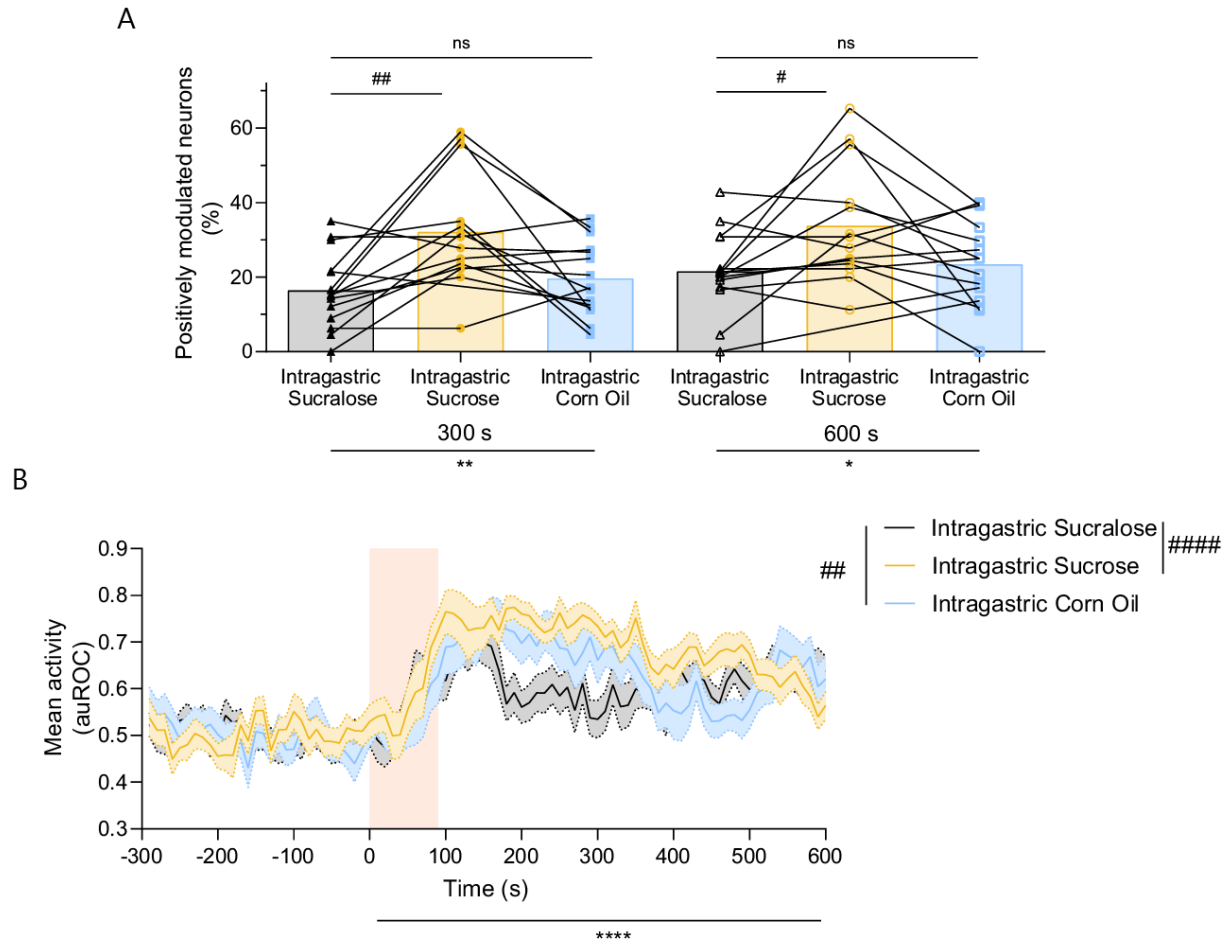

Figure 4.5 Positively modulated VTA dopaminergic neurons during intragastric delivery of reinforcers for the first 300 s vs 600 s after infusion

A Positively modulated VTA neurons, in percentage, per mouse for the first 300 s (left) and 600 s (right) after infusion. The black bar (black filled triangles) represents the sessions where IG sucralose 0.02 % was delivered, the yellow bar (yellow filled circles) represents the sessions where IG sucrose 20 % was administered, and the blue bar (blue filled squares) represents where IG corn oil 9 % was administered (n = 15). Mixed effects analysis $F_{3,34}$= 6.6, **p = 0.002. For 300 s: mixed-effects analysis

$F_{2,25}$= 8.8, ** p = 0.002. Post-hoc (Tukey test) IG sucrose vs IG corn oil $^{\#}$p = 0.03, IG sucralose vs IG sucrose $^{\#\#}$p= 0.006, and IG sucralose vs IG corn oil ns p = 0.6. For 600 s: mixed-effects analysis $F_{2,24}$= 5.0, ** p = 0.06. Post-hoc (Tukey test) IG sucralose vs IG sucrose $^{\#}$p = 0.03, IG sucrose vs IG corn oil ns p = 0.07, and IG sucralose vs IG corn oil ns p =0.8. Data is represented as mean. **B** Mean activity, in auROC, of the VTA neurons that were positively modulated by the different reinforcers. was calculated for the for the first 600 s after infusion. IG sucralose sessions are presented in black (72 neurons), IG sucrose sessions are represented in yellow (64 neurons), and IG corn oil sessions are represented in blue (58 neurons). The light orange bar represents reinforcer delivery (90 s). Mixed-effects main effect for time $F_{89,1260}$= 10.4, ****p < 0.0001; main effect for reinforcer $F2_{,2323}$= 37.9, ****p < 0.0001. Post-hoc (Tukey test) IG sucrose vs IG corn oil $^{\#\#\#\#}$p < 0.0001; IG sucralose vs IG corn oil $^{\#\#}$p= 0.006; IG sucralose vs IG sucrose $^{\#\#\#\#}$p < 0.0001. Data is presented as mean ± SEM. Shading indicates SEM.

Subsequently, it became relevant to further explore the VTA subpopulation of dopaminergic neurons based on the reinforcer administered. Our hypothesis was that a subpopulation of VTA neurons would respond specifically to PI sucrose stimuli and smaller subpopulation would respond specifically to IG corn oil. It was also relevant to understand whether a subpopulation of those neurons responded to caloric content or were nutrient-specific. Therefore, an analysis of matched cells between different sessions was performed.

Cell pairing between different reinforcer sessions was done based on nearest neighbour cell maps. Analysis was performed by comparing a session where IG sucrose was administered to the following session where IG corn oil was the reinforcer (**Figure 4.6**, 12 animals and 64 matched neurons).

Figure 4.6 A shows the heat maps for 64 neurons in an IG sucrose session and the corresponding neurons in the following IG corn oil session. Results are represented for 800 s and the orange bar represents IG infusion (90 s) of the reinforcer. A colour code was used to indicate dopaminergic neuronal activity where warmer colours (yellow) indicates higher neuronal activity and cooler colours (blue) indicates lower neuronal activity.

From the analysis of the matched neurons, 13 (20%) responded to both reinforcers, 10 (15.6%) specifically responded to sucrose, and 4 (6.3%) specifically responded to corn oil (**Figure 4.6 B** fraction represented in green, yellow, and blue, respectively). There are also a considerable number of neurons, 37 (57.8%), that were not positively modulated by PI stimuli (**Figure 4.6 B** fraction represented in grey).

Afterwards, the mean activity of the different subpopulation of neurons that specifically respond to sucrose was plotted and compared to the specific subpopulation of neurons that specifically respond to corn oil. The profile of the traces indicates that sucrose specific neurons might have higher and more sustained activity in time when compared with corn oil specific neurons, although with no statistical difference (**Figure 4.7 A**, mixed effects analysis main reinforcer ns p = 0.7). It is important to note, however, that the profiles for neurons that are corn oil specific (4 neurons) were very heterogeneous.

As expected, **Figure 4.7 B** indicates that the neuronal traces for the 13 neurons that are positively modulated by both reinforcers are very similar, indicating that a considerable percentage of neurons are probably respond to the caloric content of food. However, this analysis needs to be confirmed with IG sucralose sessions (**Figure 4.7 B**, two-way repeated measures ANOVA main effect reinforcer ns p = 0.2).

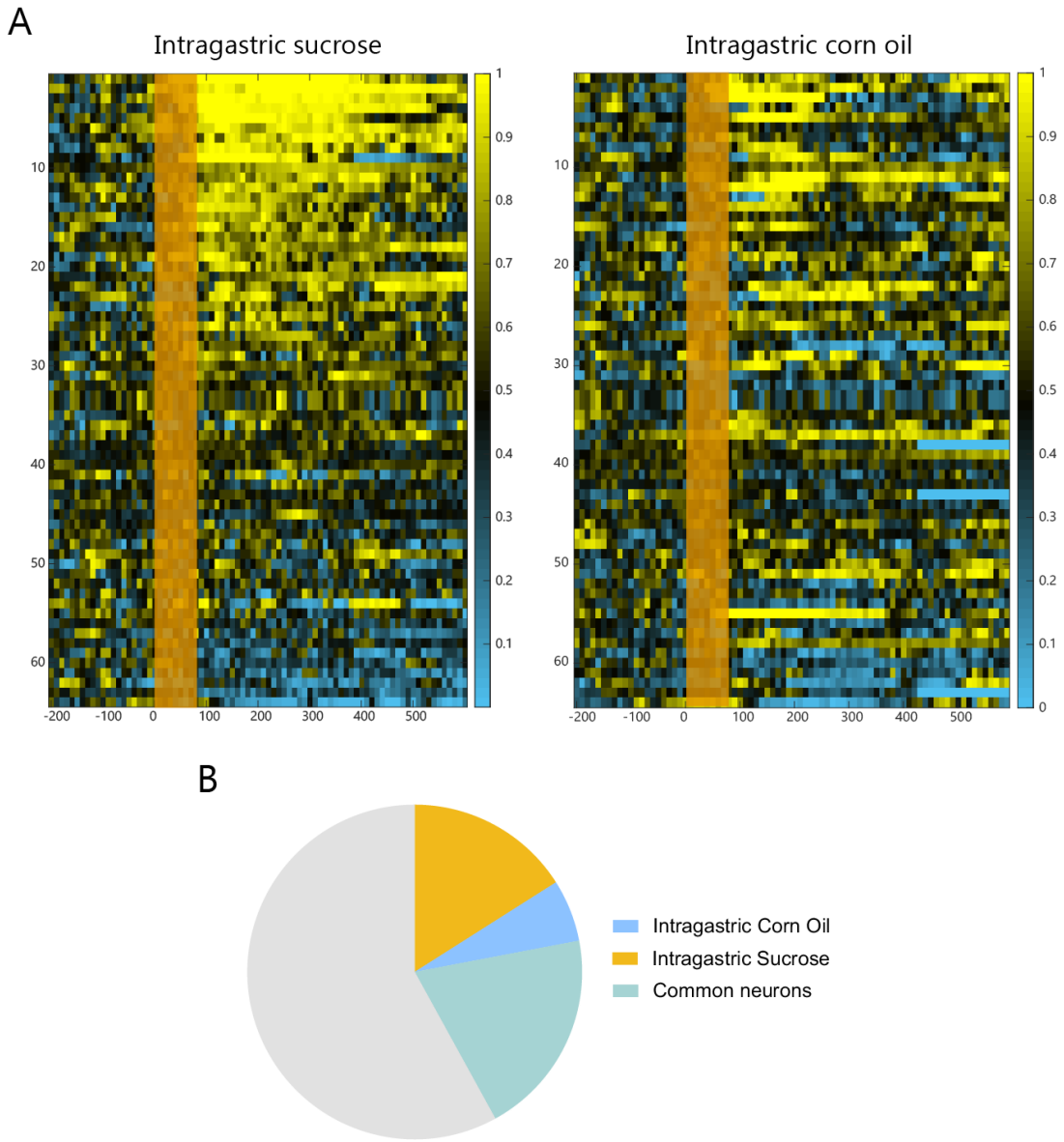

Figure 4.6. A significant subpopulation of VTA dopaminergic neurons is modulated by IG infusions of sucrose. Cell pairing between sessions was analysed for the last recording sessions, comparing the last session of IG sucrose and the following session of IG corn oil. **A** Activity of 64 neurons recorded in the last IG sucrose session (left panel) and the following IG corn oil session (right panel). Each line represents a single neuron, with a colour code that represents change in the neuronal activity relative to baseline defined according to the auROC. **B** Chart that represents the 64 paired neurons between IG sucrose and IG corn oil sessions. Yellow represents the percentage neurons that are only positively modulated by IG sucrose 20 % (10 neurons, 15.6 %), blue represents the percentage modulated by IG corn oil 9 % (4 neurons, 6.3 %), and green represents the percentage modulated by both IG reinforcers (13 neurons, 20 %). Grey represents the percentage neurons that are not positively modulated for either reinforce (37 neurons, 57.8 %).

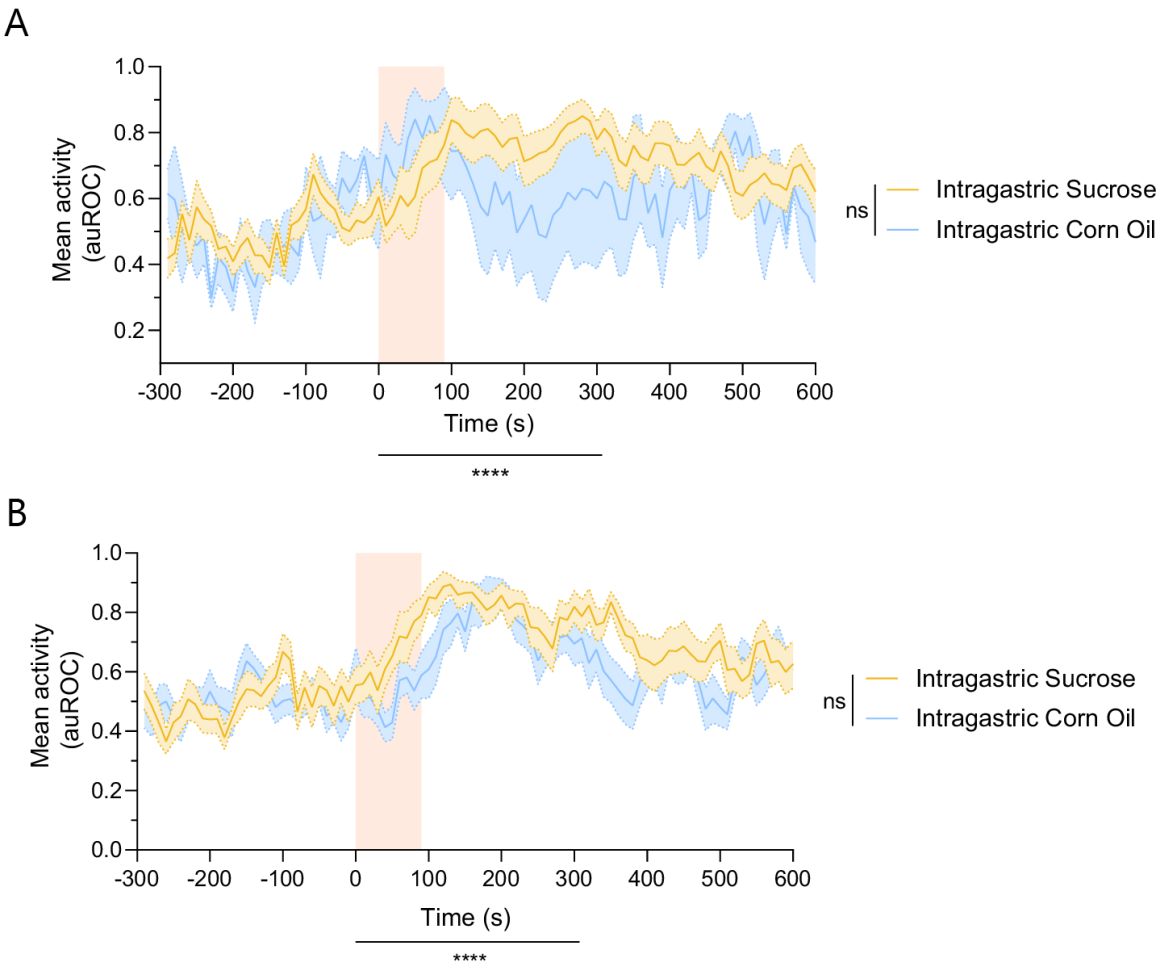

Figure 4.7 Dopaminergic VTA neurons in the that respond specifically to sucrose seem to have a higher and more sustained response throughout time when compared to corn oil specific dopaminergic VTA neurons.

A Mean activity, in auROC, of the VTA neurons that were specifically positively modulated by IG sucrose and the neurons were specifically positively modulated by IG corn oil. IG sucrose 20 % sessions are represented in yellow (10 neurons), and IG corn oil 9 % sessions are represented in blue (4 neurons). Mixed effects analysis main effect for time $F_{59,531}$= 3.82, ****p < 0.0001; main effect for reinforcer $F_{1,9}$=0.17, ns p = 0.7. **B** Mean activity, in auROC, of the VTA neurons that were positively modulated by both IG sucrose and IG corn oil. IG sucrose 20 % sessions are represented in yellow, and IG corn oil 9 % sessions are represented in blue (13 neurons). Two-way repeated measures ANOVA main effect for time $F_{7,90}$= 9.88, ****p < 0.0001; main effect for reinforcer $F_{1,12}$= 2.34 ns p = 0.2 (13 neurons). The light orange bar represents reinforcer delivery (90 s). Data is represented as mean ± SEM. Shading represents SEM.

To ensure that the results obtained were not due to any confounding variable, several control analyses were performed.

To confirm that lens placement was not affecting the results, analysis of the positively modulated neurons based on lens left or right placement was performed. As previously indicated, 15 DAT-IRES: Cre mice were unilaterally injected with a calcium sensor and implanted with a *GRIN* lens in the VTA. Approximately half of the animals were injected and implanted in the left VTA (n = 8), while the other half was injected and implanted in the right VTA (n = 7). **Figure 4.8 A** shows that the mean number of neurons detected for animals implanted in the left and the right VTA is approximately 9 (± 1 neuron) and 10 (± 1 neuron), respectively. The graph indicates that the mean number of neurons detected does not depend on lens placement (**Figure 4.8 A**, one-way repeated measures ANOVA ns p = 0.2). Also, the percentage of positively modulated neurons based on lens placement did not affect the overall conclusions of this work.

Although no statistical significance was observed in the right VTA, the biological effect is very similar and, most likely, the sample is underrepresented (**Figure 4.8 B**). Thus, it is possible to state that VTA dopamine responses to IG reinforcers is, most likely, not affected by the position of the lens lateralization of the response.

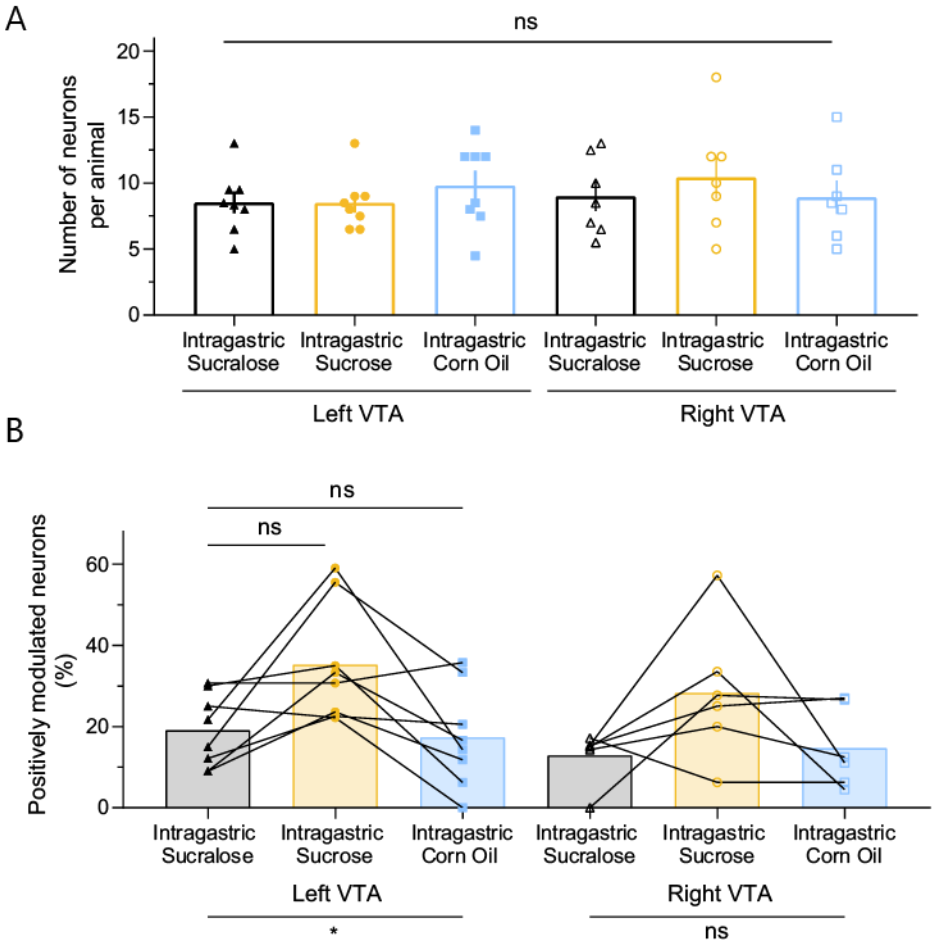

Figure 4.8 VTA dopaminergic neuronal activity in response to different IG reinforcers is not dependent on lens placement.
A Number of neurons recorded per animal in the VTA in different reinforcer sessions. The black bar (black filled triangles) represents sessions where IG sucralose 0.02 % was delivered, the yellow bar (yellow filled circles) represents sessions where IG sucrose 20 % was administered, and the blue bar (blue filled squares) represents sessions where IG corn oil 9 % was administered. One-way repeated measures ANOVA $F_{7,14}$= 6.58, ns p = 0.2. Data is represented as mean ± SEM. **B** Positively modulated VTA neurons, in percentage, per mouse based on lens placement for the first 300 s after infusion. The black bar (black filled triangles) represents the sessions where IG sucralose 0.02 % was delivered, the yellow bar (yellow filled circles) represents the sessions where IG sucrose 20 % was administered, and the blue bar (blue filled squares) represents where IG corn oil 9 % was administered (n = 15). One-way ANOVA $F_{5,39}$= 1.16, *p = 0.03. For the left VTA: one-way repeated measures ANOVA $F_{2,13}$= 4.18, *p = 0.04 (n = 8). Post-hoc analysis (Tukey test) IG sucrose vs IG corn oil $^{\#}$p = 0.03, IG sucralose vs IG sucrose ns p= 0.2, and IG sucralose vs IG corn oil ns p = 0.8. For the right VTA: one-way repeated measures ANOVA $F_{2,9}$= 1.35, ns p = 0.3 (n = 7). Data is represented as mean.

Another feature that was also important to address was the solution used to dissolve the corn oil solution. As previously mentioned, the corn oil 9 % solution was prepared with an emulsifier to dissolve the lipid in water. Thus, in order to understand whether emulsifier could have had an effect on the activity of VTA dopaminergic neurons the other 2 reinforcers, sucrose, and sucralose, were also dissolved with this

emulsifier and activity was compared. **Figure 4.9 A** shows that there is no significant difference in the percentage of positively modulated neurons between the session where sucralose (grey bar) and sucralose with emulsifier (black bar) were administered (**Figure 4.9 A**, Paired t-test IG sucralose vs IG sucralose with emulsifier ns p = 0.5). Moreover, there is also no significant difference in the percentage of positively modulated neurons between the session where sucrose (yellow bar) and sucrose with emulsifier (orange bar) were administered (**Figure 4.9 A**, Paired t-test IG sucrose vs IG sucrose with emulsifier ns p = 0.4). Therefore, presence of the emulsifier did not impact results.

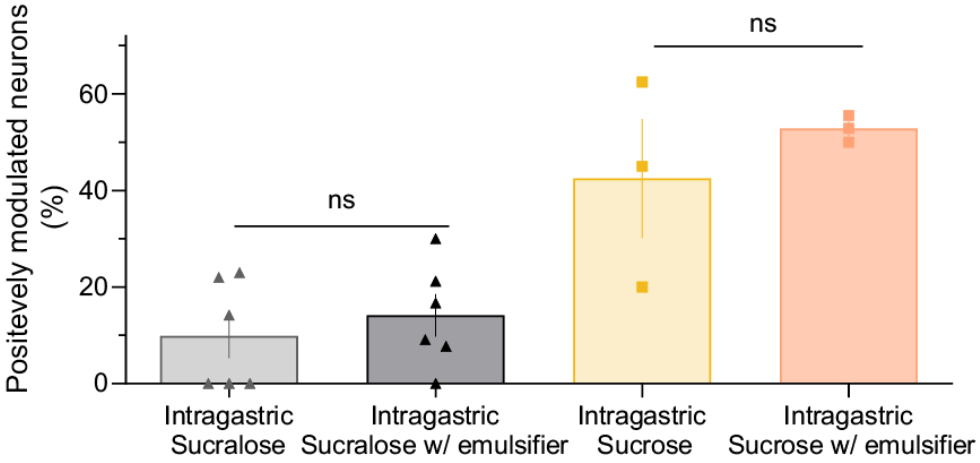

Figure 4.9 Percentage of positively modulated neurons is not affected by the presence of an emulsifier. Positively modulated VTA neurons, in percentage, per mouse for the first 300 s after infusion of sucrose and sucralose with and without emulsifier. It was necessary to add an emulsifier to dissolve corn oil 9 % in water and, therefore, the emulsifier effect on the percentage of positively modulated neurons for sucralose and sucrose sessions was further tested. Light grey bar (filled grey triangles) and black bar (filled black triangles) represent sessions where IG sucralose without and with emulsifier was administered, respectively (n = 7). Yellow bar (filled yellow squares) and orange bar (filled orange squares) represent sessions where IG sucrose without and with emulsifier were administered, respectively (n = 3). Paired t-test IG sucralose vs IG sucralose with emulsifier ns p = 0.5 and paired t-test IG sucrose vs IG sucrose with emulsifier ns p = 0.4. Data is represented as mean ± SEM.

Finally, the movement of the animal throughout each session was also and calculated based on frame-by-frame pixel changes, to ensure that movement also associated to an increase in dopamine neurons was not affecting the results previously described. The results show that movement did not differ between different reinforcer sessions (**Figure 4.10**, mixed effects analysis main effect for reinforcer ****p < 0.0001), which indicates that dopamine signals related to the movement were not a variable between different reinforcer sessions.

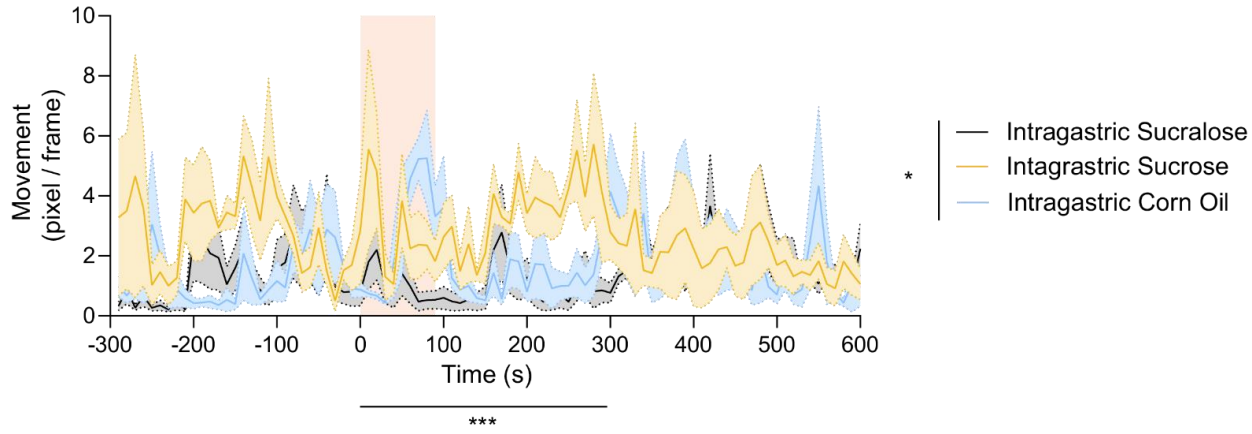

Figure 4.10 Animal movement is similar between different reinforcer sessions.
Mean animal movement, in pixel change per frame, for each reinforcer session. Animal movement was measured throughout each session and calculated based on frame-by-frame pixel change. IG sucralose 0.02 % sessions are presented in black (4 sessions), IG sucrose 20 % sessions are represented in yellow (3 sessions), and IG corn oil 9 % sessions are represented in blue (4 sessions). Mixed effects analysis main effect for time $F_{59,480}$= 1.0, ns p = 0.6; main effect for reinforcer $F_{2,437}$= 55.6, ****p < 0.0001. Data is presented as mean ± SEM. Shading indicates SEM. Unpublished data developed by Ana Fernandes, Diogo Melo ,and Albino Oliveira-Maia.

Results obtained from monitoring neuronal activity in the VTA after PI stimuli using different reinforcers indicate there is a higher percentage of dopaminergic neurons that respond to IG sucrose when compared to IG corn oil and sucralose. A subpopulation of neurons specifically respond to IG sucrose (15 out of 64 neurons) was also identified and these neurons seemed to have a higher and more sustained in time activity when compared to corn oil specific neurons (4 out of 64 neurons). Additionally, a subpopulation that seems to be responding to both reinforcers, probably respond to caloric content was also identified (20 out of 64 neurons). Results were not affected by the interval chosen for analysis neither by the lens position or the presence of an emulsifier.

.

4.1.2. Dopaminergic neurons of SNc respond independently of macronutrient

In order to understand how SNc dopaminergic neurons respond to IG infusions of different macronutrients, a similar procedure was performed as previously described for the VTA. DAT-IRES: Cre mice were injected and implanted in the SNc and, afterwards, implanted with a gastric catheter. The surgeries allowed for the monitorisation and recording of dopaminergic neuronal activity in the SNc during IG infusion of different reinforcers.

Figure 4.11 A summarizes the deep-brain calcium imaging study in the SNc. Calcium recordings were acquired in 5 DAT-IRES: Cre mice for 25 min sessions where animals were freely behaving. For each session, 1 of 3 reinforcers was delivered directly into the stomach through a previously implanted IG catheter. Reinforcer delivery occurred after a 5 min baseline period. The 3 reinforcers administered were IG isocaloric solutions of sucrose 20 % and corn oil 9%, and a control - sucralose 0.02 % solution. **Figure 4.11 B** exemplifies SNc dopaminergic neurons during a session where sucrose 20 % was administered (left top panel) and the corresponding areas of interest for each neuron detected (8 neurons, left bottom panel). A time course (10 min) of the calcium fluorescence traces of the 4 highlighted neurons (yellow, green, light blue and dark blue) are represented in the right panel.

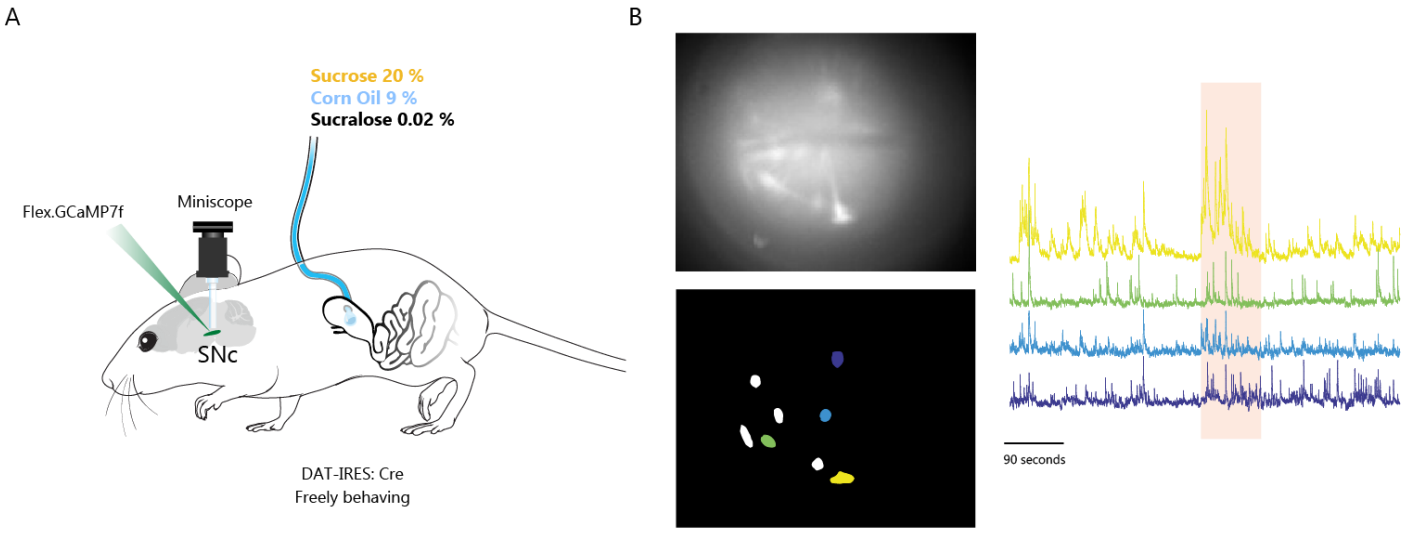

Figure 4.11 Monitoring Substantia Nigra pars compacta (SNc) dopaminergic neuronal activity during intragastric delivery of reinforcers in freely behaving mice.
A A group of 5 freely behaving DAT-IRES: Cre mice were injected with a calcium sensor, AAV.Syn.Flex.GCaMp7f, and implanted with a *GRIN* lens in the Substantia Nigra pars compacta (SNc) for deep-brain calcium imaging. Calcium recordings were acquired using a miniscope during IG delivery of three different reinforcers. The three reinforcers were isocaloric solutions of a carbohydrate - sucrose 20 %-, and a lipid - corn oil 9% -, as well as a non-caloric sweetener solution - sucralose 0.02 %. Only one reinforcer was delivered per session. Mouse drawing obtained from Scidraw.io **B** Example of SNc dopaminergic neurons during a session where sucrose 20 % was administered (top left panel) and the corresponding areas of interest (bottom left panel). A time course of the fluorescence traces of the highlighted neurons, according to colour (dark blue, blue, green, and yellow) are shown in the right panel. The light orange bar represents reinforcer delivery (90 s).

The activity of, on average, 4 (± 1) neurons per animal was recorded (**Figure 4.12 A**). No significant difference was found in the number of neurons recorded per animal between different reinforcer sessions (**Figure 4.12 B**, one-way repeated measures ANOVA ns p = 0.8).

Mean activity, in auROC, for all SNc dopaminergic neurons detected was per reinforcer session plotted for the first 15 min (**Figure 4.13**). As previously stated, the first 5 min represent baseline and the highlighted orange bar (0 to 90 s) represents reinforcer delivery. Importantly, values higher or lower than 0.5 indicated that activity is higher or lower than baseline activity, respectively.

The total number of neurons detected for the 5 animals with all sessions was 42 neurons for sucrose 20 % sessions, 35 neurons for corn oil 9 % sessions, and 35 neurons for sucralose 0.02 % sessions. First analysis of the SNc dopaminergic neuronal activity indicates that neuronal traces are similar between different reinforcer sessions (**Figure 4.13**, mixed effects analysis main effect for reinforcer ns p = 0.7).

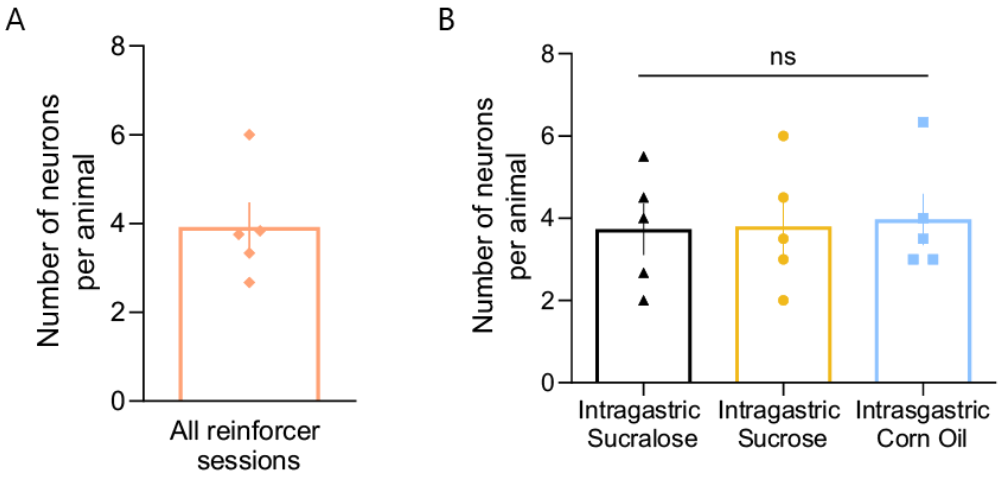

Figure 4.12 Mean number of neurons was constant between different reinforcers.
A Number of neurons recorded per animal in the SNc for all sessions (orange bar, orange filled hexagon). **B** Number of neurons recorded per animal in the SNc in different reinforcer sessions. The black bar (black filled triangles) represents sessions where sucralose 0.04 % was delivered, the yellow bar (yellow filled circles) represents sessions where sucrose 20 % was administered, and the blue bar (blue filled squares) represents sessions where corn oil 9 % was administered. Data is represented as mean ± SEM. One-way repeated measures ANOVA $F_{4,8}$= 6.9, ns p = 0.8.

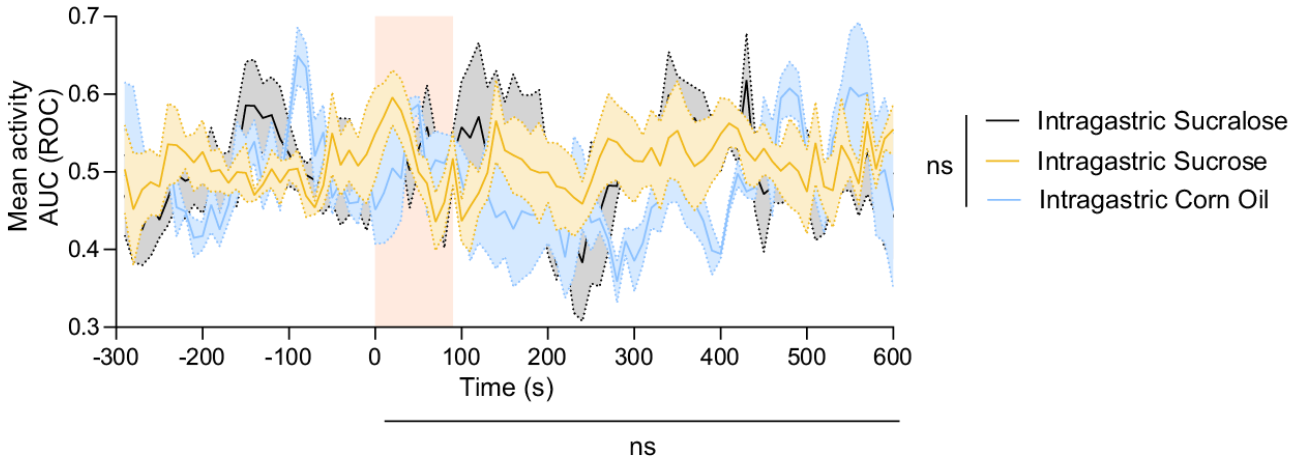

Figure 4.13 Mean auROC traces are not significantly different between different reinforcers.
Mean activity, in auROC, of all the neuronal activity recorded for all the SNc dopaminergic neurons detected per reinforcer session. IG sucralose 0.02 % sessions are presented in black (35 neurons), IG sucrose 20 % sessions are represented in yellow (42 neurons), and IG corn oil 9 % sessions are represented in blue (35 neurons). Mixed effects analysis main effect for time $F_{4,14}$= 1.1, ns p = 0.3; main effect for reinforcer $F_{1,4}$= 0.17, ns p = 0.7. Data is presented as mean ± SEM. Shading indicates SEM.

The percentage of positively modulated dopaminergic neurons, in the SNc, per reinforcer session was calculated as previously described (**Figure 4.14 A**). The results show that the percentage of positively modulated neurons does not significantly change between reinforcer sessions (**Figure 4.14 A**, one-way repeated measures ANOVA ns p = 0.7). Additionally, the curves that represent the mean activity of the positively modulated SNc neurons per reinforcer were also not significantly different (**Figure 4.14 B**, two-way ANOVA main effect for reinforcer ns p = 0.2). Therefore, dopaminergic neurons of the SNc seem to respond to IG infusions independently of the reinforcer administered. This indicates that response is independent of nutrient (sucrose vs corn oil) and, also, that SNc response is not based on caloric content (sucrose and corn oil vs sucralose).

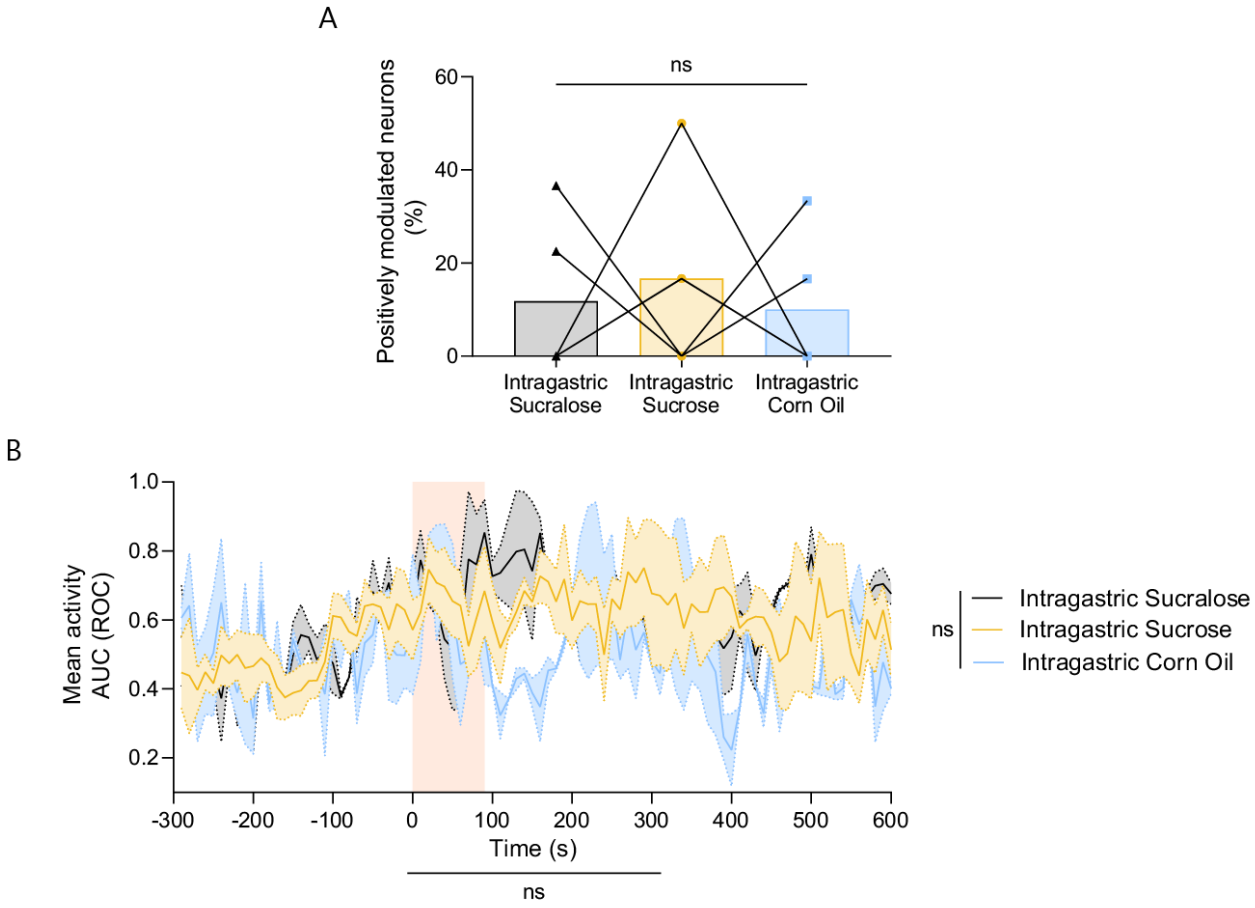

Figure 4.14 Percentage of positively modulated SNc dopaminergic neurons does not seem to differ between distinct reinforcers.

A Positively modulated SNc neurons, in percentage, per mouse for the first 300 s after infusion. The black bar (black filled triangles) represents the sessions where IG sucralose 0.02 % was delivered, the yellow bar (yellow filled circles) represents the sessions where IG sucrose 20 % was administered, and the blue bar (blue filled squares) represents the sessions where IG corn oil 9 % was administered (n = 5). One-way repeated measures ANOVA $F_{4,8}$= 0.16, ns p = 0.7. Data is presented as mean. **B** Mean activity, in auROC, of the SNc neurons that were positively modulated by the different reinforcers. The number of positively modulated neurons was calculated for the for the first 300 s after IG infusion of each reinforcer IG sucralose sessions are presented in black (5 neurons), IG sucrose sessions are represented in yellow (5 neurons), and IG corn oil 9 sessions are represented in blue (3 neurons). The light orange bar represents reinforcer delivery (90 s). Two-way ANOVA main effect for time $F_{3,12}$= 1.4, ns p = 0.3; main effect for reinforcer $F_{2,4}$=2.0, ns p = 0.2. Data is presented as mean ± SEM. Shading indicates SEM.

Importantly, neurons classified based the 600 s after infusion show the same pattern of response observed as before with no significant differences between reinforcer sessions (**Figure 4.15**, mixed effects analysis ns p = 0.5).

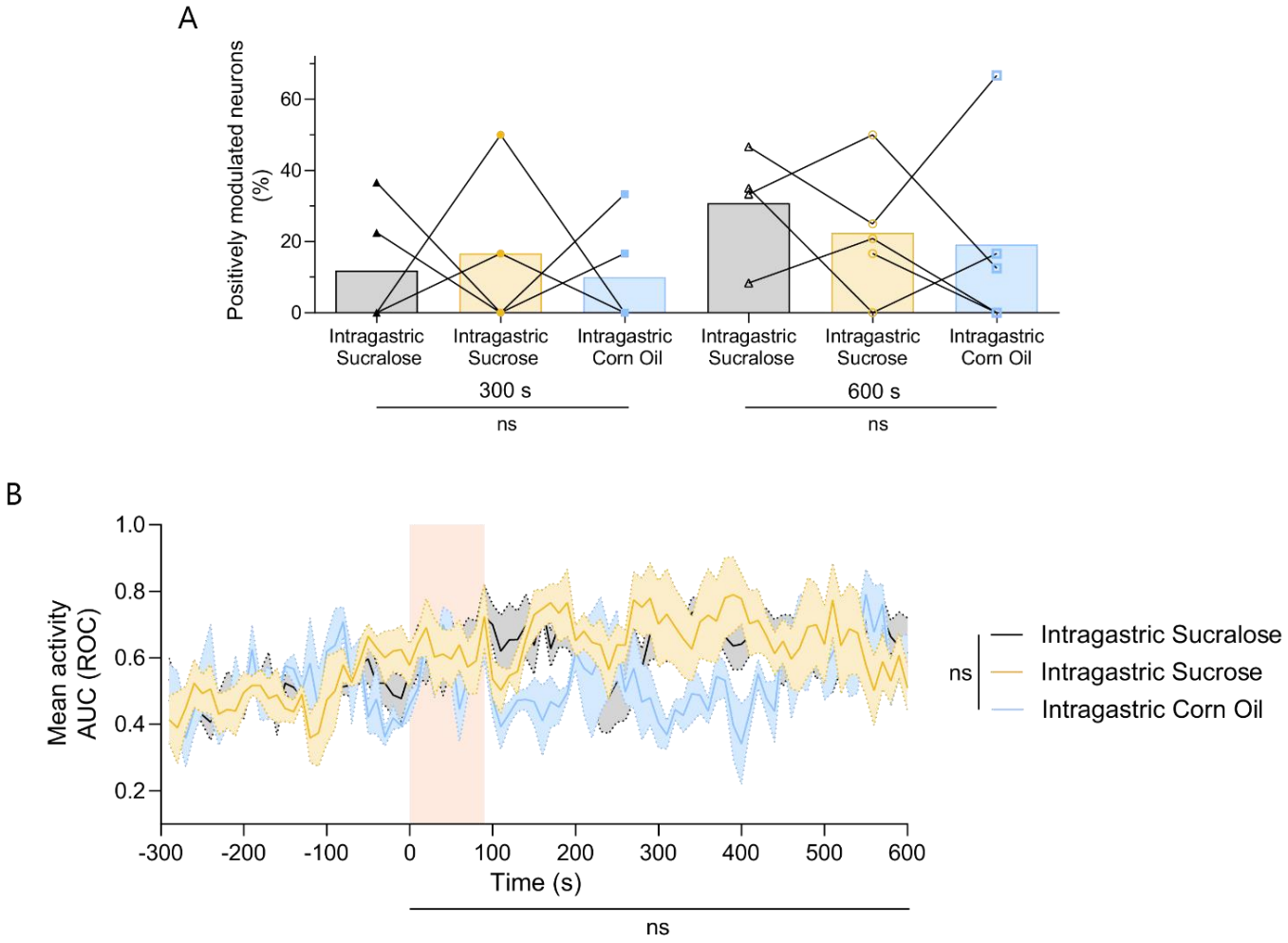

Figure 4.15 Positively modulated SNc dopaminergic neurons during IG delivery of reinforcers for the first 300 s vs 600 s after infusion.
A Positively modulated SNc neurons, in percentage, per mouse for the first 300 s (left) and 600 s (right) after infusion. The black bar (black filled triangles) represents the sessions where IG sucralose 0.02 % was delivered, the yellow bar (yellow filled circles) represents the sessions where IG sucrose 20 % was administered, and the blue bar (blue filled squares) represents sessions where IG corn oil 9 % was administered (n = 5). Mixed effects analysis $F_{1,5}$= 0.75, ns p = 0.5. For 300 s: one-way repeated measures ANOVA $F_{1,7}$= 1.2, ns p = 0.3. For 600 s: one-way repeated measures ANOVA $F_{1,4}$= 0.6, ns p = .0.7 **B** Mean activity, in auROC, of the SNc neurons that were positively modulated by the different reinforcers calculated for the for the first 600 s after infusion. IG sucralose sessions are presented in black (12 neurons), IG sucrose sessions are represented in yellow (7 neurons), and IG corn oil sessions are represented in blue (7 neurons). The light orange bar represents reinforcer delivery (90 s). Two-way ANOVA main effect for time $F_{6,50}$= 0.84, ns p = 0.5; main effect for reinforcer $F_{2,9}$= 2.30, ns p = 0.2. Data is presented as mean ± SEM. Shading indicates SEM.

Lipids are a broad group of nutrients with highly variable molecular constitutions that include fatty acids, such as corn oil. Fatty acids are a group of molecules made of very diverse types of hydrocarbon chains. Thus, it became relevant to understand whether lipid constitution impacted SNc dopaminergic neuronal response. To accomplish this, SMOF lipid was used as a reinforcer. SMOF lipid has a similar constitution to the most used lipidic solution in recent literature, the intralipid [6]. Both solutions are solution composed of several different types of lipids, with different conformations and chain types (**Table 4.1**). More specifically,

SMOF lipid contains soybean oil (60 g/L), medium-chain triglycerides (60 g/L), olive oil (50 g/L), fish oil (30 g/L) and other components in smaller concentrations.

Table 4.1 Composition of Intralipid® and SMOF lipid

Composition (g/L)	Intralipid® 20 %	SMOF lipid 20 %
Soybean oil	200	60
Egg phospholipids	12	-
Triglycerides	-	60
Olive oil	-	50
Fish oil	-	30
Fatty acids	-	2.1

Briefly, 2 DAT-IRES: Cre mice of the initial group were also reinforced with SMOF 10 %. In the same way as before, calcium recordings were acquired with a miniscope for 25 min sessions. Animals were freely behaving and the reinforcers, including SMOF, were delivered directly into the stomach after a 5 min baseline. Importantly, the concentration ensured that lipidic and carbohydrate solutions were all isocaloric.

The activity of, on average, 4 (± 1) neurons per animal was recorded. Not differences seem to have been found in the number of neurons recorded per animal between corn oil 9 % (blue bar) and SMOF 10 % (pink bar) sessions (**Figure 4.16 A**, paired t-test ns p = 0.7).

Afterwards, the percentage of positively modulated dopaminergic neurons, in the SNc, per reinforcer session was calculated. Values were calculated for the first 300 s after injection. **Figure 4.16 B** represents positively modulated SNc dopaminergic neurons, in percentage, for coin oil 9 % (blue bar) and SMOF 10 % (pink bar) sessions. The results show that the percentage of positively modulated neurons did not seem to be affected by the type of lipid used. However, it is important to note the very small number of animals and, thus, no statistical analysis was performed (**Figure 4.16 B**). Therefore, preliminary data indicates that lipid constitution does not affect SNc dopaminergic response.

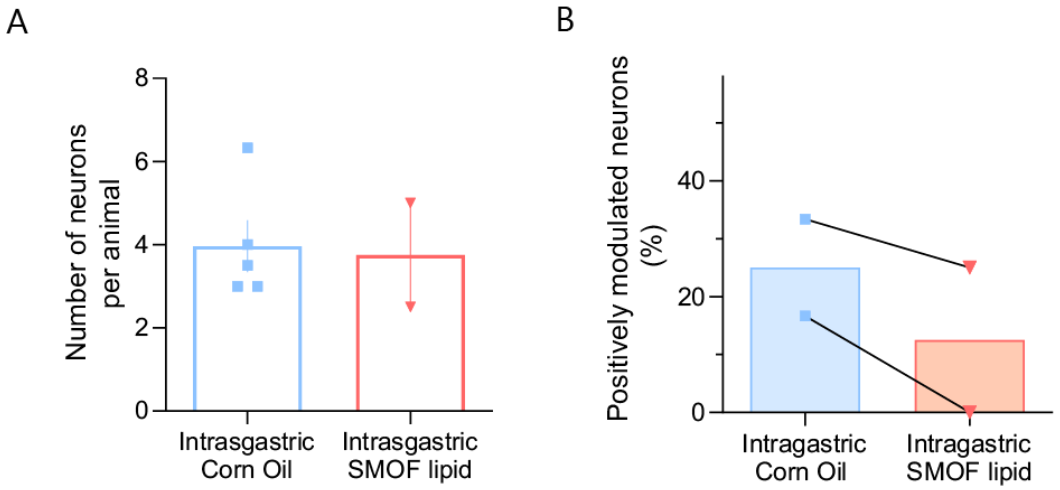

Figure 4.16 SNc dopaminergic neurons respond similarly to different types of lipids.
A Number of neurons recorded per animal in the SNc in different lipid reinforcer sessions. The blue bar (blue filled squares) represents sessions where corn oil 9 % was administered (n = 5), and the red bar (red filled upside-down triangles) represents sessions where SMOF lipid 10 % was administered (n =2). **B** Positively modulated SNc neurons, in percentage, per mouse for the first 300 s after infusion of the IG reinforcers. The blue bar (blue filled squares) represents sessions where corn oil 9 % was administered, and the red bar (red filled upside-down triangles) represents sessions where SMOF lipid 10 % was administered (n =2). Paired t-test ns p = 0.2. Data is represented as mean ± SEM.

Results regarding percentage of dopaminergic SNc positively modulated neurons and their activity in sucrose and corn oil sessions revealed that response to both nutrient is similar and, thus, SNc response does not seem to be nutrient-specific. Likewise, results between caloric – sucrose and corn oil – and non-caloric – sucralose – solutions are not significantly different which leads to the conclusion that dopaminergic SNc response might not depend on caloric content. Preliminary data also revealed that lipid constitution does not affect response in this dopaminergic area.

4.2. Response of dorsal and lateral striatum to intragastric infusions of different nutrients

It is well documented that central dopaminergic regions, such as the VTA and SNc, are anatomically and functionally connected to the ventral striatum, NAc, and dorsal striatum, respectively [7]. In fact, there is evidence indicating that dopamine levels in striatal regions increase upon PI infusion of carbohydrates [1, 2]. Based on that and results showed in this work so far, the second main objective was to record dopamine dynamics, in freely behaving mice. Dopamine transients were recorded for, simultaneously, ventral and dorsal striatal regions while infusing isocaloric reinforcers directly into the stomach through a previously implanted IG catheter. The striatal regions chosen were the NAc and DLS.

The working hypothesis is that NAc responds specifically to carbohydrates, while the DLS responds independently of the nutrient being delivered. This hypothesis is based on the pattern of responses observed in the calcium imaging of VTA and SNc from the previously presented results.

Figure 4.17 summarizes the fibre photometry study. A group of 4 WT mice were bilaterally injected with a dopamine indicator, dLight 1.2, and implanted with dual optical fibres in the NAc and DLS. For each mouse, striatal dopamine dynamics were recorded in both striatal regions using two channels, 415 and 470 nm. Session structure was similar to the one previously used for calcium imaging. Briefly, sessions lasted for 25 min and animals were freely behaving. For each session, 1 of 3 reinforcers was delivered directly into the stomach through a previously implanted IG catheter. Reinforcer delivery occurred after a 5 min baseline period at a rate of approximately 20 µL/ 3 s for 90 s. For this assay, 3 reinforcers were administered. The reinforcers administered were isocaloric solutions of a carbohydrate - sucrose 20 %-, lipid - corn oil 9% -, and a control non-caloric sweetener - sucralose 0.04 %.

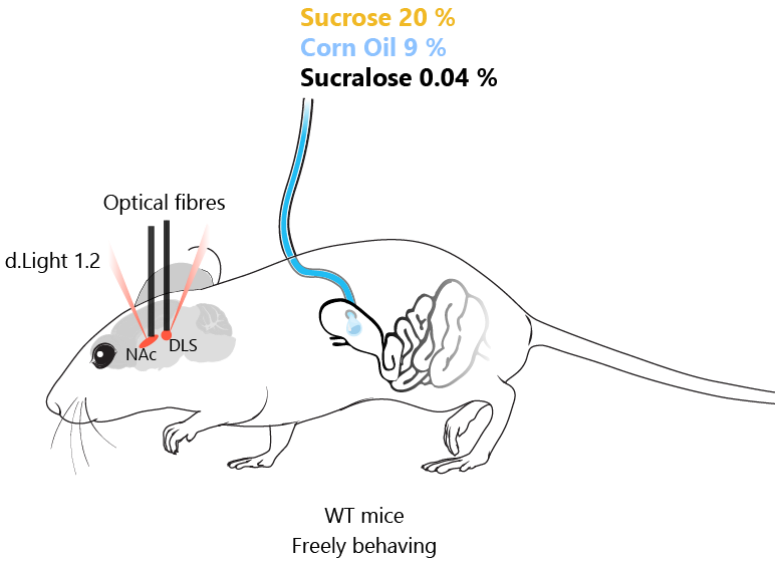

Figure 4.17 Monitoring nucleus accumbens (NAc) and dorsal-lateral (DLS) dopamine dynamics during intragastric delivery of reinforcers in freely behaving mice.
A group of 4 freely behaving WT mice were injected with a dopamine indicator, dLight 1.2, and implanted with two optical fibres in NAc and the DLS for fibre photometry experiments. Dopamine striatal dynamics were recorded during IG delivery of 3 different reinforcers directly into the stomach, through a previously implanted IG catheter. The 3 reinforcers were isocaloric solutions of a carbohydrate - sucrose 20 %-, and a lipid - corn oil 9% -, as well as a non-caloric sweetener solution - sucralose 0.04 %. Only 1 reinforcer was delivered per session. Mouse drawing was obtained from Scidraw.io.

Figure 4.18 shows the normalized changes in dopamine dynamics, z-score, in NAc and DLS in a 15 min session. The first 5 min (- 300 to 0 s) represent the baseline and the highlighted orange bar (0 to 90 s) represents reinforcer delivery.

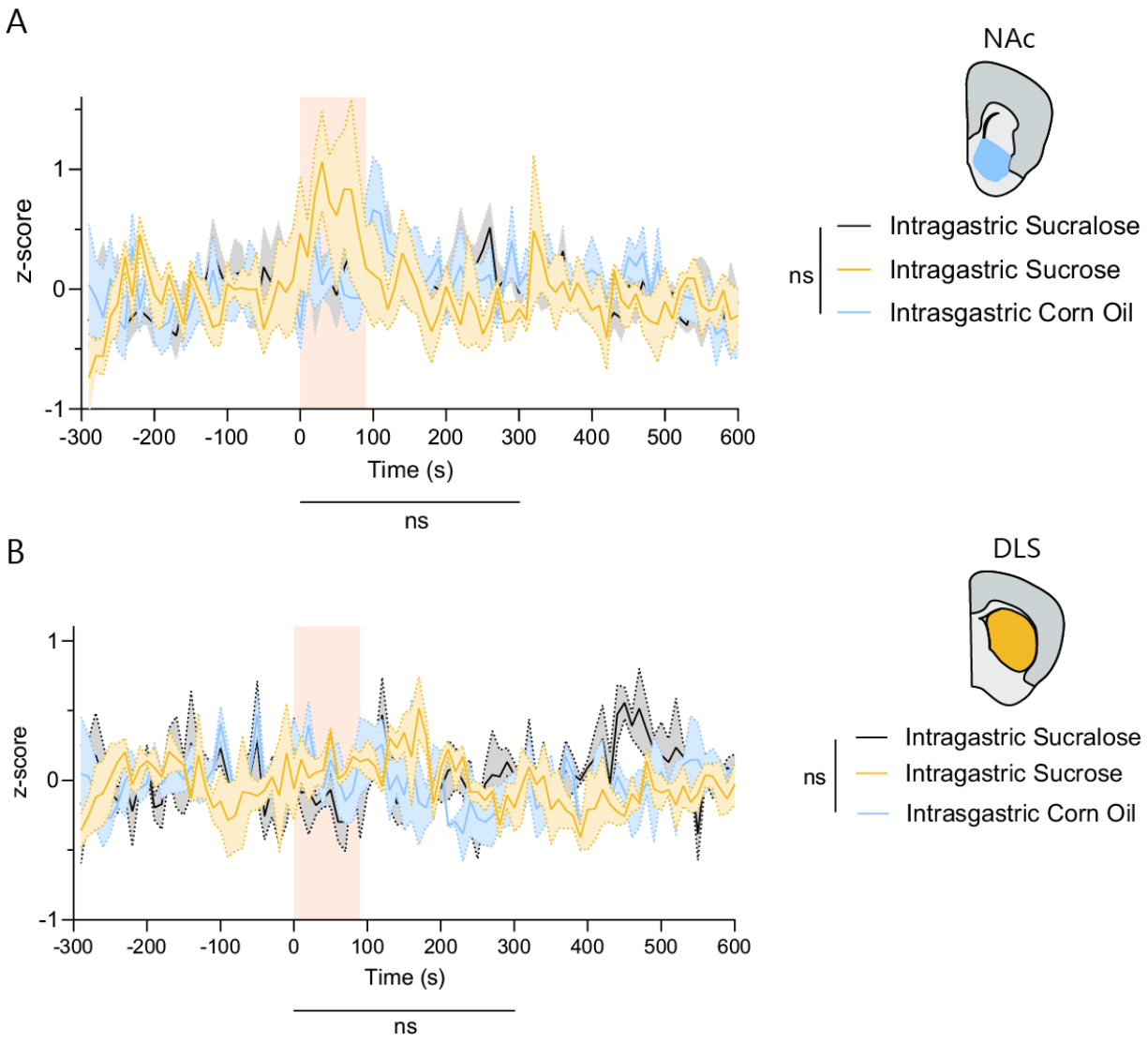

Figure 4.18 The NAc seems to specifically respond to sucrose and DLS response seems to be similar between different reinforcer sessions.
A Mean activity, z-scored, of NAc dopamine dynamics recorded per reinforcer session (n = 4). IG sucralose 0.04 % sessions are presented in black, IG sucrose 20 % sessions are represented in yellow, and IG corn oil 9 % sessions are represented in blue. Two-way repeated measures ANOVA main effect for time $F_{6,55}$= 4.3, ns p = 0.3; main effect for reinforcer $F_{2,9}$= 0.10, ns p = 0.9. **B** Mean activity, z-score, of DLS dopamine dynamics recorded per reinforcer session (n = 3). IG sucralose 0.04 % sessions are presented in black, IG sucrose 20 % sessions are represented in yellow, and IG corn oil 9 % sessions are represented in blue. Two-way repeated measures ANOVA main effect for time $F_{4,27}$= 1.03, ns p = 0.4; main effect for reinforcer $F_{2,6}$= 1.48, ns p = 0.3. Data is presented as mean ± SEM. Shading indicates SEM.

Preliminary results point to the possibility of the ventral striatum, NAc, responding to IG delivery of sucrose 20 % (**Figure 4.18 A**, yellow line) when compared to sessions where sucralose 0.04 % or corn oil 9 % (**Figure 4.18 A**, black line and blue line respectively) are delivered. This pattern, however, is not statistically

significant (**Figure 4.18 A**, two-way repeated measures ANOVA main effect for reinforcer ns p = 0.9) probably due to the low number of animals included in the analysis.

Dopamine dynamic acquired for the dorsal striatum, DLS (n = 3), did not significantly change between different reinforcer sessions (**Figure 4.18 B**, two-way repeated measures ANOVA main effect for reinforcer ns p = 0.3) corroborating previous results obtained for dopaminergic neuronal activity in the SNc. However, for the NAc analysis, the number of animals is very low and further experiments to increase the sample size and corroborate these results need to be performed.

It was important to understand whether lipid constitution impacted striatal dopamine dynamics. To accomplish this, SMOF lipid 10 % was used as a reinforcer. This lipidic solution mainly contains soybean oil, medium-chain triglycerides, olive oil and fish oil.

Therefore, in a subset of animals bilaterally injected with dLight 1.2 and implanted with dual optical fibres in the NAc and DLS, SMOF 10% was also infused directly into the stomach. Importantly, SMOF concentration was chosen so that the solution had the same caloric value as the sucrose and corn oil solutions.

Figure 4.19 shows the normalized changes in dopamine dynamics, z-score, the NAc and DLS in SMOF 10 %, corn oil 9 %, and sucrose 20 % sessions. The results show that the dopamine dynamics pattern in the ventral striatum, NAc (n = 4), seems to differ between SMOF and corn oil sessions. This apparent difference is, however, not statistically significant (**Figure 4.19 A**, two-way repeated measures ANOVA main effect for reinforcer ns p = 0.8). Again, this is most likely due to the low number of animals included in the analysis. Moreover, in the DLS, dopamine dynamics change in a similar way after intragastric injection of different types of lipidic solutions, more specifically SMOF 10 % and corn oil 9 % (**Figure 4.19 B**, pink and blue line respectively).

The results also indicate that the curve that represents response to sucrose 20 % is superimposable to the curve that represents response to SMOF 10 %, in the NAc (**Figure 4.19 B**, two-way repeated measures ANOVA main effect for reinforcer ns p = 0.8).

Overall, preliminary results show that NAc seem to increase response when IG to sucrose is infused, when compared to IG corn oil and sucralose, even knowing no significant statistically differences were observed. Interestingly, this striatal ventral region seems to respond differently to different types lipidic solutions, however, the sample size is low and analysis is underpowered. In detail, NAc seems to not respond to corn oil but the response to SMOF lipid is comparable to sucrose. On the contrary, the DLS response is very similar between different reinforcer sessions regardless of nutrient type or caloric content in a pattern of response very similar to what was observed in the SNc calcium imaging recordings. Interestingly, when comparing DLS response to sucrose and SMOF lipid these are significantly different despite the fact that patterns of response are similar.

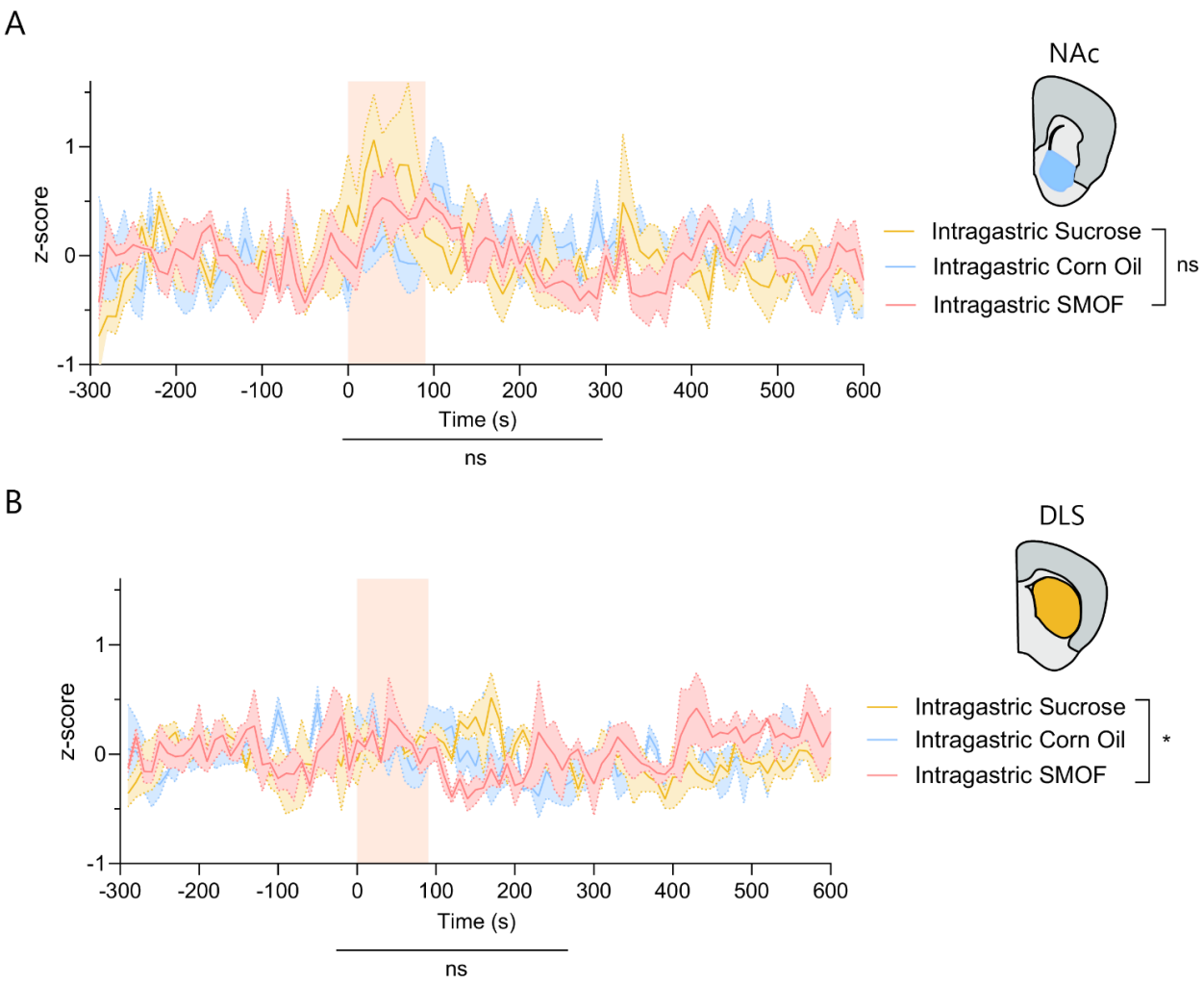

Figure 4.19 Ventral striatal response seems to be similar between sucrose and SMOF lipid sessions.
A Mean activity, z-score, of NAc dopamine dynamics recorded per reinforcer session (n = 4). IG sucrose 20 % sessions are represented in yellow and IG SMOF 10 % sessions are represented in pink. Two-way repeated measures ANOVA main effect for time $F_{2,7}$= 2.05, ns p = 0.2; main effect for reinforcer $F_{1,3}$= 0.090, ns p = 0.8. **B** Mean activity, z-scored, of DLS dopamine dynamics recorded per reinforcer session (n = 3). IG sucrose 20 % sessions are represented in yellow and IG SMOF 10 % sessions are represented in pink. Two-way repeated measures ANOVA main effect for time $F_{2,4}$= 1.51, ns p = 0.3; main effect for reinforcer $F_{1,2}$= 20.6, *p = 0.04. Data is presented as mean ± SEM. Shading indicates SEM.

4.3. Postingestive stimuli modulates food seeking behaviour in an instrumental two-action probabilistic task

Fernandes *et al.,* 2020 demonstrated that PI delivery of sucrose, directly into the stomach, was sufficient to sustain operant food-seeking behaviour. In this assay, using an instrumental one lever behavioural task, the authors showed that animals pressing for IG sucrose increased lever pressing behaviour, when compared to animals pressing for IG sucralose (non-caloric sweetener).[3]

To further explore the importance of PI stimuli in lever pressing behaviour, a novel probabilistic two-action behavioural task was developed. The major difference from previous work was the behavioural design per se and the possibility to understand the impact of PI stimuli in reinforcement learning (RL) using RL models previously described for reward based operant tasks [8, 9].

Briefly, animals had 2 available levers with different probabilities of delivering reward. During training the probabilities of reward changed between low probability (20 %) and high probability (80 %). The experimental design allowed to assess animal preference based on their choice, and therefore the possibility to infer important parameters in decision making and RL.

For this assay, animals were placed in an operant box equipped with 2 levers, each lever corresponding to a possible action that once chosen would lead to the delivery of an oral reward paired with IG reward. Oral rewards were always sucralose 0.04 % – non-caloric sweet solution. For each lever, besides the oral reward, IG sucrose or sucralose delivery was randomly assigned to a lever and the association was maintained throughout the experiment. Importantly, one lever had a probability of 80% - high probability lever - to deliver rewards and the other lever had a 20% probability - low probability lever - to deliver rewards. The probabilities switched during the session.

Accordingly, it was hypothesized that mice would develop a preference for the lever that leads to IG infusion of sucrose, the caloric solution, independently of reward probability.

The task structure encompassed two learning schedules, the continuous reinforcement (CRF) schedule and the postingestive probabilistic (PP) schedule. In the CRF schedule, to ensure lever pressing learning, mice were exposed to one lever at a time. Once they press the lever a certain number of times, the one on the opposite side would become exposed and, thus, available for lever press. Both levers would give an oral reward of sucralose 0.04 % (**Figure 3.6 A**). For this schedule, the number of lever presses per session – CRF criteria – was gradually increased and contingent on completing previous criteria.

After lever pressing acquisition animals moved to the PP schedule. In the PP schedule, each lever was associated with an oral reward - sucralose 0.04 % - paired with an IG reward delivered directly into the stomach, through a previously implanted catheter. Importantly, one lever was associated with an IG reward of a non-caloric solution - sucralose 0.04 % -, while the other was associated with an IG reward of a caloric carbohydrate solution - sucrose 20%. Association between the lever side and IG reward (sucrose or sucralose) was randomized. The association between lever side and IG reward associated was maintained throughout training. Each lever had a probability of delivering reward - oral paired with IG -, randomly assigned at the beginning of the session. One lever would give sucralose paired with IG rewards 80% of the total lever presses – high probability lever -, while the other would deliver rewards only 20% of the total lever presses - low probability lever (**Figure 3.6 B**). However, these probabilities changed according to the number of rewards obtained. Once the animal had acquired, on average, 25 rewards the probabilities associated with each lever switched. The probability switch was designated as a transition and consisted of

the high probability lever becoming the low probability lever and vice-versa. The attainment of, on average, 25 rewards and the consequent transition was designated as a block.

For this assay, a deprivation protocol was needed to ensure engagement, exploration, and better learning curves [10]. To ensure a maximal learning rate, before starting the two-action probabilistic instrumental task, a group of 7 animals was submitted to 3 different deprivation protocols.

The mean number of lever presses for the last 6 days of each deprivation protocol was plotted (**Figure 4.20**). Based on the results obtained, the water and food deprivation protocol was the protocol where mice obtained the highest number of lever presses (**Figure 4.20**, mixed effects analysis ****p < 0.0001; mean value: water and food deprivation 109.6 ± 5 presses, water deprivation 71.7 ± 4 presses, food deprivation 34.3 ± 4 presses). **Supplementary Figure 7.5** shows the mean number of lever presses per session for the 3 deprivation protocols. Therefore, the water and food deprivation protocol was the protocol chosen to proceed in the two-action probabilistic instrumental task.

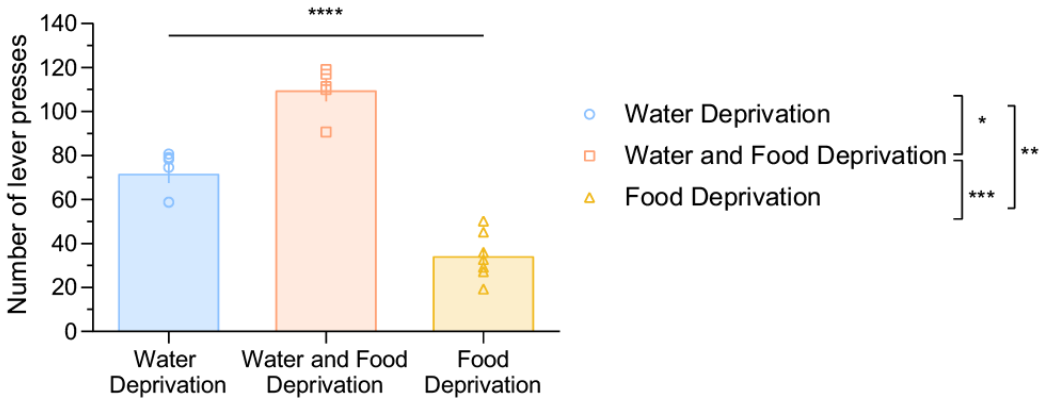

Figure 4.20 Mice press more under a water and food deprivation protocol.
Mean number of lever presses for the last 6 sessions under different deprivation protocols on the postingestive probabilistic (PP) schedule. Blue bar (with blue circles) represents animals under a water deprivation protocol (n = 7). Orange bar (with orange squares) represents animals under a water and food deprivation protocol (n = 3). Yellow bar (with yellow triangles) represents animals under a food deprivation protocol (n =4). Mixed effects analysis $F_{2,13}$ =73.4, ****p < 0.0001; post-hoc Tukey test water deprivation vs water and food deprivation *p = 0.02, water and food deprivation vs food deprivation ***p = 0.0002, water deprivation vs food deprivation **p = 0.006. Data is presented as mean ± SEM.

In a second group of animals, water and food deprived mice started the two-action instrumental task previously described, starting with a CRF schedule, in which one lever press led to an oral reward of a non-caloric solution - sucralose 0.04 %. For this schedule, the number of lever presses per session, designated as CRF criteria, was gradually increased and contingent on completing the previous criteria. This schedule was implemented so that mice could acquire lever pressing behaviour. Animals finished the CRF schedule once the last criteria, 25 presses per lever in a 60 min session, was completed twice. The number of days necessary for mice to complete the CRF schedule was designated as training days.

An interesting observation made during the training days was that mice seemed to learn and acquire lever pressing behaviour at different learning rates. Thus, the number of lever presses per training day was plotted (**Figure 4.21**). Results show that the number of days it takes an animal to finish the CRF schedule was 9 (± 1) days. While some animals needed only 5 days to complete the CRF schedule (**Figure 4.21**, M1 in purple), others needed up to 14 days to complete the same schedule (**Figure 4.21**, M3 in blue). Importantly,

all 7 mice tested mice acquired lever pressing behaviour. Interestingly, once mice learnt the association between the lever and reward delivery port (CRF10 completed), it only takes around 2 days to complete CRF25 criteria.

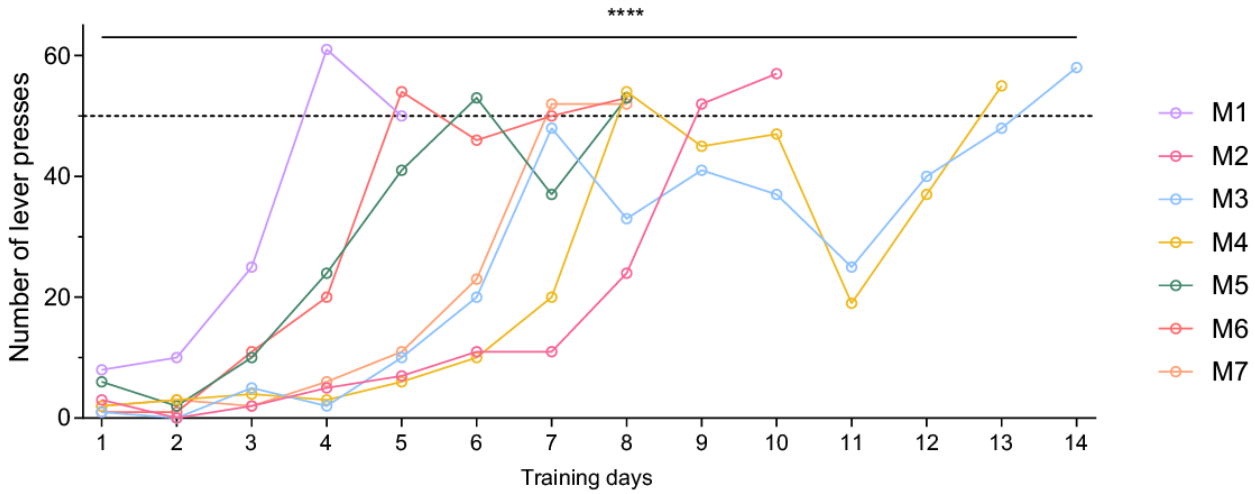

Figure 4.21 Mice learn to press a lever to obtain an oral reward at different learning rates.
Number of lever presses per training day for each mouse. Water and food deprived mice were trained to press one of two levers at a timer to obtain an oral reward of a non-caloric sweet solution - sucralose 0.04 % - in a continuous reinforcement (CRF) schedule (n = 7). The number of training days represents the time required for each animal to complete the CRF schedule or, in other wors, to press each lever 25 times (total of 50 lever presses) in a 60 min session. Each colour represents a different animal. Mixed effects analysis $F_{2,17}$= 6.60, **p = 0.006.

As previously stated, in the PP schedule each lever had a dynamic association with a probability of delivering rewards and a static association with the type of IG reward delivered. For this schedule, each lever was associated with an oral reward paired with an IG reward delivered directly into the stomach. One lever delivered an IG reward of a non-caloric solution - sucralose 0.04 % - while the other delivered a caloric carbohydrate solution – sucrose 20 %. Association between the lever side and an IG reinforcer was randomized and maintained throughout training. **Figure 4.22 A** shows the total number of presses during CRF and PP schedule. As expected, the total number of lever presses remained stable during the PP schedule. **Supplementary Figure 7.6** represents the number of lever presses per session per mouse. Additionally, the number of blocks per session did not significantly change throughout the session (**Figure 4.22 B**, mixed effects analysis ns p = 0.3). Both these results indicate that mice with a water and food deprivation protocol, on average, execute 89 (±) lever presses, and perform an average of 2 (± 1) blocks.

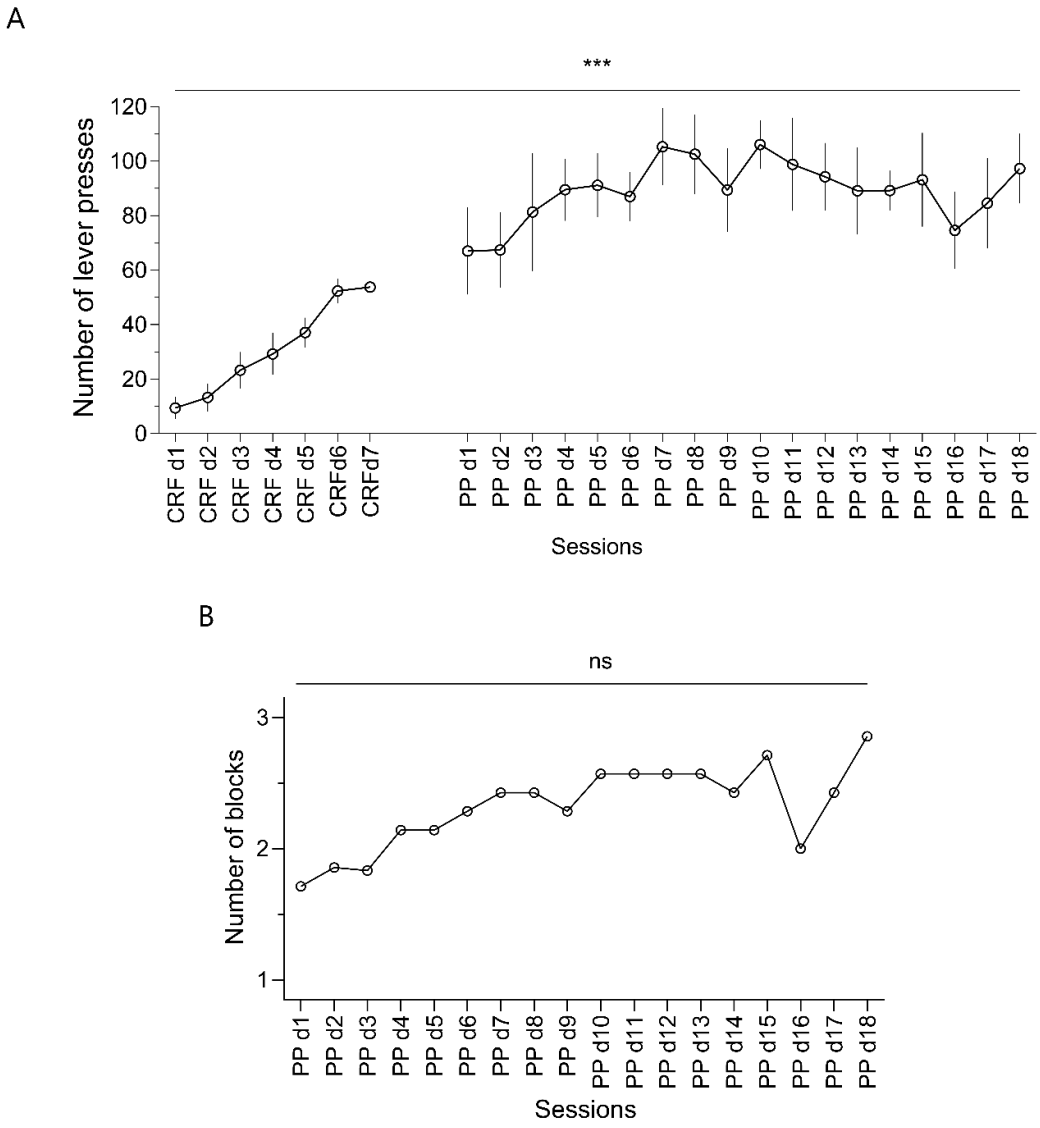

Figure 4.22 Mice learn to press a lever to obtain rewards in a two-action probabilistic instrumental task.
A Mean number of lever presses per session in a two-action probabilistic instrumental task. The first 7 days represent training in a CRF schedule (n = 7), in which only an oral reward of a non-caloric sweetener - sucralose 0.04 % - was obtained after each lever press. In the following days, mice were in a probabilistic postingestive (PP) schedule (n = 7), in which each lever could lead to an oral reward paired with postingestive reward administered directly in the stomach. The postingestive reinforcer was delivered through a previously implanted gastric catheter Importantly, one lever led to an infusion of a non-caloric reinforcer - sucralose 0.04 % - and the other lever led to an infusion of caloric carbohydrate solution - sucrose 20 %. Mixed effects analysis $F_{4,23}$= 7.17 ***p = 0.0008.l Mixed effects analysis (CRF d1 – CRF d7) $F_{2,14}$= 17.1 ***p = 0.0001. Mixed effects analysis (PP d1 – PP d8) $F_{3,21}$= ns p = 0.5. **B** Mean number of blocks per session in a two-action probabilistic instrumental task. During the PP schedule. For the PP schedule a reward consists of an oral reward – sucralose 0.04 % - paired with an IG reward – sucrose 20 % or sucralose 0.04 %. A block consists of, on average, 25 rewards. Once animals had reached the criteria to complete a full block, the lever that had high probability of delivering a reward (80 %) becomes the lever with the low probability of reward (20 %) and vice-versa. The probability switch associated with each lever was designated as a transition. Mixed effects analysis $F_{3,21}$= 1.3, ns p = 0.3. Data is presented as mean ± SEM.

Afterwards, preference for each lever during the PP schedule was evaluated (**Figure 4.23**). Preference was calculated by dividing the number of lever presses for a given lever by the total number of lever presses within a session when the lever had a high probability of delivering rewards. **Figure 4.23 A** represents the mean preference, in percentage, associated with each lever per session during the PP schedule when each lever had high probability. For this and the following figures, yellow represents the lever that led to the PI

delivery of sucrose 20 % (caloric carbohydrate solution), and black represents the lever that led to the PI delivery of sucralose 0.04 % (non-caloric solution).

The results show that preference for the sucrose lever seems to be, in the beginning, similar to the sucralose lever and, throughout time, preference for sucrose lever seems to be higher when compared with preference for sucralose lever (**Figure 4.23 A**, mixed effects analysis main effect lever *p = 0.01). Furthermore, the difference observed increases even further with training (**Figure 4.23 B**, paired t-test **p = 0.008).

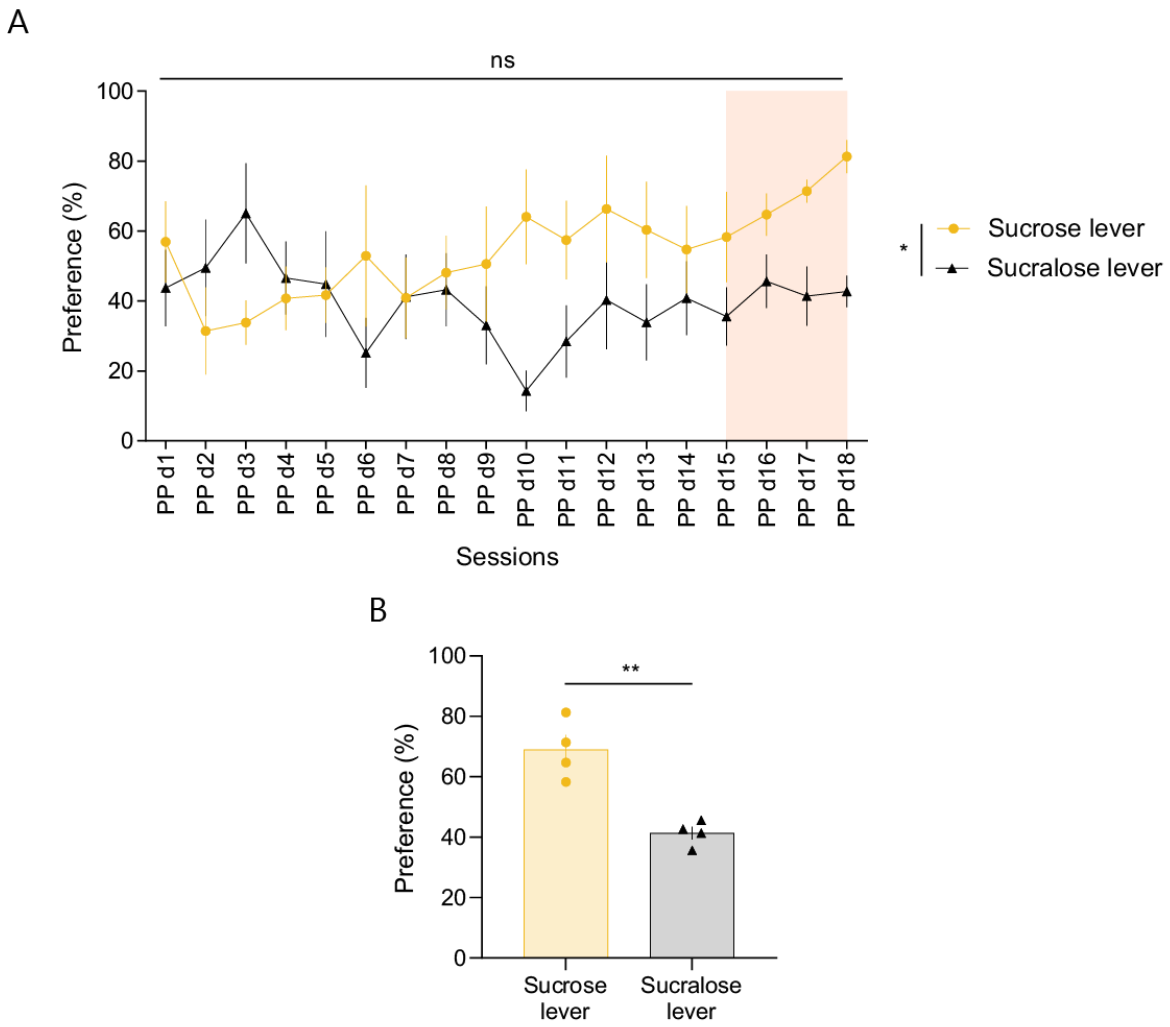

Figure 4.23 Mice seem to prefer the lever associated with intragastric delivery of sucrose.
A Mean preference, in percentage, associated with each lever per session during the PP schedule (n = 7) Preference was calculated for when each lever had high probability (80 %) of delivering rewards. In this and the following figures, the lever that led to the postingestive delivery of sucrose 20 % (caloric carbohydrate) is represented in yellow (full yellow circles) and the lever that led to the postingestive delivery of sucralose 0.04 % (non-caloric) is represented in black (full black triangles). Mixed effects analysis main effect for sessions $F_{5,49}$= 0.88, ns p = 0.5; main effect for lever $F_{1,12}$= 9.04, *p = 0.01; sessions and lever interaction $F_{31,305}$= 1.9, **p = 0.003. **B** Mean preference, in percentage, associated with each lever when the lever had high probability of delivering rewards for the last 4 sessions of the PP schedule (n = 7). Paired t-test **p = 0.008. Data is presented as mean ± SEM.

Subsequently, it became important to dissect further preference for the reinforcers associated with each lever during a transition. First, preference for each lever during a transition was plotted for the first 6 and the last 4 PP sessions (**Figure 4.24 A and C**, respectively). Preference during a transition was calculated using

a moving window of 5 lever presses for 20 trials. For **Figure 4.24 A and C** the first 5 trials (from -5 to 0) represent the time when each lever had a high probability of delivering rewards. The following 15 trials (from 0 to 15) represent the time when each lever had a low probability of delivering rewards. Mean preference values (**Figure 4.24 B and D**) were calculated using the last 5 trials where each lever had a high and low probability of delivering the rewards.

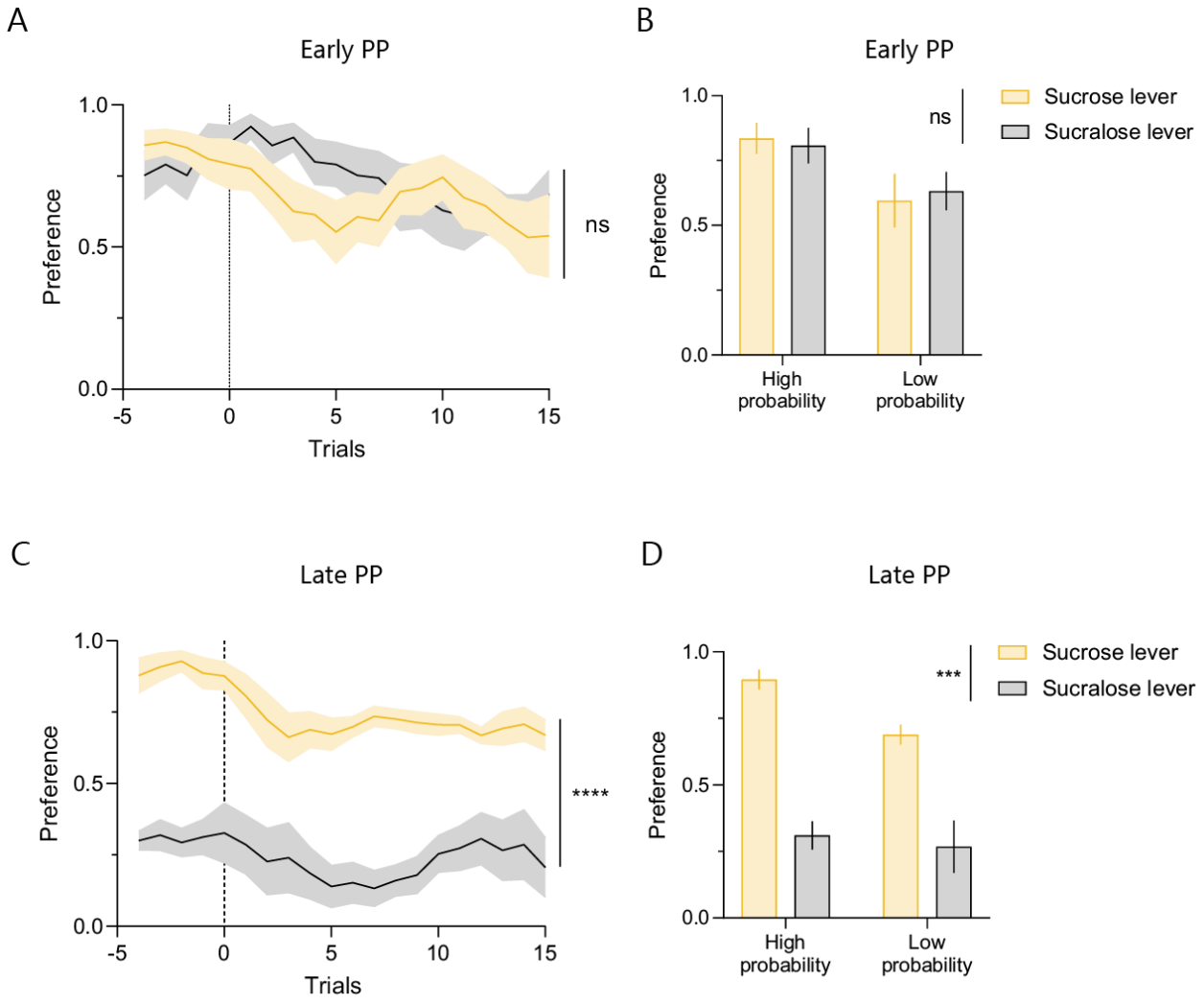

Figure 4.24 Preference for postingestive reinforcer is shaped throughout the two-action probabilistic instrumental task.

A Preference for each lever for the first 6 sessions of the PP schedule (n = 7). The lever that led to the postingestive delivery sucrose 20 % (caloric carbohydrate solution) is represented in yellow, and the lever that led to the postingestive delivery of sucralose 0.04 % (non-caloric solution) is represented in black. Preference was calculated for the first 6 sessions using a moving window (5 lever presses) for 20 trials with a transition – lever with high probability (80 %) of reward switches to lever with low probability of reward (20 %) and vice versa. The first 5 trials (from -5 to 0) represent the trials where lever had a high probability to deliver oral reward paired with an IG reward. The following 15 trials (from 0 to 15) represent the trials where lever had a low probability to deliver oral reward paired with an IG reward. Two-way ANOVA main effect for lever $F_{1,11}$= 0.39, ns p = 0.5; main effect for trial $F_{3,37}$= 4.3, **p = 0.008; lever and trial interaction $F_{19,209}$= 1.9, *p = 0.01. **B** Mean preference for each lever when they had a high and low probability to deliver oral reward paired with an IG reward for the first 6 sessions of the PP schedule (n = 7). The values were calculated using the last 5 trials where each lever had a high and low probability to deliver the rewards. Two-way ANOVA main effect for lever $F_{1,22}$= 0.003, ns p = 0.9; main effect for probability $F_{1,22}$= 7.2, *p = 0.01. **C** Preference for each lever for the last 4 sessions of the PP schedule (n = 7). Preference was calculated as described in A. Two-way ANOVA main effect lever $F_{1,10}$= 59.6, ****p < 0.0001; main effect for trial $F_{3,30}$= 3.8, *p = 0.02; lever and trial interaction $F_{19,190}$=1.1, ns p = 0.4. **D** Mean preference for each lever when they had a high and low probability to deliver oral reward paired with an IG

reward for the last 4 sessions of the PP schedule (n = 7). Mean preference was calculated as described in B. Two-way ANOVA main effect for lever $F_{1,20}$= 80.4, ****p < 0.0001; main effect for probability $F_{1,20}$= 4.9, *p = 0.04. Data is presented as mean ± SEM.

Figure 4.24 A shows no significant difference in preference between levers for the first 6 sessions of the PP schedule (**Figure 4.24 A** early PP, two-way ANOVA main effect for lever ns p = 0.5). This result along with **Figure 4.24 B** indicates that, early in training, animals follow the probabilities of receiving rewards since, for the same lever, animals would press more when the probability was high and less when the probability was low. This pattern of response occurred independently of the reinforcer infused.

After several days of PI stimuli (**Figure 4.24 C and D**), mice develop a clear preference for the lever associated with the PI delivery of the caloric carbohydrate – sucrose 20 % (**Figure 4.24 C** late PP, two-way ANOVA main effect lever ****p < 0.0001). This preference sustained and is independent of the lever switch probabilities (**Figure 4.24 D**). Meaning that the lever associated to the sucrose was always pressed independently of being highly probable or not. The opposite occurred for the lever associated to sucralose.

4.3.1. Mice do not show a clear preference upon lever reversal

In the same group of animals after observing a clear preference for the sucrose lever independently of the probabilities, a switch between the PI stimuli and lever associated with it was done. The lever that was previously associated with IG delivery of sucrose 20 % (caloric), was now associated with IG delivery sucralose 0.04 % (non-caloric). Likewise, the lever previously associated to IG delivery of sucralose 0.04 %was changed to IG delivery of sucrose 20 %. This was designated as the reversal (R) schedule which had the same structure as the PP schedule.

As previously done, the number of lever presses and the number of blocks per session was calculated and plotted (**Figure 4.25**). The results show that both the number of lever presses and the number of blocks per session did not significantly change during the R schedule (**Figure 4.25 A**, mixed effects analysis ns p = 0.3; **Figure 4.25 B**, mixed effects analysis ns p = 0.3). Comparing the number of blocks for the last day of the PP schedule (PP d18), and the last of the R schedule (R d14) corroborates the previous observation (**Figure 4.25 C**, Paired t-test ns p = 0.3). The results indicate that mice maintained performance levels after lever reversal (R schedule).

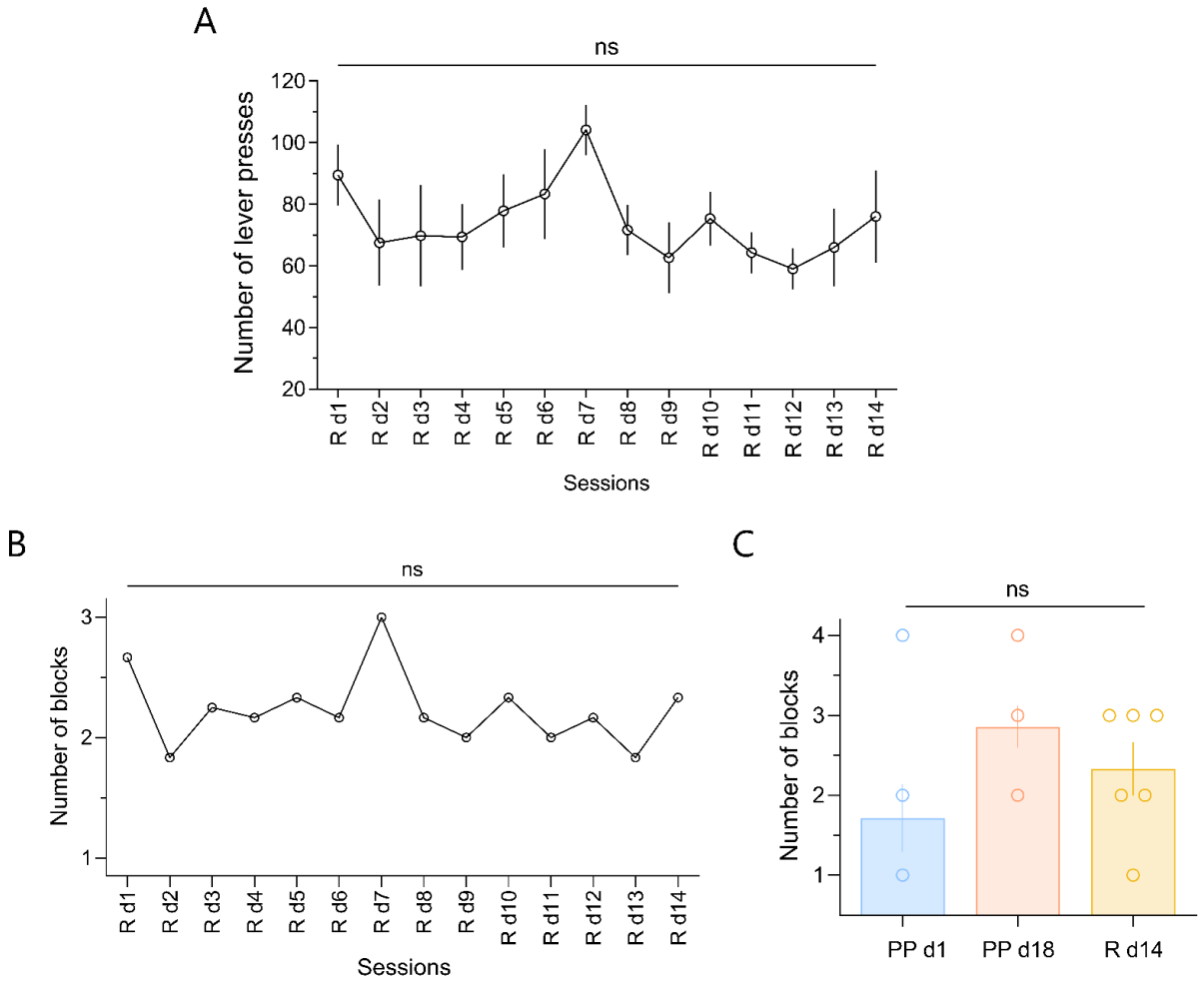

Figure 4.25 The number of lever presses and blocks did not change upon lever reversal.
A Mean number of lever presses per session in a two-action probabilistic instrumental task after lever reversal. In the last days 14 sessions, mice were in a reversal (R) schedule (n = 6), in which the IG stimuli previously associated changed to the opposite lever. As before, one lever led to an infusion of a non-caloric sweetener - sucralose 0.04 % - and the other lever led to an infusion of caloric carbohydrate - sucrose 20 %. In R schedule the postingestive rewards associated with each lever were switched in relation to the PP schedule. The lever previously associated with the non-caloric solution now delivered the caloric

carbohydrate solution and vice versa. Mixed effects analysis $F_{3,17}$= 1.29, ns p = 0.3.**B** Mean number of blocks per session during the R schedule in the two-action probabilistic instrumental task. A block consists of the number of lever presses required to reach, on average, 25 rewards, and consequently changed the probabilities of getting a reward. As previously observed, the number of blocks maintained stable during the R (n = 6) schedule. n. Mixed effects analysis $F_{3,17}$= 1.3, ns p = 0.3. **C** Mean number of blocks for three sessions (PP d1, PP d18, and R d14) in a two-action probabilistic instrumental task. Mixed effects analysis $F_{1,2}$= 1.0, ns p = 0.1. Paired t-test (PP d18 and R d14) ns p =0.3. Data is presented as mean ± SEM.

Figure 4.26 A represents the mean preference, in percentage, associated with each lever per session during the R schedule when the probability for that lever was high (80 %). The curves for sucrose and sucralose preference seem to overlap (**Figure 4.26 A**, mixed effects analysis main effect for lever ns p = 0.06). The results are similar and superimposable when restricting preference for only the last 4 sessions of the R (**Figure 4.26 A and B**, paired t-test ns p = 0.1).

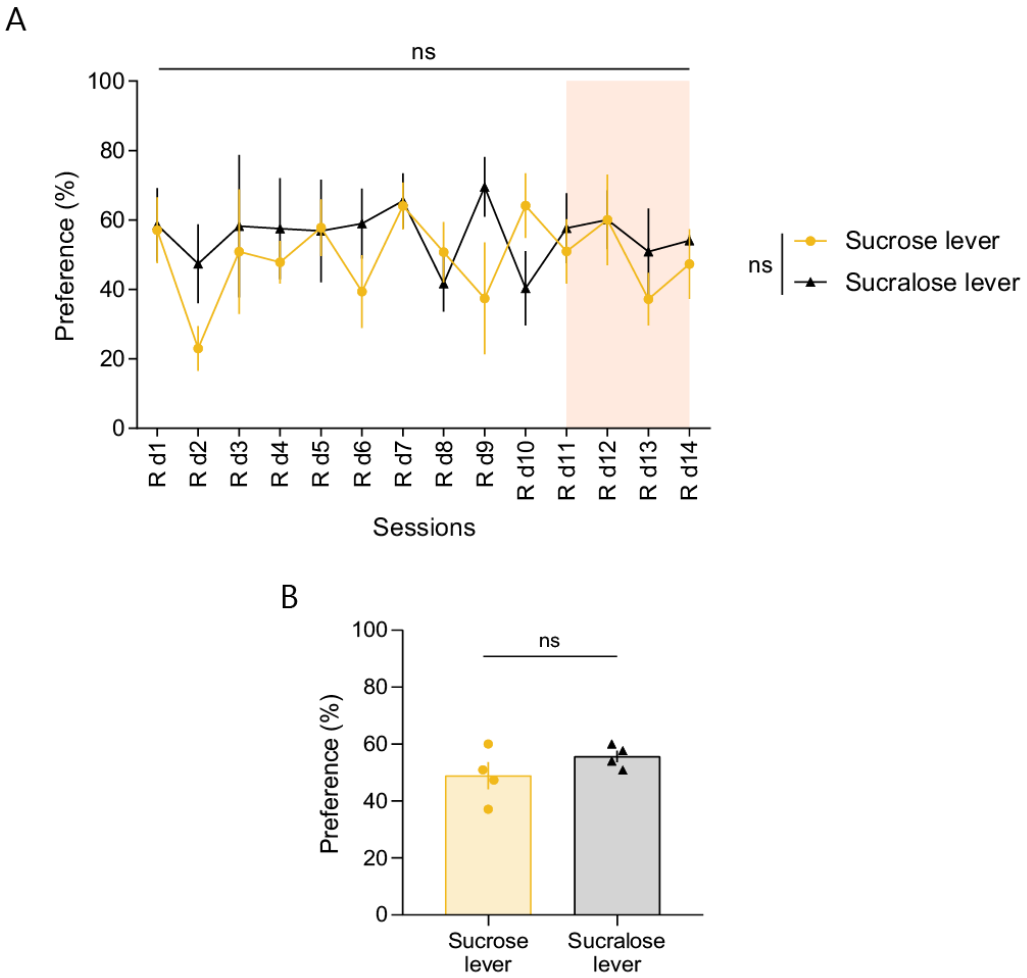

Figure 4.26 Preference does not seem to change in the R schedule.
A Mean preference, in percentage, associated with each lever per session. (R n = 6) Preference was calculated for when each lever had high probability of delivering rewards. In this and the following figures, the lever that led to the postingestive delivery sucrose 20 % (caloric carbohydrate) is represented in yellow (full yellow circles), and the lever that led to the postingestive delivery of sucralose 0.04 % (non-caloric) is represented in black (full black triangles). Mixed effects analysis main effect for sessions $F_{4,39}$= 0.97, ns p = 0.4; main effect for lever $F_{1,12}$= 4.4, ns p = 0.06; sessions and lever interaction $F_{1,128}$= 2.5, ns p = 1. **B** Mean preference, in percentage, associated with each lever when the lever had high probability of delivering rewards for the last 4 sessions of the R schedule. Paired t-test ns p = 0.1. Data is presented as mean ± SEM.

The difference observed in preference for the reinforcer associated with each lever between the PP and R schedules revealed that it was also important to explore further preference in the R schedule during a transition. Thus, preference for each lever during a transition was plotted for the last 4 sessions of R (**Figure 4.27 A**). The results show no significant difference in preference between levers (**Figure 4.27 A**, two-way ANOVA main effect for lever ns p = 0.4),

Subsequently, the mean preference for each lever was plotted for when they had a high and low probability of delivering an oral reward paired with an IG reward (**Figure 4.27 B**). Unexpectedly, **Figure 4.27 B** shows that animals always prefer the lever with a high probability of delivering a reward independently of reinforcer (**Figure 4.27 B**, two-way ANOVA main effect for probability **p = 0.009).

The R results show that animals are slowly shifting their pattern of response when compared to the PP schedule. However, due to considerable problems with the chronic intragastric catheters started to appear at this stage, it was not possible to continue this procedure for a longer period of time. Despite this, it was postulated that with more days of PI stimuli in the R schedule, a clear preference for sucrose would rise and, thus, a total reversion in lever preference would be expected.

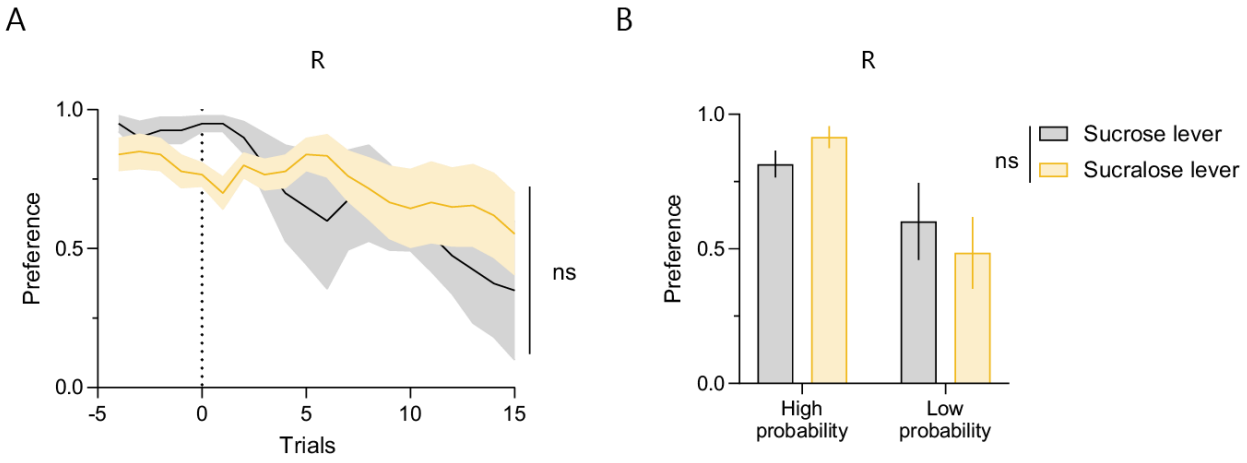

Figure 4.27 Preference seems to depend on lever probability in the R schedule.
A Preference for each lever for the first 4 sessions of R schedule (n = 6). The lever that led to the postingestive delivery sucrose 20 % (caloric carbohydrate solution) is represented in yellow, and the lever that led to the postingestive delivery of sucralose 0.04 % (non-caloric solution) is represented in black. Preference was calculated for the first 6 sessions using a moving window (5 lever presses) for 20 trials with a transition – lever with high probability (80 %) of reward switches to lever with low probability of reward (20 %) and vice versa. The first 5 trials (from -5 to 0) represent the trials where lever had a high probability to deliver oral reward paired with an IG reward. The following 15 trials (from 0 to 15) represent the trials where lever had a low probability to deliver oral reward paired with an IG reward. Two-way ANOVA main effect for lever $F_{1,155}$= 0.76, ns p = 0.4; main effect for trial $F_{19,155}$= 2.42, **p = 0.02; lever and trial interaction $F_{19,155}$= 0.75, ns p = 0.8. **B** Mean preference for each lever when they had a high and low probability to deliver oral reward paired with an IG reward for the first 4 sessions of the R schedule (n = 6). The values were calculated for the first 4 sessions using the last 5 trials where each lever had a high and low probability to deliver the rewards. Two-way ANOVA main effect for lever $F_{1,16}$= 0.0058, ns p = 0.9; main effect for probability $F_{1,16}$= 8.7, **p = 0.009. Data is presented as mean ± SEM.

It is also important to note that the body weight of every mouse was recorded and monitored to guarantee that it stayed within 85-80 % of the initial body weight. Mice that underwent 3 deprivation protocols show a decrease in weight, as expected, that stabilizes around training day 5 (**Supplementary Figure 7.7**, mixed effects analysis ***p = 0.0002. Notably, change of deprivation protocol leads to an initial weigh loss that stabilizes again (**Supplementary Figure 7.7**, days 17 - 48) after 2 days. Likewise, the body

weight of the animals from the second group initially decreased and then stabilized weight around training day 7 (**Supplementary Figure 7.8**, one-way repeated measures ANOVA (day 0 – 7, n = 7) **** $p < 0.0001$; mixed effects analysis (day 8-50) ns $p = 0.5$).

The two-action probabilistic instrumental task showed that when given the choice between an IG infusion of a non-caloric solution – sucralose - and an IG infusion of a caloric solution – sucrose – mice, after PI stimuli, choose the caloric solution and this is maintained even when the reward probabilities are low. Thus, the results shown in this work further empathize the importance of PI feedback on food-seeking behaviour. It also showed clear evidence of the impact of postingestive stimuli in learning and their importance in RL.

4.4. Bibliography

1. de Araujo IE, Oliveira-Maia AJ, Sotnikova TD, et al. Food reward in the absence of taste receptor signaling. *Neuron*. Mar 27 2008;57(6):930-41. doi:10.1016/j.neuron.2008.01.032

2. Oliveira-Maia AJ, Roberts CD, Walker QD, et al. Intravascular food reward. *PLoS One*. 2011;6(9)doi:10.1371/journal.pone.0024992

3. Fernandes AB, Alves da Silva J, Almeida J, et al. Postingestive Modulation of Food Seeking Depends on Vagus-Mediated Dopamine Neuron Activity. *Neuron*. Jun 3 2020;106(5):778-88. doi:10.1016/j.neuron.2020.03.009

4. Han W, Tellez LA, Perkins MH, et al. A Neural Circuit for Gut-Induced Reward. *Cell*. 2018;175(3):665-78. doi:10.1016/j.cell.2018.08.049

5. Tan HE, Sisti AC, Jin H, et al. The gut-brain axis mediates sugar preference. *Nature*. Apr 2020;580(7804):511-16. doi:10.1038/s41586-020-2199-7

6. Li M, Tan H-E, Lu Z, Tsang KS, Chung AJ, Zuker CS. Gut–brain circuits for fat preference. *Nature*. 2022/09/07 2022;doi:10.1038/s41586-022-05266-z

7. Beier KT, Steinberg EE, DeLoach KE, et al. Circuit Architecture of VTA Dopamine Neurons Revealed by Systematic Input-Output Mapping. *Cell*. Jul 30 2015;162(3):622-34. doi:10.1016/j.cell.2015.07.015

8. Akam T, Rodrigues-Vaz I, Marcelo I, et al. The Anterior Cingulate Cortex Predicts Future States to Mediate Model-Based Action Selection. *Neuron*. 2021;109(1):149-63. doi:10.1016/j.neuron.2020.10.013

9. Castro-Rodrigues P, Akam T, Snorasson I, et al. Explicit knowledge of task structure is a primary determinant of human model-based action. *Nat Hum Behav*. 2022;6(8):1126-41. doi:10.1038/s41562-022-01346-2

10. Tabbara RI, Maddux JM, Beharry PF, Iannuzzi J, Chaudhri N. Effects of sucrose concentration and water deprivation on Pavlovian conditioning and responding for conditioned reinforcement. *Behav Neurosci*. Apr 2016;130(2):231-42. doi:10.1037/bne0000138

5. Discussion

This study focused on the effect of postingestive (PI) nutrient sensing on dopaminergic neuronal responses. Dopaminergic neurons of the ventral tegmental area (VTA) and substantia nigra pars compacta (SNc) were recorded using calcium imaging while different reinforcers were infused directly into the stomach. Additionally, dopamine transients in the striatum, more specifically the nucleus accumbens (NAc) and dorsal-lateral striatum (DLS), were monitored using fibre photometry in the same experimental conditions.

Results show that carbohydrates lead to a consistent significant increase in VTA dopaminergic neuronal activity, which also seem to reflect an increase in dopamine release in the ventral striatum (NAc). In opposition, SNc dopaminergic neurons do not seem to be able to distinguish any of the reinforcers infused. This result seems to also be corroborated by measurements of dopamine dynamics in the dorsal striatum (DLS), where reinforcers showed superimposable profiles.

Based on the high capacity of increase and release of dopamine in the ventral areas of the brain, this project also focused on the development a novel probabilistic task based on PI sucrose stimuli response. The task was developed to further dissect the importance of PI stimuli in decision-making and reinforcement learning (RL).

Mice were trained to choose between two levers that had a given probability of delivering an oral reward paired with an intragastric (IG) reward. One lever led to the delivery of IG sucrose (caloric), while the other led to the delivery of IG sucralose (non-caloric). Results showed that, after training, mice developed a clear preference for the lever associated with the IG delivery of the caloric solution, even in conditions where the reward probability was low.

Here, we discuss the results obtained and examine how this ongoing work may impact our knowledge on feeding behaviour.

5.1. Dopaminergic regions respond differently to intragastric infusions of different nutrients

Our initial hypothesis was that central ventral regions – VTA and NAc – would respond to sucrose (carbohydrates), whereas dorsal regions – SNc and DLS – would respond to corn oil (lipids).

The work began with the monitorization of VTA dopaminergic neurons while mice were infused with three reinforcers – isocaloric solutions of sucrose and corn oil, and sucralose, a non-caloric solution. Corn oil was chosen since this lipid had reinforcing properties when given orally (**Supplementary Figure 7.4**). Sucrose and corn oil concentrations were chosen so that solutions were isocaloric. Sucralose was selected as a control since it is a non-caloric artificial sweetener and would disentangle not only stretching effects associated to IG delivery but also possible effects of activating sweet receptors in the gut. Dopaminergic activity was recorded using calcium imaging before, during and after IG solutions administration.

Results show there is a significant increase in mean activity of VTA dopaminergic neurons when IG sucrose was delivered. The pattern of response is lower in activity for both IG corn oil and IG sucralose infusions (**Figure 4.3**). Accordingly, the percentage of positively modulated neurons was significantly higher for IG sucrose when compared to the other two reinforcers (**Figure 4.4 A**).

The percentage of positively modulated neurons between corn oil and sucralose sessions did not differ. Despite this, when the mean activity of positively modulated corn oil neurons was plotted, the traces revealed a very similar profile to IG sucrose. The traces revealed higher activity that was also more sustained in time when compared to IG sucralose traces. These results indicate that, although the number of neurons

that significantly increase their activity after IG corn oil is similar to sucralose, their profile of activity is totally different, and more similar to the IG sucrose response, which indicates that corn oil pattern of response is different from the pattern of response for the non-caloric solution.

The results between VTA response to IG sucrose and sucralose infusions are in accordance with a recent study published by our group. The study that showed that VTA dopaminergic neurons respond specifically to sucrose in comparison to the same artificial non-caloric sweetener [1].

Cell pairing between different reinforcer sessions allow to track the same neuron throughout sucrose and corn oil sessions. Results from this analysis confirmed previous results that the percentage of positively modulated neurons that respond specifically to IG sucrose is higher than neurons that specifically respond to IG corn oil (**Figure 4.6 A**). From the paired neurons, around 16 % respond specifically to sucrose infusions, while only 6 % respond specifically to corn oil (**Figure 4.6 B**).

Results from this work are in accordance with several data regarding ventral dopamine responses to carbohydrates [2, 3]. Additionally, recent literature has also shown that, in vagal mediated responses from nutrients , such as fat, infused in the gut, only a small percentage of vagal neurons were activated (8 % fat specific [4]). This indicates that PI stimuli only activates a small percentage of vagal neurons, and, in turn, these neurons most likely activate a small percentage of VTA dopamine neurons. Thus, even knowing that we only found 6% of neurons that specifically respond to corn oil, this percentage could be enough to reinforce lipids and modulate feeding decisions. In fact, several lines of evidence have shown that to reinforce an action that ultimately led to addictive behaviour only an increase of small percentage of dopamine in the striatum is needed [5]. This corroborates the evidence that corn oil, although activating a small percentage of neurons in the VTA, could be sufficient to increase striatal dopamine and, most likely, shape feeding behaviour as it was observed in the one-lever pressing behavioural task (**Supplementary Figure 7.4**) and associative learning experiments [6]. Alternatively, considering that the percentage of neurons that respond to corn oil is so little, these results could be attributed to randomness. To answer this, further analysis needs to be performed, including the percentage of positively modulated neurons in a session with no IG infusion. This is a further step that needs to be addressed.

Additionally, pattern of response of hypothalamic nuclei (homeostatic circuit) is very similar to the pattern of responses observed in this work for the VTA. Meaning that neurons from the hypothalamus respond to IG ingestion of fat and sugar, when compared to water [7].

Interestingly, the percentage of positively modulated neurons that respond to both types of reinforcers is higher than both percentages for nutrient specific responses (**Figure 4.6 B**, 20 %). Furthermore, the neuronal traces are superimposable independently of the reinforcer administered (**Figure 4.7 B**, sucrose or corn oil), which could be an indicator that these neurons could be responding to the same stimuli that appears to be calorie related. This pattern of response has been observed in other circuits involved in feeding behaviour and, therefore, it is not surprising that VTA dopaminergic neurons could have different layers of responses, according to the characteristics of the food stimuli consumed.

Moreover, most of the paired neurons did not positively respond to either sucrose or corn oil. A percentage of these neurons could also be negatively modulated by one or both reinforcers. To investigate this, an analysis similar to the one performed for positively modulated neurons along with cell paring between sucrose and corn oil needs to be performed. Alternatively, some of these neurons could simply not be modulated by ingestion and, alternatively, participate in circuits related to other functions [8-10].

VTA dopaminergic neurons project to the NAc [9], which is a brain area that has been described to respond to pleasurable rewards. In the context of PI stimuli, there is clear evidence that ventral striatum respond to carbohydrates, such as glucose and sucrose [2]. However, recent data have also shown specific pattern of activity in dorsal areas when afferent gut neurons were activated. The same authors have also conflicting evidence showing higher responses for dorsal striatum when glucose and intralipid were infused in the gut. [11] These results led us to specifically target within the same animal dopamine dynamics in the NAc and DLS while infusing isocaloric reinforcers, including sucrose, corn oil and sucralose.

Fibre photometry preliminary results showed dopamine levels in the ventral striatum have a tendency to increase in sessions where sucrose is infused, when compared to corn oil and sucralose sessions (**Figure 4.18 A**). These results for sucrose corroborate evidence found in the literature and support the results we obtained for dopaminergic neuronal activity in the VTA.

Altogether, data obtained for ventral dopaminergic neurons and their projections in the ventral striatum indicate that these regions have a higher pattern of response to carbohydrates.

Dopaminergic neuronal activity was also monitored and recorded in the SNc while mice were infused with the reinforcers previously used directly into the stomach. It is important to note that the success rate for surgeries in this region was lower, when compared to the VTA, and, therefore, the number of animals recorded is much lower and had very few neurons (average of 4 neurons per animal). We believe that this is related with anatomy and size of this structure (**Figure 3.2 B**). The smaller the structure the harder it is to image the neurons and the SNc is a very thin nucleus. For most of our surgeries the position of the lens for the imaging was not satisfactory to ensure maximal recording of the dopaminergic neurons, even though the coordinates were adjusted.

Results seem to show that mean activity of SNc dopaminergic neurons was similar between the three reinforcer sessions (**Figure 4.13**). Likewise, our results show that the percentage of positively modulated neurons was not significantly different between any of the reinforcers tested (**Figure 4.14**). The traces for positively modulated neurons for different sessions also had a very similar profile. These results indicate that SNc response is not nutrient-specific, since sucrose and corn oil responses were comparable, and that pattern of response is also not based on caloric content, since sucralose response was similar to both sucrose and corn oil responses.

Fibre photometry studies in the DLS seem to support the results previously observed for the SNc, since dorsal striatal response do not show significantly differences between the reinforcers infused (**Figure 4.18 B**). The results obtained go against our initial hypothesis.

Previous literature has shown that gut-to-brain sensory responses, in awake freely behaving animals, drives dopamine release in the dorsal striatum. Additionally, there is evidence that IG infusion of fat caused an increase in dopamine in the dorsal striatum, although the concentration of lipid needed to induce significant changes in dopamine release needed to be above 30% [12]. In fact, while using a similar concentration of lipids to the one used in this project, the authors did not find an increase in dorsal striatal dopamine dynamics, corroborating our results. Considering that the objective of this work was to test isocaloric solutions, the percentage of lipids used was 9%. According to these authors, this concentration might not be enough to induce dopamine release in the dorsal striatum, which could explain our results.

Although we did not observe any significant difference in the pattern of activity between the reinforcers, there was always a significant percentage of neurons that respond after IG administration (on average 15%). This observation led us to hypothesize that SNc and its striatal projections could respond to a physiological

mechanism that always occurs after consumption, sensing mostly mechanical alterations within the gastrointestinal tract.

Considering that lipids are a very heterogenous source of fat, another lipidic solution was tested in both fibre photometry and SNc dopaminergic studies. For this, an isocaloric SMOF lipid solution, constituted of different lipids, was tested along with corn oil.

Interestingly, the response profile for SMOF lipid in the NAc seems to be very similar to the profile for sucrose in the same area (**Figure 4.19 A**). This could indicate that ventral response to lipidic solutions may depend on the type of lipid injected. In fact, it has been shown that different types of lipids condition flavour preference differently [13]. This evidence, however, needs to be further explored in order to conclude that ventral response may depend on the type of lipid. Preliminary results for central dorsal regions show that the responses of SNc to corn oil and SMOF were very similar (**Figure 4.16**). Accordingly, DLS response to these lipidic solutions was not significantly different (**Figure 4.19 B**). Contrary to what was observed for striatal ventral regions, the type of lipid does not seem to influence dorsal response.

Overall, results from our work regarding monitorization of dopaminergic neuronal activity and dopamine dynamics demonstrates that ventral and dorsal dopaminergic regions respond differently to different reinforcers. More specifically, we have shown that both the VTA and NAc have higher responses patterns to IG sucrose, a carbohydrate, when compared to an IG lipid (corn oil) or a non-caloric control (sucralose). We also identified a subpopulation of dopaminergic neurons that responds specifically to sucrose in the VTA and a second subpopulation of neurons that respond to the caloric content of the food ingested. Moreover, dorsal regions - SNc and DLS - did not specifically respond to any type of nutrient showing similar patterns of response regardless of the reinforcer infused.

5.2. Mice in a probabilistic two-action task press more to obtain intragastric infusions of a caloric solution

We developed a novel probabilistic two-action behavioural task that stands out from previous work due to its unique behavioural design and the possibility of exploring the importance of PI stimuli in RL, with the goal of exploring the importance of PI stimuli in lever pressing behaviour.

The two-action probabilistic task was purposefully designed so that animals had to make a choice between two levers. Each lever led to an oral reward paired with an IG reward. The oral reward was always sucralose, an artificial non-caloric sweetener. However, the IG reward associated with each lever was distinct. One lever was associated with IG infusions of sucrose – caloric solution -, while the other was associated with sucralose. Additionally, the probability of reward delivery associated with each lever, changed between high (80 %) and low (20 %) probability (**Figure 3.6 B**).

Our hypothesis was that mice would press more the lever associated with IG infusions of caloric solution – sucrose – independently of the probability associated with that lever.

Results from this work reveal that water and food deprived mice, in a continuous reinforcement (CRF) schedule, learn to press a lever to obtain oral rewards at distinct rates (**Figure 4.21**). The reason behind this phenomenon is unknow but, considering that animals had the same genetic background (C57BL6/J), we believed that it could connected to the deprivation state ascertain to each animal. We postulate that mice need to reach an optimal deprivation state where weight loss leads to high motivation and increased exploratory behaviours without excessive or extreme physiological phenomenon, such as extreme thirst or

hunger, that ultimate affect animal behaviour and learning. Alternatively, learning rate differences could be related to side bias or technical problems, for example, with the chronic gastric catheter implantation.

In the postingestive probabilistic (PP) schedule mice completed, on average, 89 lever press per sessions which translated to an average of 2 blocks, where each block led to, on average, 25 rewards (**Figure 4.22**). We consider that performance could be optimized with some experimental design alteration. For example, changing the operant box so that it has two magazines available, one for each lever would probably benefit the learning and the distinction between the value of each action. This design alteration would strengthen the correlation between side and reinforcer infused. Alternatively, levers could be switched to nose pokes, which would have the advantage of rewarding the action in the same place where the action is performed, enabling a clear distinction between the two actions and the two different outcomes. The concentration of the oral reward (sucralose) could be changed in order to make the solution more palatable. Palatability could be assessed using sucralose preference test as previously performed for sucrose solutions [14].

Even knowing the number of blocks could be optimized the results show that, with training mice have a clear preference for the lever that leads to IG infusions of sucrose when compared to sucralose. Moreover, this preference becomes more evident when comparing first and last training days (**Figure 4.24 A vs C**). Additionally, it was possible to observe that before IG assignment, animals consistently preferred the lever with the higher probability of delivering oral reward (**Figure 4.24 B vs D**), which is a good indication that mice were able to track the probability change.

After animals had completed a considerable amount of PP sessions, we decided to switch the IG reinforcer associated with each lever, so the lever previously associated with IG sucralose would now be associated with IG sucrose and vice-versa. Subsequently, performance and preference were assessed. Notably, the number of training days for this schedule – reversal (R) schedule – was only 7 days due to several constraints associated to the chronic gastric catheter implantation and, this, implantation and, thus, conclusions must be taken carefully.

The 7 days of R schedule already showed a slight tendency of increased preference for the lever now associated to IG sucrose and a decrease in the lever pressing behaviour for the lever now associated to the IG sucralose (**Figure 4.27**). It became clear that the preference for the lever associated to the caloric solution would become more evident with more training days. It was not possible to provide more training days because of complications with the chronic gastric catheters that lead to a reduction in the number of animals and to the end of the experiment.

Although the reversal results did not generate robust conclusions, the development of two-action probabilistic instrumental task showed that animals are able to track PI stimuli in an environment where the possibilities are uncertain. Mice clearly develop a preference for the lever associated to the IG delivery of sucrose over the lever associated with IG sucralose infusion independently of the probability assigned to that lever. One important factor to discuss is the number of training days with PI stimuli that are necessary to clearly exhibit this preference, that was higher than expected- 14 days. This could be explained based on the task structure and the temporal differences between detection of orosensory (oral sucralose reward) and PI signals by reward circuitry. As we know, preingestive signals are conveyed to central nervous regions much faster than PI signals. Therefore, animals could be already performing a second action and assigning to that action the IG value from the previous action, making it difficult to distinguish between the value of PI rewards of each lever. Additionally, since mice are consuming solution and receiving IG infusions, satiety levels during the task are not constant and could interfere with the performance level. Thus, it is important

to further explore this by constricting analysis to the first minutes of the session and compare it to the last minutes to see if there are any alterations in the lever pressing behaviour.

Our results are in accordance with previous findings that highlighted the reinforcing properties of IG delivery of a caloric solution – sucrose – in a one lever instrumental task. By applying reinforcement learning (RL) principles, this task allowed us to show that PI stimuli regarding caloric content impacts choice. This, the two-action probabilistic task confirmed the importance of PI stimuli on food-seeking behaviour. Nevertheless, there is still very limited knowledge in this area with a lot to explore regarding how PI feedback impacts decision making, and learning based on previous actions.

5.3. Bibliography

1. Fernandes AB, Alves da Silva J, Almeida J, et al. Postingestive Modulation of Food Seeking Depends on Vagus-Mediated Dopamine Neuron Activity. *Neuron*. Jun 3 2020;106(5):778-88. doi:10.1016/j.neuron.2020.03.009

2. Oliveira-Maia AJ, Roberts CD, Walker QD, et al. Intravascular food reward. *PLoS One*. 2011;6(9)doi:10.1371/journal.pone.0024992

3. de Araujo IE, Oliveira-Maia AJ, Sotnikova TD, et al. Food reward in the absence of taste receptor signaling. *Neuron*. Mar 27 2008;57(6):930-41. doi:10.1016/j.neuron.2008.01.032

4. Li M, Tan H-E, Lu Z, Tsang KS, Chung AJ, Zuker CS. Gut–brain circuits for fat preference. *Nature*. 2022/09/07 2022;doi:10.1038/s41586-022-05266-z

5. Piazza PV, Deroche-Gamonent V, Rouge-Pont F, Le Moal M. Vertical shifts in self-administration dose-response functions predict a drug-vulnerable phenotype predisposed to addiction. *J Neurosci*. 2000;20(11):4226-32. doi:10.1523/jneurosci.20-11-04226.2000

6. Sclafani A. Conditioned food preferences. *Bulletin of the Psychonomic Society*. 1991/02/01 1991;29(2):256-260. doi:10.3758/BF03335250

7. Beutler LR, Chen Y, Ahn JS, Lin YC, Essner RA, Knight ZA. Dynamics of Gut-Brain Communication Underlying Hunger. *Neuron*. 2017;96(2):461-75. doi:10.1016/j.neuron.2017.09.043

8. Wise RA, Rompre P-P. Brain Dopamine and Reward. *Annual Review of Psychology*. 1989;40(1):191-225. doi:10.1146/annurev.ps.40.020189.001203

9. Beier KT, Steinberg EE, DeLoach KE, et al. Circuit Architecture of VTA Dopamine Neurons Revealed by Systematic Input-Output Mapping. *Cell*. Jul 30 2015;162(3):622-34. doi:10.1016/j.cell.2015.07.015

10. Matsumoto M, Takada M. Distinct representations of cognitive and motivational signals in midbrain dopamine neurons. *Neuron*. Sep 4 2013;79(5):1011-24. doi:10.1016/j.neuron.2013.07.002

11. Han W, Tellez LA, Perkins MH, et al. A Neural Circuit for Gut-Induced Reward. *Cell*. 2018;175(3):665-78. doi:10.1016/j.cell.2018.08.049

12. Ferreira JG, Tellez LA, Ren X, Yeckel CW, de Araujo IE. Regulation of fat intake in the absence of flavour signalling. *J Physiol*. 2012;590(4):953-72. doi:10.1113/jphysiol.2011.218289

13. Ackroff K, Lucas F, Sclafani A. Flavor preference conditioning as a function of fat source. *Physiol Behav*. Jul 21 2005;85(4):448-60. doi:10.1016/j.physbeh.2005.05.006

14. Cagan RH, Maller O. Taste of sugars: brief exposure single-stimulus behavioral method. *J Comp Physiol Psychol*. 1974;87(1):47-55. doi:10.1037/h0036585

6. Conclusions

The present study has two main results. First, central ventral and dorsal dopaminergic regions respond differently to postingestive (PI) delivery of different nutrients. Additionally, results demonstrated that PI stimuli is capable of modulating food-seeking behaviour in a two-action probabilistic task.

Ventral tegmental area (VTA) dopaminergic neurons respond specifically to PI sucrose. This becomes evident when looking at the percentage of positively modulated neurons. For sessions where sucrose is infused the percentage of positively modulated neurons reinforcer is significantly higher when compared to sessions where corn oil or sucralose are infused. However, neuronal traces revealed that the profile of these neurons for sucrose and corn oil session are superimposable.

Cell pairing between different reinforcer sessions revealed that the percentage of neurons that are positively modulated by both intragastric (IG) sucrose and IG corn oil is higher when compared to the percentage of IG sucrose or IG corn oil specific modulated neurons. Despite the fact that there is a significant part of dopaminergic neurons responding to both reinforcers, when comparing specific sucrose neurons to specific corn oil neurons it became clear that IG sucrose activate a higher number of neurons. These results point to the possibility that VTA dopaminergic neurons have different layers of response that are significantly higher if the reinforcer is a caloric carbohydrate.

Fibre photometry results for the nucleus accumbens (NAc) seem to confirm the previous results since a trend to respond specifically to sucrose is observed. Interestingly, dopamine transient traces for sucrose and SMOF lipid are similar for this striatal region, which indicates that lipidic composition might be an important factor in the response of ventral striatal regions to PI stimuli.

Moreover, dopaminergic neuronal activity recorded in the substantia nigra pars compacta (SNc) points to a distinct pattern than the one observed for VTA dopaminergic neurons. Results show that the percentage of positively modulated neurons in this dorsal area is not significantly different between the three reinforcers tested.

The dorsal-lateral striatum (DLS) does not seem to respond specifically to any of the reinforcers since the trace patterns are similar between different sessions. Once again, fibre photometry results further corroborate what was observed with calcium imaging.

Results from the two-action probability task have given important insight on how PI stimuli can modulate food-seeking behaviour. When given the choice between two levers with different PI stimuli associated, mice have a clear preference for the lever that leads to the IG delivery of the caloric solution – sucrose. Additionally, this occurred even when the lever associated with caloric content was in a low probability schedule.

7. Supplementary information

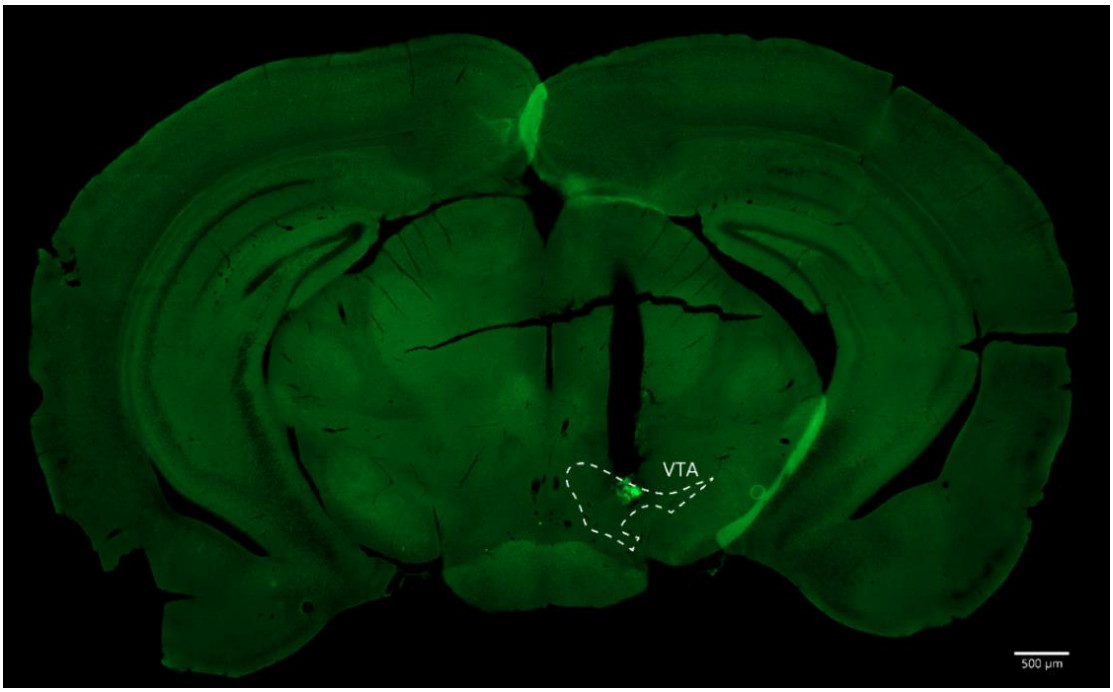

Figure 7.2 Representative images of the gradient refractive index (*GRIN*) lens track in the ventral tegmental area (VTA).
Representative image of the *GRIN* lens track in the VTA. Scale bar of 500 µm (bottom right). Image was acquired using a AxioScan.Z1 (Zeiss) microscope and a 10 X objective.

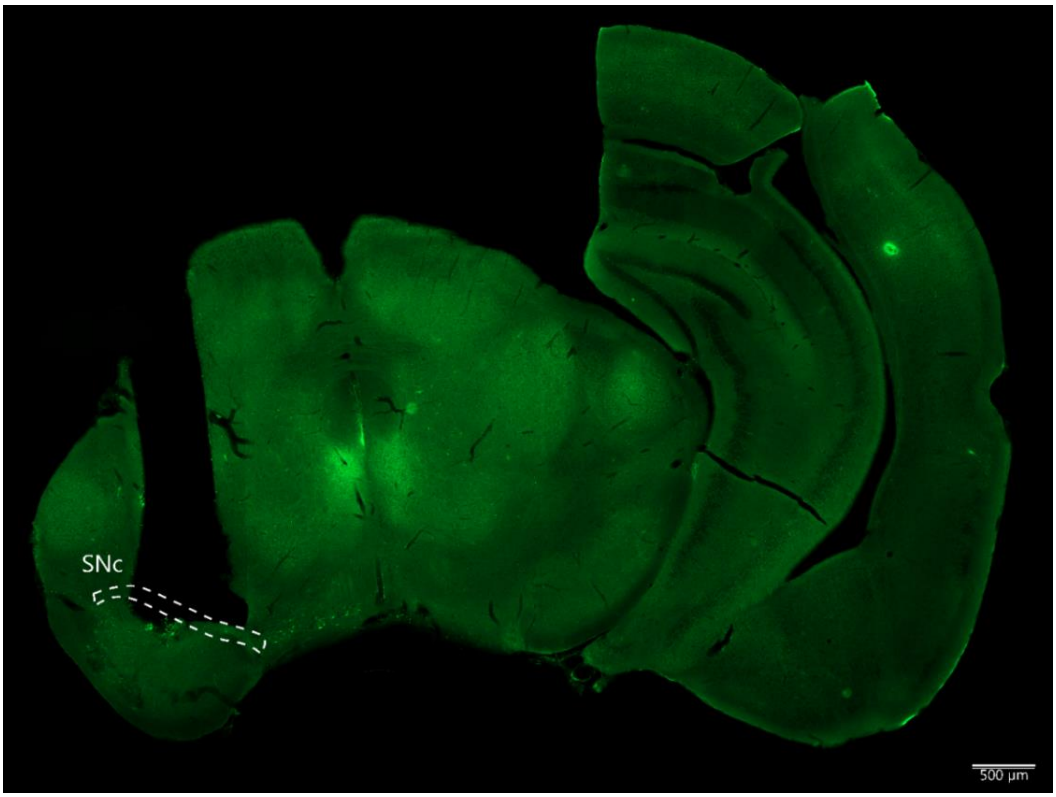

Figure 7.1 Representative images of the *GRIN* lens track in the substantia nigra pars compacta (SNc).
Representative image of the *GRIN* lens track in the SNc. Scale bar of 500 µm (bottom right). Image was acquired using a AxioScan.Z1 (Zeiss) microscope and a 10 X objective.

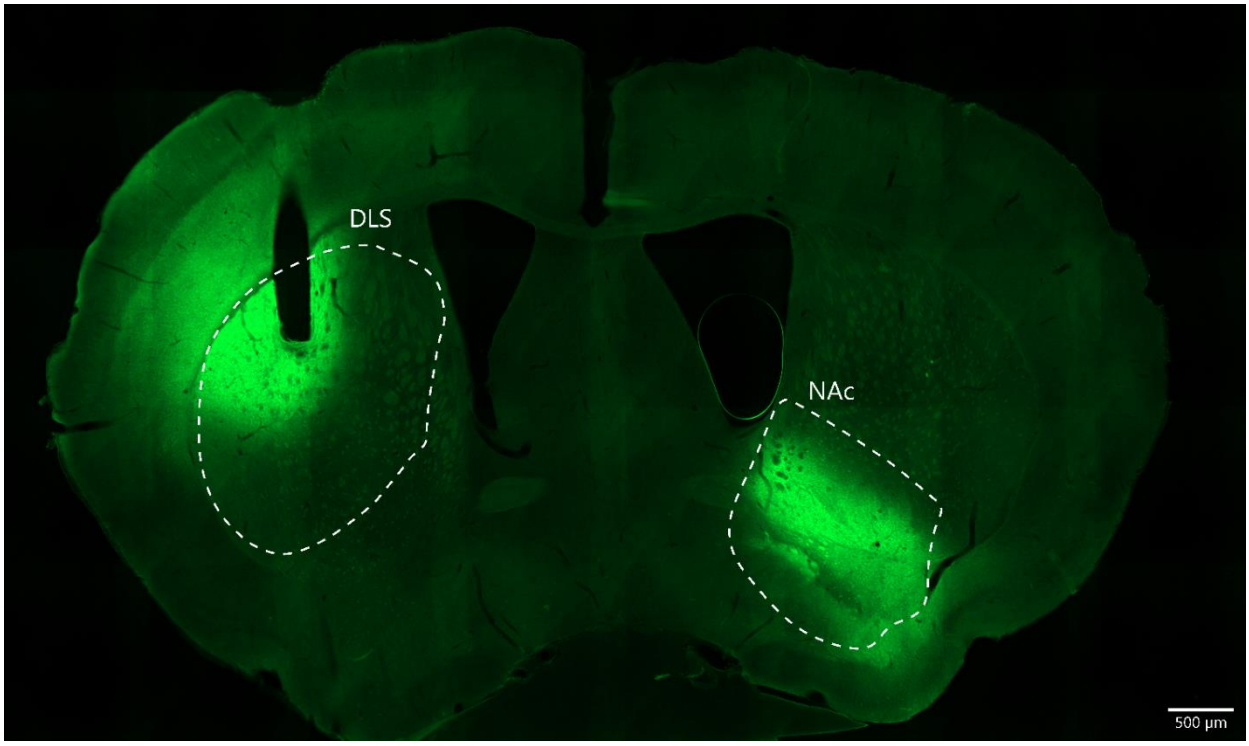

Figure 7.3 Representative image for dLight1.2 injection and dual optical fibre implantation in the striatum.
Representative image of dLight1.2 expression in the nucleus accumbens (NAc) as well as dLight1.2 expression and fibre track in the dorsal-lateral striatum (DLS). Scale bar of 500 µm (bottom right). Brain slices were stained using the anti-GFP Polyclonal Alexa Fluor™ 488 antibody. Images were acquired using a AxioScan.Z1 (Zeiss) microscope and a 10 X objective. Unpublished data developed by Tatiana Saraiva and Joaquim Alves da Silva.

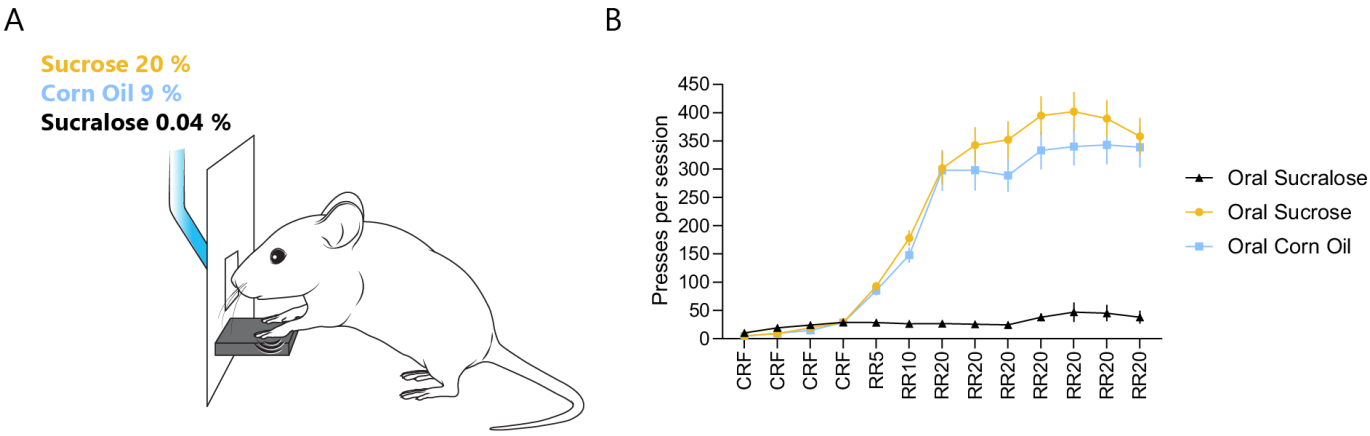

Figure 7.4 Reinforcement learning curve for isocaloric oral solutions.
A Four groups of food-deprived C57Bl6/J mice were trained to press a lever to obtain one of four oral solutions as a reward. The solutions chosen were isocaloric solutions of sucrose 20 % (n = 16), corn oil 9 % (dissolved in emulsifier 0.2 %, n = 16) and a non-caloric solution of sucrose 0.02 % (n = 8). Mouse drawing obtained from Scidraw.io. **B** Total number of presses per session for sucralose (black line, filled black triangles) sucrose (yellow line, filled yellow circles), corn oil (blue line, filled blue squares), and palm oil (pink line, filled pink upside-down triangles. In continuous reinforcement (CRF) schedule animals obtained an oral reinforcer after each lever press and in random ratio reinforcement schedule (RR) animals obtained an oral reinforcer for an average of 10 (RR 10) or 20 (RR 20) lever presses. Two-way ANOVA main effect for time ****p < 0.001; main

effect for reinforcer ****p < 0.001; post-hoc (Tukey test) analysis IG sucrose vs IG corn oil *p = 0.03; IG sucrose vs IG sucralose ####p < 0.0001; IG corn oil vs IG sucralose ####p < 0.0001). Data is presented as mean ± standard error of the mean (SEM) Unpublished data developed by Ana Fernandes and Albino Oliveira-Maia.

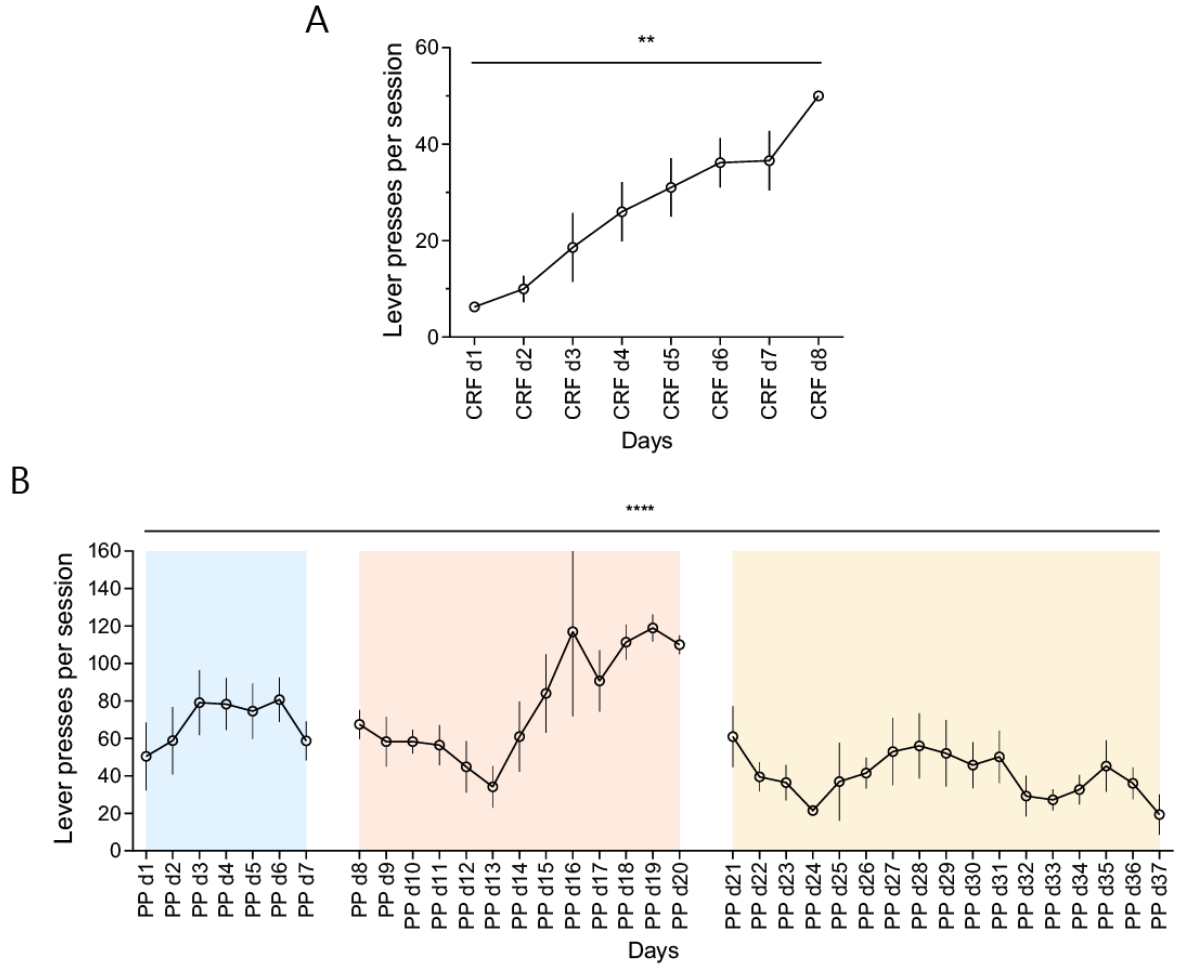

Figure 7.5 Mice can sustain lever pressing behaviour in two-action instrumental task under3 different deprivation protocols.

A Mean number of lever presses per session for continuous reinforcement (CRF) training sessions (n = 8). Water deprived mice were trained to press a lever to obtain an oral reward of a non-caloric solution - sucralose 0.04 % - under a CRF schedule, in which each lever press led to a reward. Mixed-effects analysis $F_{2,11}$ = 13.4, **p = 0.001. **B** Number of lever presses per session in a two-action instrumental task with pre and postingestive stimuli under three different deprivation protocols. After acquiring lever pressing behaviour, mice were on a probabilistic postingestive (PP) schedule, in which a lever press may lead to an oral reward – sucralose 0.04 % - paired with an IG reward delivered directly into the stomach through an IG catheter. One lever was associated with the IG delivery of the non-caloric solution – sucralose 0.04 % - and the other was associated with the delivery of a caloric carbohydrate solution – sucrose 20 %. Additionally, one lever had a high (80 %) and the other a low (20 %) low probability of delivering an oral reward paired with an IG reward. For the 7 seven days of this protocol, mice were under a water deprivation protocol (highlighted in blue, n =8); for the following 13 days, mice were under a water and food deprivation protocol (highlighted in orange, n = 8), and for the last 17 days, mice were under a food deprivation protocol (highlighted in yellow, n = 3). Mixed effects analysis $F_{3,78}$= 0.6, ***p = 0.0005. One-way repeated measures ANOVA (day PP d1- PP d7) $F_{7,42}$= 0.2, **p = 0.002. Mixed effects analysis (day PP d8 – PP d20) $F_{4,28}$= 5.8, **p = 0.002. Mixed effects analysis (day PP d21- PP d37) $F_{3,44}$= 0.9, ****p < 0.0001. Data is represented as mean ± SEM.

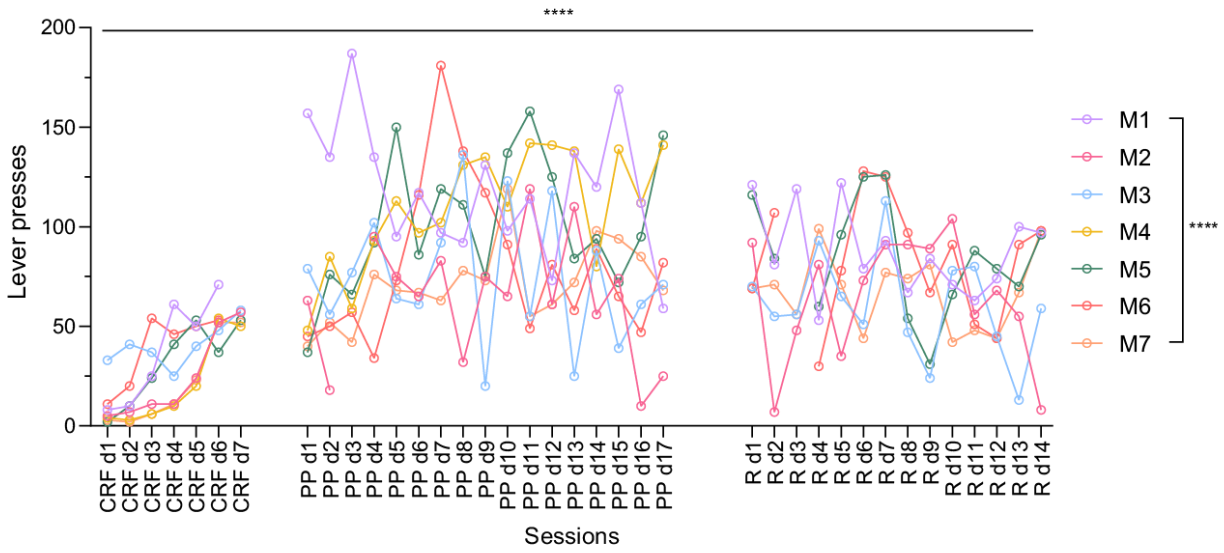

Figure 7.6 Lever presses per session is heterogenous among animals in two-action instrumental task.
Number of lever presses per session (n = 7 for CRF d1 - PP d18, n = 6 for R d1 – R d14). Each colour represents a different animal. Two-way ANOVA main effect for sessions $F_{6,203}$= 8.8, ****p< 0.0001; main effect for animal $F_{37,203}$= 5.3, ****p< 0. 0001.

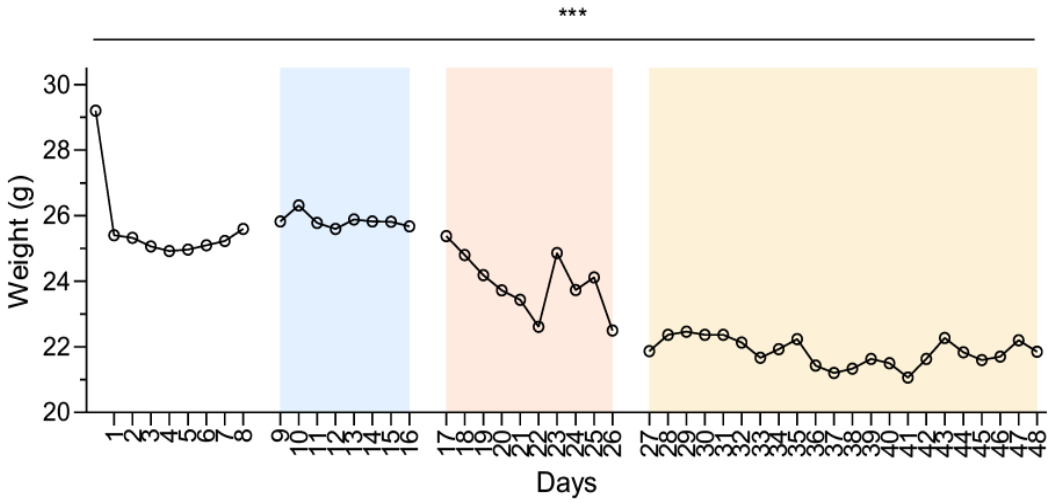

Figure 7.7 Weight of the mice fluctuates during the two-action instrumental task under 3 different deprivation protocols
Mean body weight, in grams, of mice under three different deprivation protocols throughout time. Day 0 indicates weight the day before mice started the task, designated as baseline. For the first 8 days of this protocol, mice were under a water deprivation protocol in a CRF schedule (n = 8), for the following 7 days, mice were kept in a water deprivation protocol but in a PP schedule (highlighted in blue, n = 8). Mice continued in a PP schedule for the rest of the task. For the next 13 days, mice were under a water and food deprivation protocol (highlighted in orange, n =8). For the last 17 days, mice were under a food deprivation protocol (highlighted in yellow, n = 3). Mixed effects analysis $F_{3,17}$= 13.6, ***p = 0.0001. One-way repeated measures ANOVA (day 9 – 16) $F_{7,49}$= 47.3, ns p = 0.4. Mixed effects analysis (day 17 – 26) $F_{2,12}$= 4.9, *p = 0.03. Mixed effects analysis (day 27 – 48= $F_{1,1}$= 5, ns p = 0.2.

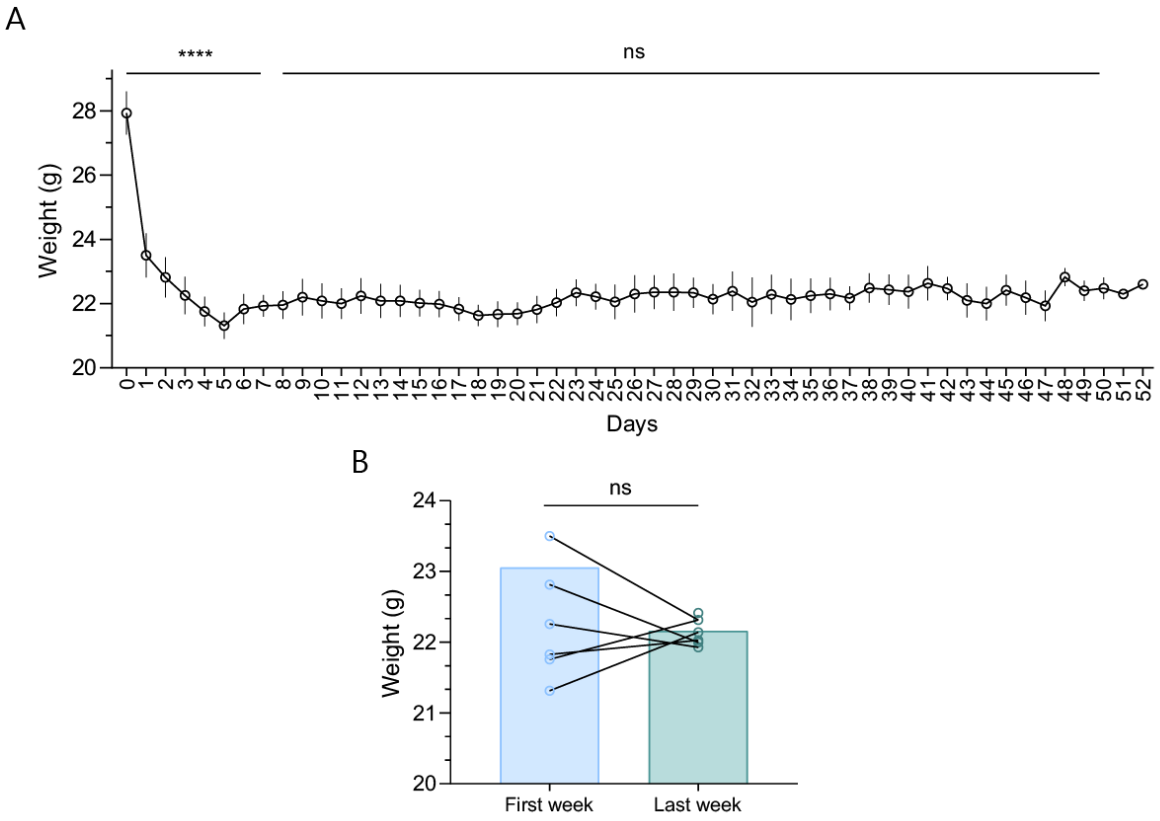

Figure 7.8 Weight of the mice initially decreases and later stabilizes during the two-action instrumental task. **A** Mean body weight, in grams (g), of water and food deprived mice throughout time. Day zero represents the day before animals started the deprivation protocol- baseline. The first 7 days correspond to the CRF schedule, and the following days correspond to the PP schedule. One-way repeated measures ANOVA (day 0 – 7, n = 7) $F_{2,12}$= 124.3, **** p < 0.0001. Mixed effects analysis (day 8-50) $F_{3,16}$= 0.7, ns p = 0.5. **B** Mean body weight, in grams (g), of water and food deprived mice for the first (blue) and last (green) weeks of each animal (n = 7). A week was defined as a period of seven days; the first week accounts for the baseline and the following six days, and the last week accounts for the last seven days the animals were weighted. Paired t-test analysis ns p = 0.3.

Table 7.1 Statistical analysis.

Figure	Sample size	Statistical test	Values
4.2 B	15 animals	One-way repeated measures ANOVA	$F_{14,28}$= 6.9, ns p = 0.5
4.3	Sucralose: 261 neurons Sucrose: 214 neurons Corn oil: 240 neurons	Two-way repeated measures ANOVA	Main effect for time $F_{8,117}$= 4.3. ***p = 0.0001; main effect for reinforcer $F_{2,27}$= 5.0, *p = 0.01
4.4 A	15 animals	Mixed-effects analysis; Multiple comparisons Tukey test	$F_{2,25}$= 8.8, ** p = 0.002 IG sucrose vs IG corn oil $^{\#}$p = 0.03, IG sucralose vs IG sucrose $^{\#\#}$p= 0.006, IG sucralose vs IG corn oil ns p = 0.6
4.4 B	Sucralose: 53 neurons Sucrose: 55 neurons Corn oil: 47 neurons	Mixed-effects analysis; Multiple comparisons Tukey test	Main effect for time $F_{7,98}$=11.4, **** p < 0.0001; main effect for reinforcer $F_{2,26}$= 4.1, * p = 0.04 IG sucrose vs IG corn oil $^{\#\#\#}$p = 0.004; IG sucralose vs IG corn oil $^{\#}$p= 0.01; IG sucralose vs IG sucrose $^{\#\#\#\#}$p < 0.0001
4.5 A	15 animals	Mixed-effects analysis; Multiple comparisons Tukey test	$F_{3,34}$= 6.6, **p = 0.002 For 300 s: mixed-effects analysis $F_{2,25}$= 8.8, ** p = 0.002 IG sucrose vs IG corn oil $^{\#}$p = 0.03, IG sucralose vs IG sucrose $^{\#\#}$p= 0.006, IG sucralose vs IG corn oil ns p = 0.6 For 600 s: mixed-effects analysis $F_{2,24}$= 5.0, ** p = 0.06, IG sucralose vs IG sucrose $^{\#}$p = 0.03, IG sucrose vs IG corn oil ns p = 0.07, IG sucralose vs IG corn oil ns p =0.8
4.5 B	Sucralose: 72 neurons Sucrose: 64 neurons Corn oil: 58 neurons	Mixed-effects analysis; Multiple comparisons Tukey test	Main effect for time $F_{89,1260}$= 10.4, ****p < 0.0001; main effect for reinforcer $F2_{,2323}$= 37.9, ****p < 0.0001. IG sucrose vs IG corn oil $^{\#\#\#\#}$p < 0.0001, IG sucralose vs IG corn oil $^{\#\#}$p= 0.006, IG sucralose vs IG sucrose $^{\#\#\#\#}$p < 0.0001
4.7 A	Sucrose: 10 neurons Corn oil: 4 neurons	Mixed-effects analysis	Main effect for time $F_{59,531}$= 3.82, ****p < 0.0001; main effect for reinforcer $F_{1,9}$=0.17, ns p = 0.7
4.7 B	Sucrose: 13 neurons Corn oil: 13 neurons	Two-way repeated measures ANOVA	Main effect for time $F_{7,90}$= 9.88, ****p < 0.0001; main effect for reinforcer $F_{1,12}$= 2.34 ns p = 0.2
4.8 A	15 animals	One-way repeated measures ANOVA	$F_{7,14}$= 6.58, ns p = 0.2
4.8 B	Left VTA: 8 animals Right VTA: 7 animals	One-way repeated measures ANOVA; Multiple comparisons Tukey test	For the left VTA: $F_{2,13}$= 4.18, *p = 0.04 (n = 8) IG sucrose vs IG corn oil $^{\#}$p = 0.03, IG sucralose vs IG sucrose ns p= 0.2, IG sucralose vs IG corn oil ns p = 0.8. For the right VTA: o $F_{2,9}$= 1.35, ns p = 0.3 .

4.9	Sucralose: 7 animals Sucrose: 3 animals	One-way ANOVA; Multiple comparisons Tukey test	$F_{3,14}$= 1.9, *** p = 0.004 IG sucralose vs IG sucralose with emulsifier ns p = 0.9, IG sucrose vs IG sucrose with emulsifier ns p = 0.7; IG sucralose vs IG sucrose #p = 0.01; IG sucralose with emulsifier vs IG sucrose with emulsifier ##p= 0.003
4.10	Sucralose: 4 sessions Sucrose: 3 sessions Corn oil: 4 sessions	Mixed effects analysis	Main effect for time $F_{59,480}$= 1.0, ns p = 0.6; main effect for reinforcer $F_{2,437}$= 55.6, ****p < 0.0001
4.12 B	5 animals	One-way repeated measures ANOVA	$F_{4,8}$= 6.9, ns p = 0.8
4.13	Sucralose: 35 neurons Sucrose: 42 neuronss Corn oil: 35 neurons	Mixed effects analysis	Main effect for time $F_{4,14}$= 1.1, ns p = 0.3; main effect for reinforcer $F_{1,4}$= 0.17, ns p = 0.7
4.14 A	5 animals	One-way repeated measures ANOVA	$F_{4,8}$= 0.16, ns p = 0.7
4.14 B	Sucralose: 5 neurons Sucrose: 5 neuronss Corn oil: 3 neurons	Two-way ANOVA	Main effect for time $F_{3,12}$= 1.4, ns p = 0.3; main effect for reinforcer $F_{2,4}$=2.0, ns p = 0.2
4.15 A	5 animals	Mixed effects analysis One-way repeated measures ANOVA	$F_{1,5}$= 0.75, ns p = 0.5 For 300 s: repeated measures ANOVA $F_{1,7}$= 1.2, ns p = 0.3. For 600 s: repeated measures ANOVA $F_{1,4}$= 0.6, ns p = .0.7
4.15 B	Sucralose: 12 neurons Sucrose: 7 neuronss Corn oil: 7 neurons	Two-way ANOVA	Main effect for time $F_{6,50}$= 0.84, ns p = 0.5; main effect for reinforcer $F_{2,9}$= 2.30, ns p = 0.2
4.18 A	4 animals	Two-way repeated measures ANOVA	Main effect for time $F_{6,55}$= 4.3, ns p = 0.3; main effect for reinforcer $F_{2,9}$= 0.10, ns p = 0.9
4.18 B	4 animals	Two-way repeated measures ANOVA	Main effect for time $F_{4,27}$= 1.03, ns p = 0.4; main effect for reinforcer $F_{2,6}$= 1.48, ns p = 0.3
4.19 A	4 animals	Two-way repeated measures ANOVA	Main effect for time $F_{2,7}$= 2.05, ns p = 0.2; main effect for reinforcer $F_{1,3}$= 0.090, ns p = 0.8
4.19 B	4 animals	Two-way repeated measures ANOVA	Main effect for time $F_{2,4}$= 1.51, ns p = 0.3; main effect for reinforcer $F_{1,2}$= 20.6, *p = 0.04
4.20	Water deprivation: 7 animals Water and food deprivation: 3 animals Food deprivation: 4 animals	Mixed effects analysis; Multiple comparisons Tukey test	$F_{2,13}$ =73.4, ****p < 0.0001 water deprivation vs water and food deprivation *p = 0.02, water and food deprivation vs food deprivation ***p = 0.0002, water deprivation vs food deprivation **p = 0.006
4.21	7 animals	Mixed effects analysis	$F_{2,17}$= 6.60, **p = 0.006

4.22 A	7 animals	Mixed effects analysis	$F_{4,23}$= 7.17 ***p = 0.0008 CRF d1 – CRF d7: $F_{2,14}$= 17.1 ***p = 0.0001. PP d1 – PP d8: $F_{3,21}$= ns p = 0.5
4.22 B	7 animals	Mixed effects analysis	$F_{3,21}$= 1.3, ns p = 0.3
4.23 A	7 animals	Mixed effects analysis	Main effect for sessions $F_{5,49}$= 0.88, ns p = 0.5; main effect for lever $F_{1,12}$= 9.04, *p = 0.01;
4.23 B	7 animals 4 sessions	Paired t test	**p = 0.008
4.24 A	7 animals 6 sessions 20 trials	Two-way ANOVA	Main effect for lever $F_{1,11}$= 0.39, ns p = 0.5; main effect for trial $F_{3,37}$= 4.3, **p = 0.008
4.24 B	7 animals 6 sessions	Two-way ANOVA	Main effect for lever $F_{1,22}$= 0.003, ns p = 0.9; main effect for probability $F_{1,22}$= 7.2, *p = 0.01
4.24 C	7 animals 4 sessions 20 trials	Two-way ANOVA	Main effect lever $F_{1,10}$= 59.6, ****p < 0.0001; main effect for trial $F_{3,30}$= 3.8, *p = 0.02
4.24 D	7 animals 4 sessions	Two-way ANOVA	Main effect for lever $F_{1,20}$= 80.4, ****p < 0.0001; main effect for probability $F_{1,20}$= 4.9, *p = 0.04
4.25 A	6 animals	Mixed effects analysis	$F_{3,17}$= 1.29, ns p = 0.3
4.25 B	6 animals	Mixed effects analysis	$F_{3,17}$= 1.3, ns p = 0.3
4.25 C	PP: 7 animals R: 6 animals	Mixed effects analysis	$F_{1,2}$= 1.0, ns p = 0.1
4.26 A	6 animals	Mixed effects analysis	Main effect for sessions $F_{4,39}$= 0.97, ns p = 0.4; main effect for lever $F_{1,12}$= 4.4, ns p = 0.06
4.26 B	6 animals 4 sessions	Paired t test	ns p = 0.1 PP d18 and R d14 ns p =0.3
4.27 A	6 animals 4 sessions 20 trials	Two-way ANOVA	Main effect for lever $F_{1,155}$= 0.76, ns p = 0.4; main effect for trial $F_{19,155}$= 2.42, **p = 0.02
4.27 B	6 animals 4 sessions	Two-way ANOVA	Main effect for lever $F_{1,16}$= 0.0058, ns p = 0.9; main effect for probability $F_{1,16}$= 8.7, **p = 0.009.